LBNL-48819

ERNEST ORLANDO LAWRENCE BERKELEY NATIONAL LABORATORY

Aspects of the Phenomenology of Superstring-Inspired Supergravity

Brent D. Nelson

Physics Division

August 2001

Ph.D. Thesis

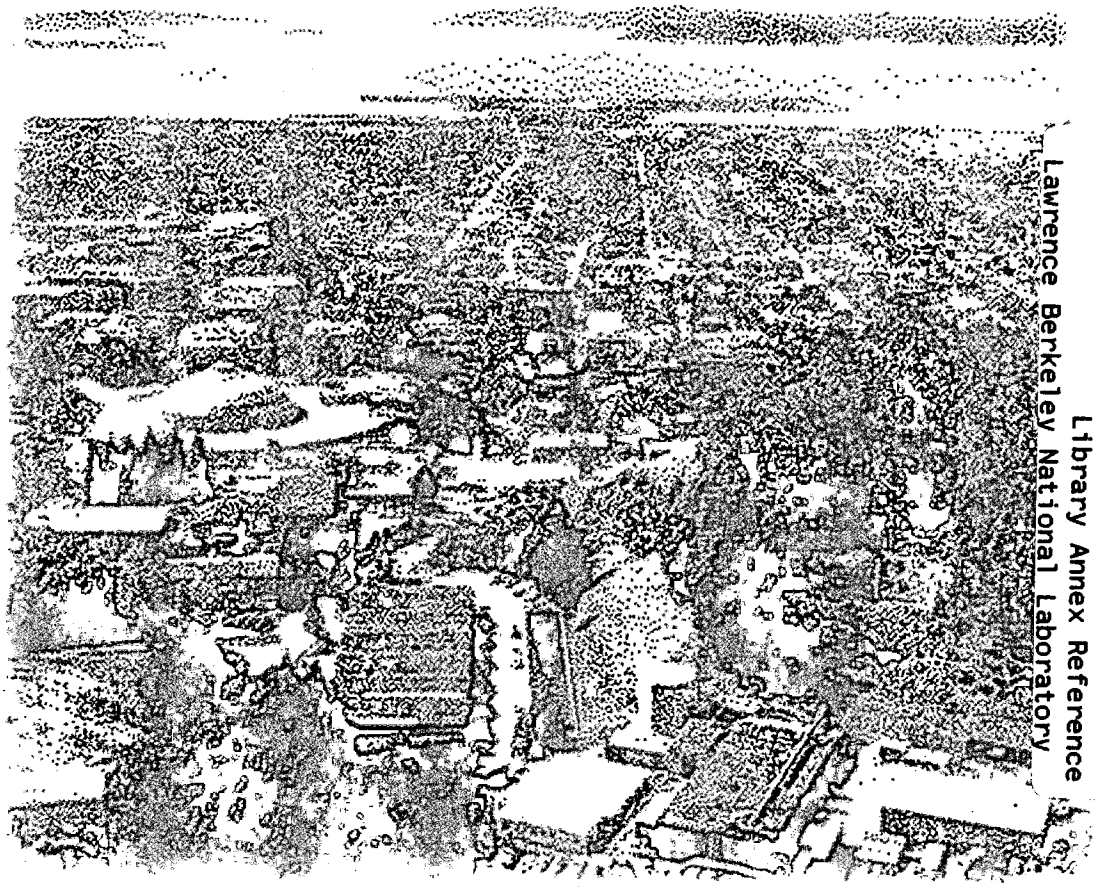

REFERENCE COPY
Does Not
Circulate

Library Annex Reference
Lawrence Berkeley National Laboratory

LBNL-48819

Copy 1

DISCLAIMER

This document was prepared as an account of work sponsored by the United States Government. While this document is believed to contain correct information, neither the United States Government nor any agency thereof, nor the Regents of the University of California, nor any of their employees, makes any warranty, express or implied, or assumes any legal responsibility for the accuracy, completeness, or usefulness of any information, apparatus, product, or process disclosed, or represents that its use would not infringe privately owned rights. Reference herein to any specific commercial product, process, or service by its trade name, trademark, manufacturer, or otherwise, does not necessarily constitute or imply its endorsement, recommendation, or favoring by the United States Government or any agency thereof, or the Regents of the University of California. The views and opinions of authors expressed herein do not necessarily state or reflect those of the United States Government or any agency thereof or the Regents of the University of California.

LBNL-48819

Aspects of the Phenomenology of Superstring-Inspired Supergravity

Brent Douglas Nelson
Ph.D. Thesis

Department of Physics
University of California, Berkeley

and

Physics Division
Ernest Orlando Lawrence Berkeley National Laboratory
University of California
Berkeley, CA 94720

August 2001

This work was supported by the Director, Office of Science, Office of High Energy and Nuclear Physics, Division of High Energy Physics and Division of Nuclear Physics, of the U.S. Department of Energy under Contract No. DE-AC03-76SF00098.

Contents

Acknowledgments **viii**

Introduction **1**

1 Supergravity Preliminaries **3**

1.1 Supergravity Model Parameters 3

1.2 Kähler $U(1)$ Superspace 4

1.3 Superstring Effective Theories 5

2 Soft Supersymmetry Breaking at One Loop **11**

2.1 Quantum-Induced Soft Supersymmetry Breaking 11

2.1.1 General Corrections to the Scalar Potential 11

2.1.2 Trilinear A-terms 15

2.1.3 Scalar Masses 16

2.2 Comparison to Anomaly Mediated Results 18

2.2.1 Gaugino Masses vs. Scalar Potential Quantities 18

2.2.2 No-Scale Models 19

2.2.3 Spurion Techniques 21

2.3 Explicit Form of the One Loop Soft Terms 23

2.3.1 Gaugino Masses 23

2.3.2 A-terms 24

2.3.3 B-terms 25

2.3.4 Scalar Masses 28

3 Orbifold Models **31**

3.1 Anomaly Dominated Scenarios 32
3.2 BIM O-II Models 35
3.3 BIM O-I Models 40
3.4 Comparisons 43

4 Dark Matter Constraints **47**
4.1 Universal Gaugino Masses 48
4.2 Nonuniversal Gaugino Masses 52

5 Phenomenology of Gaugino Condensation Models **59**
5.1 Models of Gaugino Condensation 59
5.2 Preliminary Issues 62
5.2.1 Condensation and Dilaton Stabilization 62
5.2.2 Scale of Supersymmetry Breaking 63
5.2.3 Implications for the Hidden Sector 66
5.3 Low Energy Physics Signatures 69
5.3.1 Soft Supersymmetry Breaking Terms 69
5.3.2 RGE Viability Analysis Within the MSSM 72
5.3.3 Gauge Coupling Unification 79
5.4 Dark Matter in Condensation Models 81

Conclusions **91**

A Chiral vs. Linear Multiplet Formulation for the Dilaton **93**

B Complete One Loop Expressions in Orbifold Models **97**

Bibliography **101**

List of Figures

3.1 **Soft Term Spectrum for Anomaly Dominated Scenario.** Soft term magnitudes for third generation scalars, Higgs fields and gaugino masses are given as a function of universal PV parameter p as a fraction of gravitino mass $M_{3/2}$. Scalar particles are generally much heavier than gauginos except for the limiting case of $p \to 1$. 34

3.2 **$U(1)_Y$ Gaugino Mass in the BIM O-II Model.** Contributions to the value of M_1 from F^T (dashed) and F^S (dotted) as well as total M_1 (solid) are given as a function of Goldstino angle for two values of δ_{GS} and four T-modulus *vevs*: $\langle \mathrm{Re}\, t \rangle = 0.5$ (a), $\langle \mathrm{Re}\, t \rangle = 0.9$ (b), $\langle \mathrm{Re}\, t \rangle = 5$ (c), and $\langle \mathrm{Re}\, t \rangle = 20$ (d). All values are given as a fraction of the gravitino mass $M_{3/2}$. 36

3.3 **Relative Gaugino Masses vs. $\langle \mathrm{Re}\, t \rangle$ in the BIM O-II Model with $\Lambda_{UV} = 2 \times 10^{16}$ GeV.** Relative sizes of the three gaugino masses M_1 (dashed), M_2 (dotted) and M_3 (solid) are displayed as a function of $\langle \mathrm{Re}\, t \rangle$ for two values of the Goldstino angle θ and three representative values of δ_{GS}. The vertical dotted line at $\langle \mathrm{Re}\, t \rangle = 1$ indicates the moduli self-dual point where gaugino masses become independent of δ_{GS}. When $\sin\theta = 0$ this point represents the case of leading anomaly contributions discussed in Section 3.1. All masses are relative to the gravitino mass $M_{3/2}$. 37

3.4 **Ratio M_1/M_2 in BIM O-II Model.** Contours of the absolute value of the ratio of U(1) to SU(2) gaugino masses are given for boundary scales of $\Lambda_{UV} = 2 \times 10^{16}$ GeV for panels (a) and (b), and $\Lambda_{UV} = 1 \times 10^{11}$ GeV for panels (c) and (d). The shaded area is the region of parameter space for which $|M_1| \geq |M_2|$. The arrow indicates the direction of smallest ratios as the discontinuity $M_2 = 0$ is approached. The contour $M_1 = M_2$ is given by the heavy solid line. 38

3.5 **Relative Gaugino Masses in the BIM O-II and BIM O-I Models with $\theta = 0$.** Relative sizes of the three gaugino masses M_1 (dashed), M_2 (dotted) and M_3 (solid) are displayed as a function of $\langle \mathrm{Re}\, t \rangle$ for two values of the Green-Schwarz coefficient δ_{GS} and $\Lambda_{UV} = 2 \times 10^{16}$ GeV. The top panels (a) represent the BIM O-II model from Section 3.2, the middle panels (b) represent the BIM O-I model and the bottom panels (c) represent the Love & Stadler case from [116]. All masses are relative to the gravitino mass $M_{3/2}$. 41

3.6 **Relative Gaugino Masses in the BIM O-I Models with $\theta = \pi/3$ and $\delta_{GS} = 0$.** Relative sizes of the three gaugino masses are displayed as a function of $\langle \mathrm{Re}\, t \rangle$ for the BIM O-I model (solid) and the Love & Stadler model (dashed) at $\Lambda_{UV} = 2 \times 10^{16}$ GeV. All masses are relative to the gravitino mass $M_{3/2}$. 42

4.1 **Preferred Dark Matter Region for the cMSSM.** Contours of $\Omega_\chi h^2$ of 0.1 (bottom-most contour), 0.3 and 1.0 (top-most contour) are given. The shaded region is ruled out by virtue of having the stau as the LSP. The Higgs pole region and stau coannihilation tail are clearly discernible. We have also added contours of constant Higgs mass for $m_h = 100$ GeV and $m_h = 115$ GeV. The four labeled points are examined in Figure 4.2. 50

4.2 **Annihilation Cross Sections for Selected Points from Figure 4.1.** These graphs detail the composition of the neutralino depletion cross section. The total depletion cross section is on the far left. The next two columns divide the normal annihilation channels by final state into two fermions or all other annihilation channels. The final column is the sum of all coannihilation channels. The total relic density is given at the top of each plot and the dashed horizontal line illustrates the ideal total depletion cross section for a $\Omega_\chi h^2 = 0.2$. 51

4.3 **Preferred Dark Matter Region for Nonuniversal Gaugino Masses.** Contours of $\Omega_\chi h^2$ of 0.01, 0.1, 0.3, 1.0 and 10.0 from left to right, respectively, are given as a function of the ratio of SU(2) to U(1) gaugino masses M_2/M_1 at the high scale. The cMSSM is recovered where the two masses are equal at the high scale, as has been indicated by the dashed line. The six labeled points are examined in Figure 4.4. 53

4.4 **Annihilation Cross Sections for Selected Points from Figure 4.3.** These graphs are identical in layout to those of Figure 4.2, except now the coannihilation channels are split into two columns: two-fermion final states and everything else. 54

4.5 **Preferred Dark Matter Region with Nonuniversal Gaugino Masses for Various M_3 Values [I].** Contours of constant relic density are given by the solid lines for $\Omega_\chi h^2 = 0.01$, 0.1, 0.3, 1, and 10 from left to right. The dotted lines are curves of constant wino content for $N_{12}^2 =$ 0.25, 0.04, 0.01 and 0.025 from left to right. The value of the high-scale gluino mass M_3 is given in terms of the universal gaugino mass $M_{1/2}$ at the top of each plot. This plot uses a value of $M_{1/2} = 200$ GeV except for panel (A) where $M_{1/2} = 250$ GeV. The shaded region is excluded by the constraints of Table 4.1. 55

4.6 **Preferred Dark Matter Region with Nonuniversal Gaugino Masses for Various M_3 Values [II].** Contours of constant relic density are given by the solid lines for $\Omega_\chi h^2 = 0.01$, 0.1, 0.3, and 1.0 from left to right. The value of the ratio $(M_2/M_1)_{\rm low}$ is indicated by the dashed lines for the values $(M_2/M_1)_{\rm low} = 1.15$, 1.25 and 1.50 from left to right. The shaded regions are ruled out because of a stau LSP. 57

4.7 **Preferred Dark Matter Region with Nonuniversal Gaugino Masses for Differing Signs of M_3.** The solid lines are lines of constant $\Omega_\chi h^2$ and the dashed lines represent values of $(M_2/M_1)_{\rm low} = 1.15$, 1.25 and 1.50 as in Figure 4.6. The shaded regions are excluded by virtue of having a stau for the LSP. We have indicated the Higgs mass constraint in panels (A) and (B). Here $M_{1/2}$ is taken to be 500 GeV in all panels. 58

5.1 **Condensation Scale as a Function of Hidden Sector Gauge Configuration.** Contours give the scale of gaugino condensation in GeV for $(c_\alpha)_{\rm eff} = 3$. 65

5.2 **Gravitino Mass as a Function of Hidden Sector Gauge Configuration.** Contours of gravitino mass for 10^2 GeV through 10^5 GeV are given for $(c_\alpha)_{\rm eff} = 3$. 66

5.3 **Gravitino Mass Regions as a Function of Yukawa Parameter.** Gravitino mass contours for (a) 100 GeV and (b) 10 TeV are shown for $(c_\alpha)_{\text{eff}} = 50$ and $(c_\alpha)_{\text{eff}} = 0.1$ with $\alpha_{\text{STR}} = 0.04$. The region between the two sets of curves can be considered roughly the region of phenomenological viability. 67

5.4 **Constraints on the Hidden Sector.** The shaded regions give three different "viable" regions depending on the value of the unified coupling strength at the string scale. The upper limit in each case represents a 10 TeV gravitino mass contour with $(c_\alpha)_{\text{eff}} = 1$, while the lower bound represents a 100 GeV gravitino mass contour with $(c_\alpha)_{\text{eff}} = 10$. 68

5.5 **Gaugino Masses in the Model of Section 5.1.** Gaugino masses M_1 (dashed), M_2 (dotted) and M_3 (solid) are given at a scale $\Lambda_{\text{UV}} = 1 \times 10^{14}$ GeV as a function of the condensing group β-function coefficient b_+^0. The vertical dotted line in the left panel is the benchmark case of E_6 condensation in the hidden sector with 9 **27**s of hidden sector matter studied in [84]. The right panel focuses on the region where the three masses are approximately unified. 70

5.6 **Spectrum of Soft Supersymmetry Breaking Terms in the Model of Section 5.1.** All values are given relative to the gravitino mass $M_{3/2}$ at a scale $\Lambda_{\text{UV}} = 1 \times 10^{14}$ GeV as a function of the condensing group β-function coefficient b_+. 71

5.7 **Region with Correct Symmetry Breaking for Scenario A.** The maximum value of $\tan\beta$ consistent with electroweak symmetry breaking and positive squark masses is displayed as a function of the gravitino mass. The plot is shown with $b_+ = 0.08$ but the values are extremely insensitive to the choice of this parameter. 73

5.8 **Region with Correct Symmetry Breaking for Scenario D.** Three pairs of curves are shown for $b_+ = 0.084, 0.087, 0.090$. For values of $\tan\beta$ between the curves the heavy scalar contribution at two loops to the running of $m_{U_3}^2$ drives its value negative. 74

5.9 **Chargino/Neutralino Mass Degeneracy in Scenario A.** The mass difference between the $\chi_1^\pm$ and the $\tilde{N}_1$ is given in GeV. 75

5.10 **Wino-like and Bino-Like LSPs in Scenario A.** The difference in mass between the two lightest neutralinos $\tilde{N}_2$ and $\tilde{N}_1$ is given. Note that a level crossing occurs and there exists a region in which the $\tilde{W}_3$ becomes the LSP, as is to be expected when the anomaly contribution to gaugino masses dominates. 76

5.11 **Constraints from Table 4.1 for Scenario A.** Exclusion curves for lightest chargino (solid), gluino (dashed), lightest neutralino (dotted) and lightest Higgs mass (dashed-dotted) for weak coupling at the string scale. The region below the curves fails to meet the corresponding constraint from Table 4.1. The upper left corner represents the region where the difference in mass between the $\chi_1^\pm$ and the $\tilde{N}_1$ falls below 2 GeV. 77

5.12 **Constraints from Table 4.1 for Scenario D.** Exclusion curves for lightest chargino (thick solid), gluino (dashed), lightest neutralino (dotted), lightest Higgs (dashed-dotted) and lightest stop (thin solid) mass. Curves are for weak coupling at the string scale. The region below the curves fails to meet the corresponding constraint from Table 4.1. 78

5.13 **Mass Contours for Scenario A.** *Panel A:* Contours for the lightest neutralino mass of 40, 80, 120, 160 and 240 GeV. *Panel B:* Contours of lightest chargino mass of 40, 80, 120, 160, 240 and 400 GeV. *Panel C:* Contours of lightest Higgs mass of 90, 100, 110, 120 and 130 GeV. *Panel D:* Contours of lightest stop mass of 200, 500, 1000, 2000 and 4000 GeV. All contours increase from the bottom to the top of each panel. 79

5.14 **Mass Contours for Scenario D.** *Panel A:* Contours for the lightest neutralino mass of 40, 80, 120, 160, 240 and 400 GeV. *Panel B:* Contours of lightest chargino mass of 40, 80, 120, 160, 240 and 400 GeV. *Panel C:* Contours of lightest Higgs mass of 80, 90, 100, 110, 120, 130 and 140 GeV. *Panel D:* Contours of lightest stop mass of 200, 500, 1000, 2000 and 4000 GeV. All contours increase from the bottom to the top of each panel. 80

5.15 **Gauge Coupling Unification.** Results of adding one pair of $(Q, \overline{Q})$ and two pairs of $(D, \overline{D})$ at the condensation scale. Contours of constant implied Planck mass are overlaid on the region for which $\Delta = \alpha_3^{\rm RGE} - \alpha_3^{\rm OBS}$ is within the two-sigma experimental limit of $\delta\alpha = \pm 0.004$. The dotted line represents the maximum value of b_+ consistent with $M_{3/2} \leq 10$ TeV and the RGE determined string coupling. The values of $\alpha_{\rm STR}$ here range from 0.044 at the $\Delta = +0.004$ contour to 0.050 at the $\Delta = -0.004$ contour. 82

5.16 **Cosmologically Preferred Region in Gaugino Condensation Models.** Contours of constant relic density are given as a function of M_0 and b_+ by the solid lines while the Higgs resonance and $W^\pm$ resonance are indicated by the upper and lower dotted lines, respectively. Moving outward from the lower dotted line are contours of $\Omega_\chi h^2 = 0.01$, 0.1, 0.3, 1.0 and 10. The labeled points are examined in detail in Figure 5.18. 83

5.17 **Cosmologically Preferred Region and Experimental Constraints.** Contours of $\Omega_\chi h^2 =$ 0.01, 0.1, 0.3, 1.0 and 10 are again shown along with the experimental constraints from Table 4.1. The shaded region is excluded: the dashed curve represents a 190 GeV gluino mass while the two parallel solid curves represent a 75 GeV and a 90 GeV chargino mass from bottom to top. . 84

5.18 **Annihilation Cross Sections for Selected Points From Figure 5.16.** These graphs are identical in nature to those of Figure 4.4. 85

5.19 **Relic Densities vs. Wino Content in Gaugino Condensation Models.** Contours of constant relic density are given as in Figure 5.16 by the solid lines for $\Omega_\chi h^2 = 0.1$, 0.3, and 1.0 only. Dotted lines are contours of constant wino content of 25%, 4%, 1%, 0.25% from left to right. 86

5.20 **Relic Densities vs. Gaugino Mass Ratios in Gaugino Condensation Models.** Contours of constant relic density are given as in Figure 5.16 by the solid lines for $\Omega_\chi h^2 = 0.1$, 0.3, and 1.0. Dashed lines are contours of constant ratio $(M_2/M_1)_{\rm low}$ of 1.15, 1.25, and 1.5 from left to right. 87

5.21 **Preferred Dark Matter Region in Hidden Sector Configuration Space.** This plot illustrates the dark matter parameter space in terms of the gauge group and matter content parameters of the hidden sector. The fine points on the left have the preferred value $0.1 \leq \Omega_\chi h^2 \leq 0.3$ and the coarse points have $0.3 < \Omega_\chi h^2 \leq 1.0$. The swath bounded by lines (a) and (b) is the region in which the $0.1 \leq (c_\alpha)_{\rm eff} \leq 10$ and the gravitino mass is between 100 GeV and 10 TeV. The dotted lines are the possible combination of gauge parameters for different hidden sector gauge groups. 88

List of Tables

3.1 **Regions of Positive Squared-Mass in the Anomaly Dominated Scenario.** Range of $\tan\beta$ for which scalar squared-masses are positive at the boundary scale Λ_{UV} using the PV scenario (A). The value of $\tan\beta$ was varied over the range for which the third generation Yukawa couplings remain perturbative up to the scale Λ_{UV}. This corresponds to the range $1.3 \leq \tan\beta \leq 44$ for $\Lambda_{UV} = 1 \times 10^{11}$ GeV and $1.6 \leq \tan\beta \leq 48$ for $\Lambda_{UV} = 2 \times 10^{16}$ GeV. 33

3.2 **Sample Spectra (in GeV) for Typical Models of Sections 3.1, 3.2 and 3.3.** All cases are for PV scenario (A), $\tan\beta = 3$ and $\Lambda_{UV} = 2 \times 10^{16}$ GeV ($\tilde{B}$ % and $\tilde{W}_3$ % represent the content of the lightest neutralino in per cents). The first O-II case considered, while clearly ruled out experimentally, is presented as an illustrative example. 43

3.3 **Sample Spectra (in GeV) for Typical Models of Sections 3.1, 3.2 and 3.3.** The same as in Table 3.2 but for $\tan\beta = 10$. Neither of the large threshold models are viable at this value of $\tan\beta$. 45

4.1 **Superpartner and Higgs mass constraints imposed [125, 53].** 56

5.1 **Gauge group Casimirs and allowed condensate numbers.** Possible hidden sector gauge group configurations that might give rise to thermal relic neutralino densities compatible with observations. 89

Acknowledgments

I offer my thanks and appreciation to Professors Marc Rieffel and Hitoshi Murayama for serving as members of my dissertation committee. I would further like to thank Marjorie Shapiro for serving on my qualifying committee and for providing much needed guidance and support, particularly early in my graduate student career.

I have benefited in my research and found great inspiration through conversations with Professors Shapiro and Murayama, as well as Professors Nima Arkani-Hamed, Robert Cahn, Lawrence Hall, Ian Hinchliffe, David Jackson, Robert Jacobsen, Jim Siegrist, and Bruno Zumino of U.C. Berkeley and Lawrence Berkeley Laboratory. I particularly wish to thank Pierre Binétruy of the Université Paris-Sud in Orsay, France for his support and collaboration, as well as his hospitality during my stay at the Université de Paris-Sud.

The staff at LBL and at U.C. Berkeley have made the challenges of life as a graduate student far less daunting through their cheerful attitude and ability to solve problems and for that I am grateful. I have also found working with my fellow graduate students and researchers at LBL to be the most rewarding element to my time as a student and I would be remiss if I did not thank Andreas Birkedal-Hansen, Dan Brace, Andre de Gouvea, Alex Friedland, Joel Giedt, Christophe Grojean, Chris Kolda, Bogdan Morariu, Aaron Pierce and Jonathan Tannenhauser.

Finally my most heartfelt thanks goes to Mary K. Gaillard whose counsel has been appreciated and whose efforts on my behalf have been extraordinary. I owe my success as a student to the knowledge I have gained under her tutelage, and any future success I may enjoy in the field of high energy theoretical physics will only serve as partial repayment for that debt.

This work was supported in part by the Director, Office of Science, Office of High Energy and Nuclear Physics, of the U.S. Department of Energy under Contract DE-AC03-76SF00098.

LBNL-48819

Aspects of the Phenomenology of Superstring-Inspred Supergravity

Brent Douglas Nelson

Department of Physics, University of California at Berkeley, and

Theoretical Physics Group, Lawrence Berkeley National Laboratory.

Abstract

In this dissertation we calculate the one loop quantum contributions to soft supersymmetry breaking terms in the scalar potential as well as gaugino masses in supergravity theories regulated à la Pauli-Villars. We find "universal" contributions, independent of the regulator masses and tree level soft supersymmetry breaking, that contribute gaugino masses and A-terms equal to the "anomaly mediated" contributions found in analyses using spurion techniques, as well as a scalar mass term not identified in those analyses. The universal terms are in general modified – and in some cases canceled – by model-dependent terms. We emphasize the model dependence of loop-induced soft terms in the potential, which are much more sensitive to the details of Planck scale physics then are the one loop contributions to gaugino masses.

Next, a systematic analysis of soft supersymmetry breaking terms at the one loop level is performed in a large class of string effective field theories. We show that the pattern of supersymmetry breaking depends on the detailed prescription of the regularization process which is assumed to represent the Planck scale physics of the underlying fundamental theory. The usual anomaly mediation case with vanishing scalar masses at one loop is not found to be generic. We also discuss the supersymmetric spectrum of O-I and O-II orbifold compactification models.

Finally, we study the phenomenology of a class of models describing modular invariant gaugino condensation in the hidden sector of a low energy effective theory derived from the heterotic string. Placing simple demands on the resulting observable sector, such as a supersymmetry breaking scale of approximately 1 TeV, a vacuum with properly broken electroweak symmetry, superpartner masses above current direct search limits, etc., results in significant restrictions on the possible configurations of the hidden sector. We include in this analysis an investigation of the dark matter prospects of supersymmetric models such as these with nonuniversal gaugino masses. The cosmologically viable regions of parameter space are investigated, allowing very specific statements to be made about the content of the supersymmetry breaking hidden sector.

Introduction

Our ultimate goal is to study the phenomenology of string-inspired supergravity models. The low energy physics in such models is determined by the pattern of soft supersymmetry breaking parameters: scalar masses, gaugino mass and bilinear/trilinear couplings in the scalar potential referred to commonly as "B-terms" and "A-terms," respectively. When these soft supersymmetry breaking patterns are taken to be universal – that is, a single common gaugino mass $M_{1/2}$, a common scalar mass M_0 and a common trilinear coupling A_0 at the supersymmetry breaking scale Λ_{SUSY} – the model is designated "minimal" supergravity or mSUGRA. The phenomenology of these types of unified models has been extensively studied in the past [19, 51, 106, 107].

We would like to instead consider here the case of nonuniversalities – in particular those that arise from loop corrections to tree level soft terms. In general these tree level terms are indeed universal, but if the loop corrections are significant, or at least competitive in size with these tree level pieces, then departures from the standard phenomenology may result. Our tool for addressing these loop computations in the context of a nonrenormalizable theory such as supergravity is the method of Pauli-Villars regularization. We will perform explicit loop computations using component fields in this context in Section 2.

A secondary motivation for this study is to understand recent results involving the super-Weyl anomaly of standard $\mathcal{N} = 1$ supergravity referred to in Section 1. There has been considerable interest recently in soft supersymmetry breaking induced by quantum corrections, starting with the observation [93, 131] that there are several "anomaly mediated" contributions arising from the super-Weyl (or superconformal) anomaly: a gaugino mass term proportional to the β-function, a trilinear A-term proportional to the chiral multiplet (matrix-valued) γ-function, and a scalar mass term proportion to the derivative of the γ-function, arising first at the two loop level. The claim in the literature is that these quantum corrections are independent in their details of the high energy physics represented by the underlying theory (namely, a string theory) – thus they are claimed to be "universal" contributions to soft supersymmetry breaking. We will look closely at these claims in Section 2.2

In any given supersymmetric theory, a consistent analysis of the soft terms is necessary in order to make reliable predictions. Such a systematic analysis was performed at tree level by Brignole, Ibáñez and Muñoz [35, 36] some time ago for a large class of four-dimensional string models. One of the nice features of this analysis was to make explicit the dependence of the soft terms on the auxiliary field vacuum expectation values (*vevs*) and thus to relate them directly to the supersymmetry breaking mechanism. In this respect, the auxiliary fields F^S and F^α associated respectively with the string dilaton and the moduli fields are expected to play a central role in these superstring models.

This analysis showed that, besides a universal contribution associated with the dilaton field, soft terms generically receive from moduli fields a nonuniversal contribution which may lead to a very different phenomenology from the standard one referred to as the minimal supergravity model. In Section 2, new contributions to the soft supersymmetry breaking terms are exhibited that are truly supergravity contributions in the sense that they involve the auxiliary fields of the supergravity multiplet, more precisely the complex scalar auxiliary field M in the minimal formulation. In Section 3 we present the general form of these contributions, expressed in terms of the auxiliary fields, and we discuss them for several classes of superstring models. We stress that some of the contributions depend on the way the underlying theory regulates the low energy effective field theory. In particular we find a model of anomaly mediation where the scalar masses might be nonvanishing at one loop.

Having found sources of nonuniversality – particularly in the important gaugino sector of the theory – we test supergravity models in the arena of thermal relic dark matter densities. Models of the sort we investigate in Section 3 tend to provide far too much or far too little neutralino relic density to account for cosmological observations. Supergravity models where anomaly contributions to gaugino masses are competitive with tree level contributions may provide the best solution to the problem of dark matter in the universe, as is demonstrated in Section 4.

When considering the subject of effective field theories from strings, the notion of "phenomenological viability" has in the past been a very loose standard. Indeed some of the well-known problems facing such low energy theories seemed quite intractable, depressing the prospects of ever being able to refer to a meaningful superstring phenomenology. The problems to which we refer include the need to generate a hierarchy between the supersymmetry breaking scale and the Planck scale, the cosmological dangers of moduli fields with Planck-suppressed interactions, the desire for a weakly-coupled effective quantum field theory, and most significantly the need to stabilize the dilaton [16, 37, 58].

Recently, however, it was shown that by incorporating postulated nonperturbative string-theoretical effects in a modular invariant low energy field theory the above problems can be addressed in a simple manner with tuning required only in the vanishing of the cosmological constant [27, 28, 29, 84]. Having passed these initial tests it now becomes possible to ask for a slightly higher standard in "viability."

The philosophy behind the study presented in Section 5 is to probe this class of models in a series of phenomenological arenas to uncover relations between the dynamics of the hidden sector and the nature of our observable world. After a review in Section 5.1 of the class of models we will consider we investigate in Section 5.2 the initial challenge of setting the supersymmetry breaking scale that all effective field theories from strings must confront. In Section 5.3 we turn to the pattern of soft supersymmetry breaking parameters and look for the implications of current mass bounds arising from searches at LEP and the Tevatron. We also investigate phenomenological challenges arising from gauge coupling unification and cosmological relic densities in an effort to further constrain these models.

Chapter 1

Supergravity Preliminaries

This section collects some of the concepts that reappear throughout this study in the form of a very brief introduction to supergravity effective theories that derive from models of weakly-coupled heterotic string theory.

1.1 Supergravity Model Parameters

A supersymmetric model which is covariant under general coordinate transformations possesses a local, or gauged, supersymmetry and becomes a supergravity theory. In this text we will consider a set of chiral superfields Z^M (the associated scalar field will be denoted by z^M with $z^M = Z^M|_{\theta=\bar{\theta}=0}$) which belong to two distinct classes: the first class Z^i denotes observable superfields charged under the gauge symmetries of the Standard Model (SM) while the second class Z^n describes hidden sector fields. By "hidden sector" we will typically be referring to either chiral matter multiplets charged under the gauge symmetries of the hidden sector gauge group(s) $\mathcal{G}_{\text{hid}}$ and/or some set of moduli fields which parameterize the compactification of the string theory. We will return to these moduli fields in Section 1.3.

The interactions of the chiral multiplets and gauge fields of the observable sector in a generic supergravity model are described by three functions: the Kähler potential $K(Z^M, \overline{Z}^{\overline{M}})$, the superpotential $W(Z^i, Z^n)$ and the gauge kinetic functions $f^a(Z^n)$, one for each gauge group $\mathcal{G}^a$.

The auxiliary fields of the chiral multiplets are denoted F^M and are obtained by solving their corresponding equations of motion. They read for the chiral superfields:

$$F^M = -e^{K/2} K^{M\overline{N}} \left(\overline{W}_{\overline{N}} + K_{\overline{N}} \overline{W} \right), \tag{1.1}$$

where, as is standard, $\overline{W}_{\overline{N}} = \partial \overline{W} / \partial \overline{Z}^{\overline{N}}$ and $K^{M\overline{N}}$ is the inverse of the Kähler metric $K_{M\overline{N}} = \partial^2 K / \partial Z^M \partial \overline{Z}^{\overline{N}}$. The supergravity auxiliary field M simply reads:

$$M = -3e^{K/2} W. \tag{1.2}$$

As a sign of spontaneous breaking of supersymmetry, the gravitino mass is directly expressed in

terms of its *vev* (in reduced Planck scale units $M_{\rm PL}/\sqrt{8\pi} = 1$ which we use from now on):

$$M_{3/2} = -\frac{1}{3}\langle \overline{M} \rangle = \left\langle e^{K/2}\overline{W} \right\rangle . \tag{1.3}$$

In terms of these fields, the F-term part of the potential reads:

$$\widehat{V} = F^I K_{I\overline{J}} \overline{F}^{\overline{J}} - \frac{1}{3} M\overline{M} = F^I K_{I\overline{J}} \overline{F}^{\overline{J}} - 3M_{3/2}^2 . \tag{1.4}$$

Since in what follows we will assume vanishing D-terms (to preserve the gauge invariance of the Standard Model after supersymmetry breaking) we will only be interested in this part of the scalar potential. Finally, the holomorphic function $f_a(Z^n)$ is the coefficient of the gauge kinetic term in superspace. Its *vev* yields the gauge coupling associated with the gauge group $\mathcal{G}_a$:

$$< \mathrm{Re}\, f_a >= \frac{1}{g_a^2} . \tag{1.5}$$

1.2 Kähler $U(1)$ Superspace

In constructing supersymmetric Lagrangians, and extracting the component field expressions from the corresponding superfield operator expressions, we will use the Kähler $U(1)$ formalism of [31, 32, 33] which differs from the formalism of Wess and Bagger [142]. In this section we present the key differences and features of this formulation of supergravity.

The kinetic energy of the chiral superfields in the standard formulation for flat superspace involves the superspace volume integral

$$\mathcal{L}_{\rm KE} = \int \mathrm{d}^4\theta \, K(Z^M, \overline{Z}^{\overline{M}}) \tag{1.6}$$

and thus possesses a classical symmetry under the transformation

$$K(Z^M, \overline{Z}^{\overline{M}}) \to K(Z^M, \overline{Z}^{\overline{M}}) + F(Z^M) + \overline{F}(\overline{Z}^{\overline{M}}) . \tag{1.7}$$

When a superpotential is included with Lagrangian density $\mathcal{L}_{\rm pot} = \int \mathrm{d}^2\theta \, W(Z^M) + \text{ h.c.}$, then this symmetry can be preserved provided we simultaneously make the transformation

$$W(Z^M) \to e^{F(Z^M)} W(Z^M) \tag{1.8}$$

on the superpotential. This is a Kähler transformation and it manifests itself as a chiral phase rotation, with phase given by the function $F(Z^M)$ in (1.7), on the fields of the theory. As such it is vulnerable to a chiral anomaly when the theory is treated quantum mechanically.

In curved superspace the kinetic term must be modified to include the effects of curvature by amending (1.6) to read

$$\mathcal{L}_{\rm KE} = -3 \int \mathrm{d}^4\theta \, E e^{-\frac{1}{3}K(Z^M, \overline{Z}^{\overline{M}})} \tag{1.9}$$

where E is the superdeterminant of the vielbein superfield E_M^A. Note that (1.9) reduces to (1.6) to leading order in $M_{\rm PL}$ when expanding the exponential. Now the Kähler transformation (1.7)

must be accompanied by a compensating Weyl rescaling of the supervielbein E to preserve the classical symmetry, *i.e.* a "super-Weyl" transformation. In supergravity this symmetry can be incorporated into the structure of superspace in a natural way by including this chiral $U(1)$ factor in the structure group of the superspace geometry and assigning each field in the theory a weight under the transformation (1.7) called its Kähler weight. The covariant derivatives are then modified to include a $U(1)$ gauge connection corresponding to this transformation. In this formulation the kinetic action then becomes simply related to the volume of superspace. This is the essence of the Kähler $U(1)$ superspace formalism [31].

As a practical matter, supersymmetric Lagrangians can be constructed in supergravity as either "D-terms" involving integration of a real function of the fields over all of superspace $\int \mathrm{d}^4\theta$ or "F-terms" involving the integration of a holomorphic function over half of the superspace coordinates $\int \mathrm{d}^2\theta$. The former can be converted to the latter via superspace integration by parts as follows

$$\mathcal{L} = \int \mathrm{d}^4\theta\, E\, X = -\frac{1}{16}\int \mathrm{d}^4\theta\, \frac{E}{R}\left(\overline{\mathcal{D}}^2 - 8R\right) X + \text{ h.c.}\,, \tag{1.10}$$

where R is the chiral curvature superfield whose lowest component is the auxiliary field of supergravity $M = -6R|_{\theta=\bar{\theta}=0} = (\overline{M})^*$ and $(\overline{\mathcal{D}}^2 - 8R)$ is the covariant chiral projection operator. Having made this transformation the component Lagrangian is obtained using the standard construction [31]

$$\begin{aligned} \mathcal{L} &= \frac{1}{2}\int \mathrm{d}^4\theta\, \frac{E}{R}\mathbf{r} = \sqrt{g}\left(s - r\overline{M}\right) + \text{ h.c. } + \mathcal{O}(\psi_\mu), \\ r &= \mathbf{r}\Big|_{\theta=\bar{\theta}=0}, \quad s = -\frac{1}{4}\mathcal{D}^2\mathbf{r}\Big|_{\theta=\bar{\theta}=0}. \end{aligned} \tag{1.11}$$

1.3 Superstring Effective Theories

Our interests lie in a specific class of supergravity models which we can refer to as "string-inspired," which is to say that the field content and couplings can be constrained – and in some cases completely determined – by imposing symmetries arising from the underlying string theory which gives rise to the low energy effective supergravity model. Throughout this work the string theories considered are of the weakly-coupled heterotic variety and we will restrict ourselves to orbifold compactifications of the six extra spacetime dimensions to obtain a low energy effective four-dimensional theory.

Of central importance is the dilaton field which is universally present in all string theories. The vacuum expectation value of this field determines the value of the string coupling constant g_{STR} at the scale of compactification, which we denote Λ_{STR}. Here we will assume that this scale of compactification is somewhere between the Grand Unified scale $\Lambda_{\text{GUT}} \approx 2 \times 10^{16}$ GeV or the Planck scale $\Lambda_{\text{PL}} \approx 1 \times 10^{18}$ GeV. Taking the approximate unification of gauge couplings in the minimal supersymmetric standard model (MSSM) at Λ_{GUT} as a guide we will assume $g^2_{\text{STR}} = 1/2 \to \alpha^{-1}_{\text{STR}} \approx 24.7$.

The string dilaton can be represented as a chiral superfield S or as a linear superfield L [30, 33, 38, 43, 55]. While the former is very prevalent in the literature, in the context of string theory the dilaton ℓ is the lowest component of a vector superfield L which includes the degrees

of freedom of the dilaton and of the antisymmetric tensor present among the massless string modes, and which satisfies the modified linearity condition

$$-(\overline{\mathcal{D}}^2 - 8R)L = W^\alpha W_\alpha, \quad -(\mathcal{D}^2 - 8\overline{R})L = \overline{W}_{\dot\alpha}\overline{W}^{\dot\alpha}, \tag{1.12}$$

where the superfield R is related to elements of the supervielbein as mentioned in Section 1.2, W^α is a Yang-Mills superfield strength, and the summation over gauge indices is suppressed. The Bianchi identity

$$(\mathcal{D}^2 - 24\overline{R})W^\alpha W_\alpha - (\overline{\mathcal{D}}^2 - 24R)\overline{W}_{\dot\alpha}\overline{W}^{\dot\alpha} = \text{total derivative} \tag{1.13}$$

follows immediately from (1.12) – an important constraint when we eventually modify (1.12) to include the presence of gaugino condensates in Section 5. The chiral multiplet formulation can be recovered by a duality transformation, at least at the classical level. However the linear multiplet formulation provides a simpler implementation of the Green-Schwarz anomaly cancellation mechanism and a better framework for constructing an effective Lagrangian for gaugino condensation, both of which will be addressed below.

In the weak coupling regime, the models that we consider have a simple tree level gauge kinetic function when written in the chiral formulation:

$$f_a(Z^n) = k_a S, \tag{1.14}$$

where S is the string dilaton and k_a is the affine level[1]. At tree level this chiral superfield is related to the string coupling constant at the string scale through the relation

$$\langle \mathrm{Re}\, s\rangle = \frac{1}{g^2_{\mathrm{STR}}(\Lambda_{\mathrm{STR}})}, \tag{1.15}$$

where $s = S|_{\theta=\bar\theta=0}$, and has a tree level Kähler potential given by $K(S,\overline{S}) \equiv k(S,\overline{S}) = -\ln(S+\overline{S})$. We will employ this chiral formulation when we wish to make contact with results found in the literature.

The calculation of various quantities in the Kähler $U(1)$ formalism is facilitated by placing the dilaton in the linear multiplet. At tree level the two formalisms can be related by $S+\overline{S} = 1/L$ so that the tree level dilaton Kähler potential can be written $k(L) = \ln L$. In the linear mutliplet formulation the string coupling constant is given by $g^2_{\mathrm{STR}}/2 = \langle \ell\rangle = \langle L|_{\theta=\bar\theta=0}\rangle$. As the dilaton determines the gauge coupling constants of the observable sector it is imperative that the field ℓ be stabilized at a finite field value. This is accomplished by appealing to nonperturbative corrections [16, 135] to the Kähler potential of string-theoretic origin. We will parameterize these corrections in the linear multiplet case by modifying the kinetic energy term in the Lagrangian and the dilaton Kähler potential by a pair of functions:

$$\mathcal{L}_{\mathrm{KE}} = \int \mathrm{d}^4\theta\, E\left[-2 + f(L)\right], \quad k(L) = \ln L + g(L), \tag{1.16}$$

which satisfy the conditions

$$Lg'(L) = f - Lf'(L), \quad g(0) = f(0) = 0, \tag{1.17}$$

[1]From now on, we will only consider affine level one nonabelian gauge groups *i.e.* $k = 1$ ($k = 5/3$ for the abelian group $U(1)_Y$ of the Standard Model).

which ensure that the Einstein term of the gravity action has canonical form [27], and that they vanish in the weak coupling limit: $g^2/2 = \langle \ell \rangle = \langle V|_{\theta=\bar{\theta}=0} \rangle \to 0$. In the presence of such corrections the string coupling constant is given by a modified relation

$$g^2_{\rm STR}(\Lambda_{\rm STR}) = 2\,\langle \ell \rangle \,/\, (1 + f(\ell))\,. \tag{1.18}$$

In Appendix A we give the correspondence between various terms in the component Lagrangian in the chiral and linear multiplet formalisms.

In addition to the dilaton all of the orbifold compactification models we will consider here contain a set of moduli fields which parameterize the string compactification. The size of the compact dimensions are determined by the vacuum expectation values of a set of three complex fields T^α with $\alpha = 1, 2, 3$. The Kähler potential for these moduli is known at the tree level from the underlying string theory, and we can include the entire string moduli sector in the expression

$$K(S,T) = k(S+\overline{S}) - \sum_{\alpha=1}^{3} \ln\left(T^\alpha + \overline{T}^\alpha\right) = k(S+\overline{S}) + \sum_\alpha g^\alpha, \tag{1.19}$$

with $g^\alpha \equiv -\ln(T^\alpha + \overline{T}^\alpha)$.

Of central importance at the perturbative level are the diagonal modular transformations:

$$T^\alpha \to \frac{aT^\alpha - ib}{icT^\alpha + d}, \quad ad - bc = 1, \;\; a,b,c,d \in \mathrm{Z}, \tag{1.20}$$

that leave the classical effective supergravity theory invariant. This symmetry is known to remain a symmetry of the underlying string theory to all orders in string perturbation theory, so it must remain a perturbative symmetry in our low energy effective theory. This is one of the key constraints imposed on our supergravity models and we will refer to the symmetry with the words "modular invariance." Under the transformation (1.20) the fields of the theory transform as follows:

$$\begin{aligned} g^\alpha &\to F^\alpha + \overline{F}^\alpha, \quad F^\alpha = \ln(icT^\alpha + d), \quad \Phi^A \to e^{\sum_\alpha F^\alpha n^\alpha_A}\Phi^A, \\ \lambda_a &\to e^{-\frac{i}{2}\sum_\alpha \mathrm{Im}F^\alpha}\lambda_a, \quad \theta \to e^{-\frac{i}{2}\sum_\alpha \mathrm{Im}F^\alpha}\theta. \end{aligned} \tag{1.21}$$

Thus a matter field which transforms as

$$Z^A \to (icT^\alpha + d)^{n^\alpha_A} Z^A \tag{1.22}$$

under the modular transformations (1.20) is said to have a *modular weight* of n^α_A.

To preserve the classical modular invariance both the Kähler potential and superpotential for the matter terms must be modified to include functions of the moduli. We will assume for the simplicity of the expressions which follow that the Kähler metric for the matter fields Z^i has the form:

$$K_{i\bar{j}} = \kappa_i(Z^n)\delta_{i\bar{j}} + \mathcal{O}(|Z^i|^2), \tag{1.23}$$

and a matter field with modular weight n^α_i has

$$\kappa_i = \prod_\alpha (T^\alpha + \overline{T}^\alpha)^{n^\alpha_i}. \tag{1.24}$$

Because (1.20) has the form of a Kähler transformation (1.7) on (1.19), it is necessary to ensure that the superpotential transforms as

$$W(Z^M) \to W(Z^M) \prod_\alpha (icT^\alpha + d)^{-1}, \tag{1.25}$$

so the moduli dependence of the superpotential for the matter fields can be determined. If we denote $W_{ijk} = \partial^3 W(z^M)/\partial z^i \partial z^j \partial z^k$ then we must have

$$W_{ijk} = \lambda_{ijk} \prod_\alpha [\eta(T^\alpha)]^{2(1+n_i^\alpha+n_j^\alpha+n_k^\alpha)}, \tag{1.26}$$

where $\eta(T)$ is the classical Dedekind function:

$$\eta(T) = e^{-\pi T/12} \prod_{n=1}^{\infty} (1 - e^{-2\pi n T}), \tag{1.27}$$

which transforms as

$$\eta(T^\alpha) \to (icT^\alpha + d)^{-1/2} \eta(T^\alpha) \tag{1.28}$$

under the modular transformation (1.20). We will also use in the following the Riemann zeta function:

$$\zeta(T) = \frac{1}{\eta(T)} \frac{\mathrm{d}\eta(T)}{\mathrm{d}T}. \tag{1.29}$$

Let us note that the non-holomorphic Eisenstein function

$$\hat{G}_2(T,\overline{T}) \equiv -2\pi \left(2\zeta(T) + \frac{1}{T+\overline{T}}\right) \equiv -2\pi G_2(T,\overline{T}), \tag{1.30}$$

vanishes at the self-dual points $T = 1$ and $T = e^{i\pi/6}$.

From (1.21) we can see that the chiral superfields Φ^A receive a chiral phase rotation, so we would expect that this modular transformation would possess an anomaly. That is in fact the case at the quantum level [6, 39, 54, 59, 87, 110, 121], so modular invariance must be restored by an appropriate choice of local counterterms. There are two sources of such terms arising from string theory: the universal Green-Schwarz (GS) counterterm [39, 54] and model-dependent string threshold corrections [6, 59].

The Green-Schwarz counterterm has the following form

$$\mathcal{L}_{\mathrm{GS}} = \int \mathrm{d}^4\theta \, E L V_{\mathrm{GS}}, \tag{1.31}$$

in the linear multiplet formalism [38, 26] where the real function V_{GS} reads:

$$V_{\mathrm{GS}} = \frac{\delta_{\mathrm{GS}}}{24\pi^2} \sum_\alpha \ln\left(T^\alpha + \overline{T}^\alpha\right) + \sum_i p_i \prod_\alpha \left(T^\alpha + \overline{T}^\alpha\right)^{n_i^\alpha} |\phi^i|^2 + \mathcal{O}\left(\phi^4\right). \tag{1.32}$$

The group-independent factor δ_{GS} is simply equal to $-3C_{E_8}$, where $C_{E_8} = 30$ is the Casimir operator of the group E_8 in the adjoint representation, if there are no Wilson lines. Otherwise,

it can be smaller in magnitude. The coefficients p_i represent the couplings of the observable sector fields to the Green-Schwarz counterterm. They are *a priori* unknown model-dependent variables, though they are (in principle) calculable in the underlying string theory. The string threshold corrections can be thought of as corrections to the string gauge coupling constant due to string states above the compactification scale and take the form

$$\mathcal{L}_{\rm th} = -\frac{1}{64\pi^2}\sum_\alpha \int \mathrm{d}^4\theta \frac{E}{R} \ln \eta^2(iT^\alpha) \left(\sum_a b_a^\alpha (W^\alpha W_\alpha)_a \right) + \text{ h.c. }. \tag{1.33}$$

In the chiral multiplet formalism for the dilaton these terms can be thought of as corrections to the gauge kinetic functions f_a in (1.14). The parameters b_a^α vanish for orbifold compactifications with no $\mathcal{N} = 2$ supersymmetry sector [6].

Chapter 2

Soft Supersymmetry Breaking at One Loop

2.1 Quantum-Induced Soft Supersymmetry Breaking

The points we wish to emphasize in the Pauli-Villars (PV) calculation given here are (1) the presence in general of $\mathcal{O}(M_{3/2})$ contributions to the scalar masses that are proportional to the chiral supermultiplet γ-function (rather than its derivative, which is a two loop effect), and (2) the difference between gaugino masses and soft terms in the scalar potential with respect to dependence on the details of Planck scale physics. To this end we will present our calculations under the simplifying assumption that the Pauli-Villars squared-mass matrix commutes with other operators that are relevant to quantum corrections. We further restrict our analysis to one loop order and retain only terms of lowest order in $M_{3/2}/M_{\rm PL}$, where $M_{3/2}$ and $M_{\rm PL}$ are the gravitino mass and the reduced Planck mass, respectively. We then use our results to address the issue of anomaly mediated supersymmetry breaking [7, 93, 95, 131].

2.1.1 General Corrections to the Scalar Potential

The one loop logarithmic divergences of standard chiral supergravity were determined in [80, 81, 82], and it was shown in [77, 78, 79] that they can be regulated[1] by a set of Pauli-Villars chiral superfields Φ^A. As in these references we denote the light superfields by Z^i, and introduce covariant derivatives of the superpotential $W(Z^i)$ as follows:

$$\begin{aligned} A &= e^K W, \quad A_i = D_i A = \partial_i A, \quad A_{ij} = D_i D_j A = \partial_i \partial_j A - \Gamma^k_{ij} A_k, \\ \overline{A}^i &= K^{i\overline{m}} \overline{A}_{\overline{m}}, \quad \text{etc.}, \quad K_{i\overline{m}} = \partial_i \partial_{\overline{m}} K(Z^i, \overline{Z}^{\overline{m}}), \quad \partial_i = \frac{\partial}{\partial Z^i}, \end{aligned} \tag{2.1}$$

where Γ^k_{ij} is the affine connection associated with the Kähler metric $K_{i\overline{m}}$ and its inverse $K^{i\overline{m}}$. In the regulated theory, the one loop correction to the chiral multiplet Kähler potential is given by [79] the superfield operator (up to a Weyl transformation necessary to put the Einstein term

[1] The full regulation of gravity loops requires the introduction of Abelian gauge superfields as well; these play no role here and we ignore them.

in canonical form[2])

$$\Delta L = -\frac{1}{32\pi^2}\int \mathrm{d}^4\theta\, E\, e^{-K}\sum_{AB}\eta_A \overline{A}^{AB} A_{AB}\ln(m_A^2/\mu^2) = \int \mathrm{d}^4\theta\, E\,\delta K(Z^i,\overline{Z}^{\overline{m}}), \tag{2.2}$$

where $A_{AB}(Z^i,\overline{Z}^{\overline{m}})$ is defined as in (2.1), with the light field indices i,j replaced by PV indices A,B, $\eta_A = \pm 1$ is the PV signature, m_A is the (supersymmetric) PV mass, and μ is the (scheme-dependent) normalization point. The wave function renormalization matrix is given by

$$\begin{aligned}\gamma_i^j &= \left\langle K^{j\bar{n}} D_{\bar{n}} D_i \frac{\partial}{\partial \ln\mu^2}\delta K\right\rangle = \frac{1}{32\pi^2}\left\langle D^j D_i \sum_{AB}\eta_A (e^{-K}\overline{A}^{AB} A_{AB})\right\rangle \\ &= \frac{1}{32\pi^2}\left\langle e^{-K}\sum_{AB}\eta_A \overline{A}^{jAB} A_{iAB}\right\rangle + \cdots ,\end{aligned} \tag{2.3}$$

where here and throughout ellipses represent terms of higher dimension.

The regulation of matter and Yang-Mills loop contributions to the matter wave function renormalization requires the introduction of PV chiral superfields $\Phi^A = \Phi^i, \widehat{\Phi}^i$ and Φ^a which transform according to the chiral matter, anti-chiral matter and adjoint representations of the gauge group and have signatures $\eta_A = -1, +1, +1$, respectively. These fields couple to the light fields through the superpotential[3]

$$W(\Phi^A, Z^i) = \frac{1}{2}W_{ij}(Z^k)\Phi^i\Phi^j + \sqrt{2}\Phi^a\widehat{\Phi}_i(T_a Z)^i + \cdots , \tag{2.4}$$

where T_a is a generator of the gauge group, and their Kähler potential takes the schematic form

$$K_{\mathrm{PV}} = \sum_A \kappa_A\left(Z^N\right)|\Phi^A|^2, \tag{2.5}$$

where the functions κ_A are functions of the hidden sector (moduli) fields as defined by (1.23).

We are interested here in string-derived models which are modular invariant and we wish the quantum corrected theory to be perturbatively invariant under the modular transformation (1.20) as well. This can be achieved if the couplings of the relevant PV fields are modular invariant. For the fields $\Phi^i, \Phi^a, \widehat{\Phi}^i$ that contribute to the renormalization of the Kähler potential we then know that their dependence on the dilaton and T-moduli must be identical in form to the light observable sector fields whose loops they regulate. Therefore we can separate the function κ_A into a piece dependent on the dilaton and a piece dependent on the moduli fields. Then we have [77, 78, 79] for typical orbifold models,

$$\begin{cases} \Phi^i: & \kappa_i^\Phi = \kappa_i = \prod_\alpha (T^\alpha + \overline{T}^\alpha)^{n_i^\alpha}, \\ \widehat{\Phi}^i: & \hat{\kappa}_i^\Phi = \kappa_i^{-1}, \\ \Phi^a: & \kappa_a^\Phi = g_a^{-2}e^K = g_a^{-2}e^k \prod_\alpha (T^\alpha + \overline{T}^\alpha)^{-1}. \end{cases} \tag{2.6}$$

[2]This brings in terms with factors of V_{tree} that we neglect since if $\langle V_{\mathrm{tree}}\rangle = 0$, they can at most give small corrections to the tree level soft terms.

[3]Full regulation of the theory requires several copies of fields with the same gauge quantum numbers, and the coupling parameters and signatures given here actually represent weighted average values.

With these choices, the ultraviolet divergences cancel, and, for the leading (lowest dimension) contribution, one obtains the standard result for the matter wave function renormalization in the supersymmetric gauge [18]

$$\gamma_i^j = \frac{1}{32\pi^2} e^K \sum_{AB} \eta_A W_{iAB} \overline{W}^{jAB} = \frac{1}{32\pi^2} \left[4\delta_i^j \sum_a g_a^2 (T_a^2)_i^i - e^K \sum_{kl} W_{ikl} \overline{W}^{jkl} \right]. \tag{2.7}$$

The matrix (2.7) is diagonal in the approximation in which generation mixing is neglected in the Yukawa couplings; in practice only the $T^c Q_3 H_u$ Yukawa coupling is important. We will make this approximation in the following, and set

$$\begin{aligned} \gamma_i^j &\approx \gamma_i \delta_i^j, \quad \gamma_i = \gamma_i^W + \gamma_i^g, \quad \gamma_i^W = \sum_{jk} \gamma_i^{jk}, \quad \gamma_i^g = \sum_a \gamma_i^a, \\ \gamma_i^a &= \frac{g_a^2}{8\pi^2} (T_a^2)_i^i, \quad \gamma_i^{jk} = -\frac{e^K}{32\pi^2} (\kappa_i \kappa_j \kappa_k)^{-1} |W_{ijk}|^2 . \end{aligned} \tag{2.8}$$

The Lagrangian (2.2) generally contains soft supersymmetry breaking terms, displayed below, that are proportional to those of the tree level Lagrangian. What are usually referred to as "anomaly mediated" soft supersymmetry breaking terms are finite contributions that are not remnants, like (2.2), of the ultraviolet divergences. To evaluate such terms in the framework of PV regularization, we must retain all contributions that do not vanish in the limit $m_A^2 \to \infty$. Here we are interested in the scalar potential, given by

$$\begin{aligned} \mathcal{L} &= \frac{i}{2} \int \frac{d^4 p}{(2\pi)^4} \mathrm{STr}\, \eta \ln \left(p^2 - m^2 - H \right) \\ &= -\frac{1}{32\pi^2} \mathrm{STr}\, \eta \left[\left(h m^2 + \frac{1}{2} g^2 \right) \ln(m^2) + \frac{1}{2} h^2 \ln \left(\frac{m^2}{\mu^2} \right) + \frac{H^3}{6m^2} - \frac{H^4}{24 m^4} \right] \\ &\quad + \mathcal{O}\left(\frac{1}{m^2} \right), \end{aligned} \tag{2.9}$$

where H is the effective field-dependent squared mass with the supersymmetric PV mass matrix m^2 separated out:

$$H_{\mathrm{PV}} = H + m^2, \quad H = h + g, \quad h \sim m^0, \quad g \sim m^1. \tag{2.10}$$

The terms in (2.9) proportional to $\ln(m^2/\mu^2)$ are the bosonic part of (2.2). The first term in (2.9) proportional to m^2 is the remnant of the quadratically divergent contribution [77, 78]. It is completely controlled by Planck scale physics, and can be made to vanish with appropriate conditions on m^2. If it is present it contains A-terms and scalar masses proportional to the tree potential soft terms with coefficients suppressed by $1/32\pi^2$; we neglect it in the following.

The PV loops contribute soft supersymmetry breaking terms to the light field effective Lagrangian if the PV tree Lagrangian contains such terms. In the presence of supersymmetry breaking one generally expects the matrix g in (2.10) which is linear in m to contain "B-terms". Indeed it is these B-terms that generate the "anomaly mediated" contributions to the gaugino masses and the A-terms of the light theory[4] that have been discussed in the literature [93, 128, 131]. As we shall see below, there are two contributions to supersymmetry

[4]There may also be B-terms generated at one loop in the light theory if there are quadratic holomorphic terms in its tree level superpotential or Kähler potential. These contributions were considered in [79]; we ignore them and use the expression "B-term" to designate the B-term proportional to the PV mass.

breaking scalar masses that arise from a double B-term insertion in a Feynman diagram. These two contributions cancel, resulting in the assertion [128, 131] that there is no anomaly mediated contribution to scalar masses at one loop. However, there can in general be soft masses and A-terms in the matrix h in (2.10). In leading order in $M_{3/2}^2/\mu^2$, A-terms are present in the PV part of h only if there are dimension-three soft supersymmetry breaking operators in the tree Lagrangian. Soft PV mass terms, which in leading order contribute only to scalar masses, are not similarly restricted by the low energy theory. Specifically, if the regulator masses are constant there are always soft squared-mass terms in the PV sector.

The PV mass for each superfield Φ^A is generated by coupling it to a field Π^A in the representation of the gauge group conjugate to that of Φ^A through the superpotential term

$$W_m = \sum_A \mu_A\left(Z^N\right)\Phi^A\Pi^A, \tag{2.11}$$

where $\mu_A\left(Z^N\right)$ can in general be a holomorphic function of the light superfields. There is no constraint on the Kähler potential for the fields Π^A similar to those of the Φ^A allowing us to determine the analogous expressions to (2.6). We will set, for $\Pi^A = (\Pi^i, \widehat{\Pi}^i, \Pi^a)$,

$$\Pi^A: \quad \kappa_A^{\Pi} = h_A(S+\overline{S})\prod_\alpha (T^\alpha + \overline{T}^\alpha)^{q_A^\alpha}, \tag{2.12}$$

and then the functions $\mu_A(Z^N)$, and therefore the PV masses, are fixed up to a constant by modular covariance. Note that the modular weights of the fields Π^A which are given by q_A^α are not necessarily related to those of the fields of the observable sector and thus represent an undetermined set of parameters in the theory. Now with PV Kähler potential given by (2.5), (2.6) and (2.12) and the superpotential (2.11) we have explicitly

$$m_A^2 = e^K(\kappa_A^\Phi)^{-1}(\kappa_A^\Pi)^{-1}|\mu_A|^2, \tag{2.13}$$

which we also have occasion to write in the form

$$m_A^2 = m_\alpha^2 = f_A\mu_A^2, \quad f_A = e^K(\kappa_A^\Phi)^{-1}(\kappa_A^\Pi)^{-1}. \tag{2.14}$$

The general field-dependent matrix H in (2.9) has been evaluated in [80, 81, 82]. Denoting by H^χ and H^ϕ the matrices H in (2.10) for fermions and bosons, respectively, we have, with constant background fields,

$$\begin{aligned} H^\chi &= h^\chi + \frac{r}{4}, \quad (h^\chi)_B^A = e^{-K}A_{BC}\overline{A}^{AC}, \quad (h^\chi)_\beta^\alpha = 0, \\ (h^\chi)_D^\alpha &= K^{\alpha\bar\beta}\mu_B K^{\overline{B}C}A_{CD} = g_D^\alpha = e^{-K}f_A\mu_{A\alpha}A_{AD}, \\ (h^\chi)_\beta^A &= \overline{A}^{AB}\mu_B = g_\beta^A, \quad H^\phi = h^\chi + \widehat{V} + M_{3/2}^2 + R, \end{aligned} \tag{2.15}$$

where $M_{3/2}^2 = e^K|W|^2$, $\widehat{V} = e^{-K}A_j\overline{A}^j - 3M_{3/2}^2$. The last term in (2.15) depends on the curvature of the PV metric:

$$R_B^A = R_{B\overline{m}i}^A e^{-K}A^{\overline{m}}\overline{A}^i = -\delta_{AB}F^i\overline{F}^{\overline{m}}\partial_{\overline{m}}\left(\kappa_A^{-1}\partial_i\,\kappa_A\right) = -\delta_{AB}F^i\overline{F}^{\overline{m}}\partial_{\overline{m}}\partial_i\ln\kappa_A, \quad A = \Phi^A, \Pi^A, \tag{2.16}$$

where $F^i = -e^{-K/2}\overline{A}^i$ is the auxiliary field of the supermultiplet Z^i. Terms involving the space-time curvature r are replaced by terms proportional to the tree potential V after a Weyl transformation that restores the one loop corrected Einstein term to canonical form. We assume throughout a vanishing cosmological constant, $\langle V\rangle = 0$, so we can drop them. Similarly, we can drop $\widehat{V}$ if D-terms vanish in the vacuum: $V = \widehat{V} + \mathcal{D}$, $\mathcal{D} = \frac{1}{2}g^2\sum_a D_a^2$, $(T^a z)^i K_i$, $z^i = Z^i|$, $\langle D_a\rangle = 0$. Terms containing only powers of h^X cancel in the supertrace, so we get contributions only from scalar trace terms that include the scalar mass term $M_{3/2}^2 + R$ in (2.15) or factors of $H_{XY} = K_{X\overline{X}}H_Y^{\overline{X}}$:

$$\begin{aligned} H_{AB} &= h_{AB} = e^{-K}\left(\overline{A}^i D_i A_{AB} - A_{AB}\overline{A}\right), \quad h_{\alpha\beta} = 0, \\ H_{A\beta} &= g_{A\beta} = e^{-K}\overline{A}^i D_i\left(e^K W_{A\beta}\right) - \overline{A}W_{A\beta} = -\delta_{A\beta}\mu_{A\alpha}\left(\overline{A} - \overline{A}^i\partial_i \ln f_A\right). \end{aligned} \tag{2.17}$$

$H_{A\alpha}$ is the B-term mentioned above, and the part of h_{AB} linear in $z^i - \langle z^i\rangle$ is the A-term.

2.1.2 Trilinear A-terms

Neglecting B-terms in the tree Lagrangian, the leading contribution to W_{AB} is linear in a gauge nonsinglet field Z^i. Explicitly expanding H_{AB} gives

$$H_{AB} = e^K K^{i\bar{j}}\overline{W}_{\bar{j}}W_{iAB} - e^{K/2}F^n\partial_n \ln(\kappa_i\kappa_A\kappa_B e^{-K})z^i W_{iAB}. \tag{2.18}$$

The second term in (2.18) is the A-term where $\langle F^n\rangle \neq 0$ with Z^n a gauge singlet in the supersymmetry breaking sector. Assuming that the matter superpotential is independent of Z^n, the tree-level A-terms are given by

$$\langle\partial_i\partial_j\partial_k V\rangle = A_{ijk}\left\langle e^{K/2}W_{ijk}\right\rangle, \quad A_{ijk} = \left\langle F^n\partial_n \ln(\kappa_i\kappa_j\kappa_k e^{-K})\right\rangle, \tag{2.19}$$

and the tree level gaugino masses are given by

$$M_a = \frac{1}{2}\left\langle F^n\partial_n \ln(g_a^{-2})\right\rangle. \tag{2.20}$$

Using the couplings given in (2.4), we have

$$F^n\partial_n \ln(\kappa_i\kappa_{\Phi^J}\kappa_{\Phi^K}e^{-K}) = A_{ijk}, \quad F^n\partial_n \ln(\kappa_i\kappa_{\widehat{\Phi}^I}\kappa_{\Phi^a}e^{-K}) = 2M_a. \tag{2.21}$$

Then we obtain

$$\begin{aligned} \mathrm{Tr}\eta h^2 &\ni 2\sum_{AB}\eta_A h_{AB}h^{AB} \ni -2e^{3K/2}W_j z^i\sum_{AB}\eta_A W_{iAB}\overline{W}^{jAB}F^n\partial_n \ln(\kappa_j\kappa_A\kappa_B e^{-K}) + \text{h.c.} \\ &= -64\pi^2 e^{K/2}W_i z^i\left[\sum_{jk}\gamma_i^{jk}A_{ijk} + 2\sum_a \gamma_a^i M_a\right] + \text{h.c.}, \end{aligned} \tag{2.22}$$

for the leading contribution to the A-term from the second term in (2.9), *i.e.* the contribution from the shift in the potential due to the shift in the Kähler potential. The leading order

contribution to the "anomaly-induced" A-term arises from a PV loop diagram with one B-term insertion:

$$
\begin{aligned}
\mathrm{Tr}\eta\frac{H^3}{6m^2} &\ni \mathrm{Tr}\eta\frac{hg^2}{2m^2} \ni \sum_{AB}\frac{\eta_A}{2m_A^2}h^A_{\overline{B}}\left(g^{\overline{B}}_{\gamma}g^{\gamma}_A + g^{\overline{B}}_{\bar{\gamma}}g^{\bar{\gamma}}_A\right) + \text{ h.c.} \\
&\ni -32\pi^2 e^{K/2}W_i z^i\left[\gamma_i M_{3/2} + F^n\partial_n\left(\sum^a \gamma_i^a \ln f_{ia} + \sum_{jk}\gamma_i^{jk}\ln f_{jk}\right)\right] + \text{ h.c.}\,, \\
f_{AB} &= \sqrt{f_A f_B}, \quad f_{jk} = \sqrt{f_{Z^J}f_{Z^K}}, \quad f_{ia} = \sqrt{f_{\varphi^a}f_{Y_I}},
\end{aligned}
\tag{2.23}
$$

which reduces to the "anomaly mediated term" found in [93] provided that $\langle F^n\partial_n \ln f_A\rangle = 0$. We discuss below the circumstances under which this is the case. The full leading-order A-term Lagrangian is

$$
\begin{aligned}
\mathcal{L}_A &= e^{K/2}\sum_i W_i z^i\Big[\gamma_i M_{3/2} + \sum_a \gamma_i^a\left(2M_a\ln(m_{ia}^2/\mu^2) + F^n\partial_n\ln f_{ia}\right) \\
&\quad + \sum_{jk}\gamma_i^{jk}\left(A_{ijk}\ln(m_{jk}^2/\mu^2) + F^m\partial_n\ln f_{jk}\right)\Big] + \text{ h.c. } + \cdots, \\
m_{AB}^2 &= m_A m_B, \quad m_{jk}^2 = m_{\Phi^J}m_{\Phi^K}, \quad m_{ia}^2 = m_{\Phi^a}m_{\widehat{\Phi}^I}.
\end{aligned}
\tag{2.24}
$$

2.1.3 Scalar Masses

Scalar masses get a contribution from the term quartic in H:

$$
\begin{aligned}
\mathrm{Tr}\eta\frac{H^4}{24m^2} &\ni \mathrm{Tr}\eta\frac{g^4}{24m^2} \\
&\ni \sum\frac{\eta_A}{12m_A^2}\left[2\left(g^A_\beta g^\beta_C g^C_{\bar{\delta}} g^{\bar{\delta}}_A + g^\alpha_B g^B_\gamma g^\gamma_{\overline{D}} g^{\overline{D}}_\alpha\right) + g^A_\beta g^\beta_{\overline{C}} g^{\overline{C}}_{\bar{\delta}} g^{\bar{\delta}}_A + g^\alpha_B g^B_{\bar{\gamma}} g^{\bar{\gamma}}_{\overline{D}} g^{\overline{D}}_\alpha\right] + \text{ h.c.} \\
&\ni e^{-K}\sum_{AB}\eta_A|M_{3/2} + F^i\partial_i\ln f_A|^2 A_{AB}\overline{A}^{AB},
\end{aligned}
\tag{2.25}
$$

which corresponds to two B-term insertions in the PV loop. The contribution from the cubic term is

$$
\begin{aligned}
\mathrm{Tr}\eta\frac{hg^2}{2m^2} &\ni \frac{1}{2}\sum_{AB}\eta_A h^A_{\overline{B}}\left[g^{\overline{B}}_\beta g^\beta_A\frac{1}{m_B^2} + g^{\overline{B}}_{\bar{\alpha}} g^{\bar{\alpha}}_A\frac{1}{m_A^2}\right] \\
&\quad + \frac{1}{2}M_{3/2}^2\sum_{AB}\eta_A g^A_\beta g^\beta_A\left(\frac{1}{m_B^2} + \frac{1}{m_A^2}\right) \\
&\quad - \frac{1}{2}\sum_{AB}\eta_A g^A_\beta g^\beta_A\left(\frac{1}{m_B^2}F^n\overline{F}^{\overline{m}}\partial_n\partial_{\overline{m}}\ln g_\beta + \frac{1}{m_A^2}F^n\overline{F}^{\overline{m}}\partial_n\partial_{\overline{m}}\ln g_A\right) \\
&\quad + \frac{1}{2}\sum_B \eta_B m_B^{-2} g_{B\beta}g^{B\beta}h^B_B + \text{ h.c.}
\end{aligned}
$$

$$\begin{aligned}
\mathrm{Tr}\eta\frac{hg^2}{2m^2} \ni\ & \frac{1}{2}e^{-K}\sum_{AB}\eta_A\left[F^n\partial_n\ln\left(\kappa_i\kappa_A\kappa_B e^{-K}\right)\right]\left(M_{3/2}+\overline{F}^{\overline{m}}\partial_{\overline{m}}\ln f_B\right)z^iA_{iAB}\overline{A}^{AB}\\
&+\frac{1}{2}e^{-K}\sum_{AB}\eta_A A_{AB}\overline{A}^{AB}\left(F^n\overline{F}^{\overline{m}}\partial_n\partial_{\overline{m}}\ln f_A-M_{3/2}^2\right)\\
&+\frac{1}{2}e^{-K}\sum_{AB}\eta_A A_{AB}\overline{A}^{AB}|M_{3/2}+\overline{F}^{\overline{m}}\partial_{\overline{m}}\ln f_B|^2+\ \text{h.c.}\ ,
\end{aligned}\tag{2.26}$$

where we used the vacuum condition (1.4). The last term in (2.26) is a double B-term insertion; it cancels (2.25) in the Lagrangian (2.9). The first term on the right hand side of (2.26) corresponds to one B-term and one A-term insertion, and the second term corresponds to a PV soft squared-mass insertion. Explicitly,

$$F^n\overline{F}^{\overline{m}}\partial_n\partial_{\overline{m}}\ln f_A-M_{3/2}^2=\mu_{\Phi^A}^2+\mu_{\Pi^A}^2,\tag{2.27}$$

where

$$\mu_A^2=M_{3/2}^2-F^n\overline{F}^{\overline{m}}\partial_n\partial_{\overline{m}}\ln\kappa_A,\quad A=\Phi^A,\Pi^A\tag{2.28}$$

is the soft supersymmetry breaking squared mass of the field Φ^A or Π^A. For $A\to\Phi^A$ the masses are determined by the supersymmetry breaking masses of the tree Lagrangian

$$\mu_{\Phi^I}^2=\mu_{z^i}^2\equiv\mu_i^2,\quad \mu_{\widehat{\Phi}^I}^2=2M_{3/2}^2-\mu_i^2,\quad \mu_{\Phi^a}^2=-2M_{3/2}^2-M_a^2,\tag{2.29}$$

so these terms give no contribution if $\mu_i=M_a=0$. However, even if no soft supersymmetry breaking masses are present in the tree Lagrangian, one cannot *a priori* exclude such terms in the theory above the effective cut-off, that could be reflected in soft supersymmetry breaking masses $\mu_{\Pi^A}^2$ in the PV sector that parameterizes the underlying Planck scale physics. Finally we have

$$\begin{aligned}
\mathrm{Tr}h^2 \ni\ & 2\sum_{AB}\eta_A\left(H_B^AH_A^B+H_{AB}H^{AB}\right)\\
\ni\ & 2e^{-K}\sum_{AB}\eta_A\Big[2\mu_A^2\overline{W}^{AB}W_{AB}\\
&+z^i\bar{z}^{\bar{j}}F^n\overline{F}^{\overline{m}}\left(\partial_n\ln(\kappa_i\kappa_A\kappa_Be^{-K})\right)\left(\partial_{\overline{m}}\ln(\kappa_j\kappa_A\kappa_Be^{-K})\right)\overline{W}_{\bar{j}}^{AB}W_{iAB}\Big],
\end{aligned}\tag{2.30}$$

for the part of the renormalization of the Kähler potential that contributes to scalar masses. Using (2.21) and (2.27)–(2.29), the full scalar mass term is

$$\begin{aligned}
\mathcal{L}_m\ =\ & \sum_i|z^i|^2\Bigg(M_{3/2}^2\gamma_i+\sum_a\gamma_i^a\left\{\left(3M_a^2-\mu_i^2\right)\ln(m_{ia}^2/\mu^2)\right.\\
&\left.+F^n\overline{F}^{\overline{m}}\partial_{\overline{m}}\partial_n\ln f_{ia}+M_a\left[\left(\overline{F}^{\overline{m}}\partial_{\overline{m}}+F^n\partial_n\right)\ln f_{ia}+2M_{3/2}\right]\right\}\\
&+\sum_{jk}\gamma_i^{jk}\Bigg\{\left(\mu_j^2+\mu_k^2+A_{ijk}^2\right)\ln(m_{jk}^2/\mu^2)+F^n\overline{F}^{\overline{m}}\partial_{\overline{m}}\partial_n\ln f_{jk}\\
&\qquad+\frac{1}{2}A_{ijk}\left[\left(\overline{F}^{\overline{m}}\partial_{\overline{m}}+F^n\partial_n\right)\ln f_{jk}+2M_{3/2}\right]\Bigg\}\Bigg)+\cdots.
\end{aligned}\tag{2.31}$$

In the absence of tree level soft supersymmetry breaking, this expression reduces to the first ("universal") term if $\left\langle F^n \overline{F}^{\overline{m}} \partial_n \partial_{\overline{m}} f_A \right\rangle = 0$.

The soft supersymmetry breaking Lagrangian for the canonically normalized scalars ϕ_R is obtained by making the substitution $\phi^i = g_i^{-\frac{1}{2}} \phi_R^i$ in $\mathcal{L}_A + \mathcal{L}_m$. For completeness and comparison we give the result for the one loop induced (left-handed) gaugino mass [13, 86] under the same assumptions used here to calculate $\mathcal{L}_A + \mathcal{L}_m$:

$$\begin{aligned}
\Delta M_a &= -\frac{g_a^2(\mu)}{16\pi^2}\left[(3C_a - C_a^M)M_{3/2} + \sum_X \eta_X C_a^X F^n \partial_n \ln f_X\right] + \cdots \\
&= -\frac{g_a^2(\mu)}{16\pi^2}\left[(3C_a - C_a^M)M_{3/2} + C_a F^n \partial_n K - \sum_i F^n C_a^i \partial_n \ln f_i\right] + \cdots, \\
f_i &= \kappa_i^{-2} e^K,
\end{aligned} \tag{2.32}$$

where C_a, C_a^X and C_a^i are the quadratic Casimirs in the adjoint of the gauge subgroup $\mathcal{G}_a$ and in the representations of Φ^X and Z^i respectively, with $C_a^M = \sum_i C_a^i$. The second equality in (2.32) follows from the requirements of finiteness [77, 78] and supersymmetry [87] of the chiral/conformal anomaly proportional to the squared gauge field strength.

2.2 Comparison to Anomaly Mediated Results

In this section we wish to focus our attention on those parts of the one loop result found in Section 2.1 which are "universal" in their nature – that is, which depend only on the gravitino mass $M_{3/2}$, anomalous dimensions and β-function coefficients. Since the super-Weyl anomaly is associated with the Kähler transformation (1.20), which is explicitly canceled in models that ensure modular invariance one might expect the mass terms found in [93, 131] that arise from the super-Weyl anomaly to be absent in this class of models. However, this term has its origin in the running of the couplings from the string scale to the scale of supersymmetry breaking, and is therefore independent of the string scale physics. In addition, we found a contribution that depends on the unknown couplings of matter fields in the GS term.

2.2.1 Gaugino Masses vs. Scalar Potential Quantities

The one loop contributions to A-terms (and to scalar masses and B-terms discussed below) are considerably more sensitive to the details of Planck scale physics than the gaugino masses. The most straightforward way to regulate an effective theory is by introducing heavy fields – such as the Pauli-Villars fields – with masses of the order of the effective cut-off, and couplings to light fields chosen so as to cancel quadratic divergences. The PV masses can be interpreted as parameterizing effects of the underlying theory. These masses are to some extent constrained by supersymmetry. These constraints are much more powerful in determining the loop-corrected gaugino masses than the other soft parameters, for the reasons that follow.

All gauge-charged PV fields contribute to the vacuum polarization and to the gaugino masses. Their gauge-charge weighted masses are constrained by finiteness and supersymmetry to give the result in (2.32). The superfield operator that corresponds to these terms is the same one that

contains the field theory chiral and conformal anomalies under Kähler transformations of the type (1.20), and is therefore completely determined by the chiral anomaly which is unambiguous. Specifically, the conformal and chiral anomalies are the real and imaginary part of an F-term operator; the former is governed by the field dependence of the PV masses that act as an effective cut-off and are determined by supersymmetry from the latter [87].

On the other hand, only a subset of charged PV fields Φ^A contribute to the renormalization of the Kähler potential, which determines the matter wave function renormalization and governs the loop corrections to soft parameters in the scalar potential. Their PV masses are determined by the product of the inverse metrics of these fields and of fields Π^A to which they couple in the PV superpotential to generate Planck scale supersymmetric masses, as well as by *a priori* unknown holomorphic functions $\mu_A(Z^N)$ of the light fields that appear in the PV superpotential. While the Kähler metrics of the Φ^A are determined by finiteness requirements, the metrics of the Π^A are arbitrary. In operator language, the conformal anomaly associated with the renormalization of the Kähler potential is a D-term; it is supersymmetric by itself and there is no constraint, analogous to the conformal/chiral anomaly matching in the case of gauge field renormalization with an F-term anomaly, on the effective cut-offs – or PV masses – for this term. As a consequence the soft terms in the scalar potential cannot be determined precisely in the absence of a detailed theory of Planck scale physics.

Relating this to the results of the previous section, unlike the expressions in (2.24) and (2.31) the leading one loop contribution to the gaugino masses (2.32) is completely determined by the low energy theory. In this case all gauge-charged PV fields Φ^X contribute, their mass matrix is block diagonal and commutes with the relevant operators, and the gauge-charge weighted masses are constrained to give the second equality in (2.32). Since the conformal anomaly associated with the renormalization of the Kähler potential is a D-term, it is supersymmetric by itself and there is no constraint analogous to the conformal/chiral anomaly matching in the case of gauge field renormalization with an F-term anomaly. As a consequence the "nonuniversal" terms appearing in $\mathcal{L}_A + \mathcal{L}_m$ cannot be determined precisely in the absence of a detailed theory of Planck scale physics.

2.2.2 No-Scale Models

As a check of our results, consider the "no-scale" model defined by

$$K = k(S) + G, \quad G = -3\ln(T + \overline{T} - \sum_i |\Phi^i|^2), \quad W = W(\Phi^i) + W(S), \tag{2.33}$$

which has no soft supersymmetry breaking in the observable sector Φ^i at tree level. If we regulate the theory so as to preserve the no-scale structure, we have $\kappa_{\Phi^A} = \kappa_{\Pi^A}$, and

$$f_A = f_i = h_i(s)e^{G/3}. \tag{2.34}$$

Then

$$\partial_t \ln f_A = \frac{1}{3}G_t, \quad \partial_{\bar{t}}\partial_t \ln f_A = \frac{1}{3}G_{t\bar{t}}. \tag{2.35}$$

Vanishing vacuum energy at tree level requires $F^s = 0$, so if $\langle\phi^i\rangle = 0$, $\phi^i = \Phi^i|_{\theta=\bar{\theta}=0}$, the no-scale Kähler potential satisfies

$$-F^n G_n = e^{K/2} W G_{\bar{t}} K^{\bar{t}t} G_t = 3M_{3/2}, \quad F^n \overline{F}^{\bar{m}} G_{n\bar{m}} = e^{K/2}|W|^2 G_{\bar{t}} K^{\bar{t}t} G_t = 3M_{3/2}^2, \tag{2.36}$$

and all the soft supersymmetry breaking terms, (2.24), (2.31) and (2.32), cancel, in agreement with explicit calculations [22] and nonrenormalization theorems [24] in the context of this type of model.

In one of the earlier papers related to "anomaly mediated" supersymmetry breaking, Randall and Sundrum [131] considered a class of models defined by a Kähler potential

$$K = -3\ln\left[1 - \sum_i |\Phi^i|^2 - f(Z^n, \overline{Z}^{\bar{m}})\right], \tag{2.37}$$

where the Φ^i represent gauge-charged matter, and the Z^n are in a hidden sector where supersymmetry is broken: $\langle\Phi^i\rangle = \langle F^i\rangle = 0$, $\langle F^n\rangle \neq 0$. For these models

$$\langle K_{i\bar{j}}\rangle = \left\langle e^{K/3}\delta_{i\bar{j}}\right\rangle = \kappa_i\delta_{i\bar{j}}, \quad \mu_i^2 = A_{ijk} = 0, \tag{2.38}$$

from the definitions (2.19) and (2.28) and the vacuum condition (1.4). In addition there is no dilaton: g_a = constant, $M_a = 0$, so there is no soft supersymmetry breaking in the tree Lagrangian. If we *assume* $\kappa_{\Phi A} = \kappa_{\Pi A}$, there are also no soft supersymmetry breaking parameters in the PV Lagrangian. Then the scalar masses indeed vanish at one loop, and we obtain:

$$\begin{aligned}
\ln f_{jk} &= g_a^{-1}\ln f_{ia} = \ln f_i = K/3, \\
\mathcal{L}_A &= -\frac{1}{32\pi^2}e^{K/2}W_i z^i\gamma_i\left(M_{3/2} + \frac{1}{3}F^n K_n\right) + \text{h.c.} + \cdots, \\
\Delta M_a &= -\frac{g_a^2(\mu)}{16\pi^2}(3C_a - C_a^M)\left(M_{3/2} + \frac{1}{3}F^n K_n\right) + \cdots.
\end{aligned} \tag{2.39}$$

To determine the model-dependent contribution proportional to $\langle F^n K_n\rangle$, we study the vacuum conditions $\langle V\rangle = \langle V_z\rangle = 0$ for the potential $V(z = Z|)$ derived from $W(Z)$ and $K(Z) = -3\ln[1 - f(Z)]$, with the gauge-charged fields Φ set to zero. This potential is classically invariant under the Kähler transformation

$$K(Z) \to K^\xi(Z) = K(Z) + \xi\ln|W(Z)|^2, \quad f^\xi = (1-f)|W|^{\frac{2\xi}{3}}, \quad W(Z) \to W^{1-\xi}(Z). \tag{2.40}$$

If one imposes a "separability" condition [131] on the superpotential

$$W = W(\Phi^i) + W(Z^n), \tag{2.41}$$

the redefinition (2.40) is not a classical invariance of the full theory with $\Phi \neq 0$, but rather defines a one-parameter family of models of the general form defined by (2.37) and (2.41), with the same vacuum, but with different couplings of the hidden sector to gauge-charged matter.

If $f(Z, \overline{Z}) = f(|Z|^2)$ and $\langle z\rangle = \langle Z|\rangle = 0$, then $\langle K_z\rangle = \langle 3f'(z)\bar{z}\rangle = 0$, and the "anomaly mediated" results are recovered in the dimension-three soft operators (2.39). An example of this type is given in [131] for the case of a single hidden sector field Z. For the family of models generated from that one by the redefinitions (2.40), we obtain for the coefficient of the soft terms in (2.39):

$$B^\xi = M_{3/2} + \frac{1}{3}\left\langle F^z K_z^\xi\right\rangle = M_{3/2} + \frac{\xi}{3}\left\langle F^z\frac{W_z}{W}\right\rangle = (1-\xi)M_{3/2}, \tag{2.42}$$

since $\left\langle F^z \overline{F}^{\bar{z}} K_{z\bar{z}} \right\rangle = -\left\langle F^z (K_z W + W_z) \right\rangle = 3M_{3/2}^2$ is invariant under (2.40).

For $\langle z \rangle = \xi = 0$, we have $\langle F^z K_z \rangle = 0$, giving the standard result [93, 128, 131] $B^\xi = M_{3/2}$. In the literature the point $\xi = 0$ is referred to as "minimal anomaly mediated supersymmetry breaking." For $\xi = 1$, this model is precisely the one defined by (2.33), with $B^\xi = 0$. Quite generally, if $\langle F^n W_n \rangle = 0$ in the class of models defined by the separability conditions (2.37), (2.41) *and* $\kappa_{\Phi A} = \kappa_{\Pi A}$ for the PV fields, the soft supersymmetry breaking terms all vanish, since in this case $\langle F^n K_n \rangle = \left\langle F^n \overline{F}^m K_{i\bar{m}} \right\rangle / M_{3/2} = -3M_{3/2}$ by the vacuum condition (1.4).

In the context of string theory however, the "no-scale" regularization is unacceptable, because it leads to a loop-corrected Lagrangian that is anomalous under modular transformations, which are known to be perturbatively unbroken in string theory. Therefore one must restore modular invariance by including, for example, a modular covariant field dependence in the PV mass parameters in (2.13) $\mu_A = \mu_A(T)$, which might reflect string loop threshold corrections; since these necessarily break the no-scale structure of the theory soft supersymmetry breaking parameters would be generated since $F^T \neq 0$ in this toy model. Alternatively, as shown in [79], this theory can be regulated with field-independent masses for the PV fields that contribute to the renormalization of the Kähler potential: $\partial_n f_A =$ constant, in which case the A-terms are precisely those found above for this no-scale case, but scalar masses are also generated at one loop: $\Delta\mu_i^2 = \gamma_i M_{3/2}^2$. Gauginos remain massless since their masses are insensitive to the specific choice of PV regulator masses.

2.2.3 Spurion Techniques

To summarize, we have found that the "anomaly mediated" results for soft supersymmetry breaking rest on the separability assumptions stated above, but also on more specific assumptions on the form of the hidden sector potential and PV sector couplings. We now address the question as to why these same results were obtained by spurion analyses.[5] In its original incarnation [7, 92, 95], these techniques of deriving observable sector soft supersymmetry breaking terms were applied solely to models in flat superspace (such as models of gauge mediated supersymmetry breaking). In these cases the Kähler potential and superpotential obeyed the separability conditions between observable and hidden sectors

$$K_{\text{tot}} = K_{\text{obs}}\left(\Phi, \overline{\Phi}\right) + K_{\text{hid}}\left(Z, \overline{Z}\right), \quad W_{\text{tot}} = W_{\text{obs}}(\Phi) + W_{\text{hid}}(Z). \tag{2.43}$$

Furthermore, the observable sector Kähler potential was of a minimal variety: $K_{\text{obs}}\left(\Phi, \overline{\Phi}\right) = \sum_i |\Phi^i|^2$.

The key properties of models in which the leading contributions to soft terms arise from the conformal anomaly were enumerated by Randall and Sundrum and are encapsulated in the form of the Kähler potential (2.37). This Kähler potential was the result of demanding separability in the function $\Omega = -3e^{-K/3}$:

$$\Omega_{\text{tot}} = -3 + \Omega_{\text{obs}}\left(\Phi, \overline{\Phi}\right) + \Omega_{\text{hid}}\left(Z, \overline{Z}\right), \quad W_{\text{tot}} = W_{\text{obs}}(\Phi) + W_{\text{hid}}(Z), \tag{2.44}$$

where the factors -3 ensure the canonical normalization of the Einstein term in the supergravity Lagrangian. The separability condition (2.44) and the requirement that $\Omega_{\text{obs}} \propto \sum_i |\Phi^i|^2$ (necessary to ensure vanishing tree level soft supersymmetry breaking in the visible sector as stated

[5] The authors of [128] also pointed out that these results are correct only if $\langle F^n K_n \rangle$ can be neglected.

in Section 2.2.2) give rise to (2.37). Of course in the flat space limit Kähler separability (2.43) and separability in Ω (2.44) are equivalent statements. Thus the Kähler potential assumed in (2.37) is of precisely the limited class of potentials for which the flat-space spurion techniques can be imported into a supergravity context, as in Refs. [131] and [128], without complication. This intimate connection between (2.37) and the canonical flat space of the spurion technique is not surprising as the ansatz of (2.44) represents a set of models with very special conformal properties, as we will elucidate below.

For dimension-three soft terms the distinction between curved and flat superspace is irrelevant, and the dependence of the anomaly-induced soft terms (2.39) on the auxiliary multiplet of supergravity is fixed by the conformal properties of the operators involved [93]. The complete anomaly contribution for the dimension-two soft terms given in (2.31) not proportional to the normal logarithmic running can in fact be obtained from the spurion technique by use of the following construction. We promote the wave function renormalization coefficient Z to a spurion superfield $\mathcal{Z}$ as in [92]. However, this field is not only dependent on the chiral compensator $\eta = 1 + F_\eta \theta^2$ and its Hermitian conjugate, but also on a *real* superfield. Using the PV soft term definitions in (2.21) we can see that this spurion is given schematically by

$$V = 1 - (a + 2m_a)\theta^2 - (a + 2m_a)\bar{\theta}^2 + \mu_a^2 \theta^2 \bar{\theta}^2, \tag{2.45}$$

where here a and $2m_a$ generically represent the tree-level A-terms of the Pauli-Villars sector that correspond, respectively, to the tree-level A-terms A and gaugino masses M_a of the light field sector, and μ_a represents the soft scalar masses of the Pauli-Villars sector. The functional dependence of the superfield $\mathcal{Z}$ on these spurions is given by

$$\mathcal{Z} = \mathcal{Z}\left(\frac{\mu \mathrm{V}}{(\eta\bar{\eta})^{1/2}}\right) \tag{2.46}$$

with μ the renormalization point as before, in analogy with Ref. [7, 95, 131].

We can now perform a Taylor series expansion of this expression about $\theta = 0$ to obtain

$$\begin{aligned} \ln \mathcal{Z} &= \ln Z(\mu) + \frac{\partial \ln Z(\mu)}{\partial \ln \mu}\left[-\left(a + 2m_a + \frac{F_\eta}{2}\right)\theta^2 - \left(a + 2m_a + \frac{\overline{F}_\eta}{2}\right)\bar{\theta}^2\right] \\ &\quad + \frac{\partial \ln Z(\mu)}{\partial \ln \mu}\left[\left(\mu_a^2 + \frac{(a+2m_a)F_\eta}{2} + \frac{(a+2m_a)\overline{F}_\eta}{2} + \frac{|F_\eta|^2}{4}\right)\theta^2\bar{\theta}^2\right] + \cdots \end{aligned} \tag{2.47}$$

Now the *chiral* field redefinition

$$\eta \to \eta' = Z(\mu)^{1/2} \exp\left(-\frac{1}{2}\frac{\partial \ln Z(\mu)}{\partial \ln \mu} F_\eta \theta^2\right)\eta \tag{2.48}$$

can be performed as usual in the spurion derivation to eliminate the one loop contribution to soft masses arising from the supergravity auxiliary field and generate the one loop contribution to the A-terms. This process is equivalent to the cancellation of the double B-term insertions mentioned above (2.27). Note the importance of the assumptions of (2.37), in particular the fact that the Kähler potential for the observable sector is minimal to lowest order in $1/M_{\mathrm{PL}}$, for the rotation (2.48) to be performed.

This same chiral rotation cannot be performed on the real superfield contributions of the Pauli-Villars soft supersymmetry breaking terms. This real superfield is not itself the product of

a chiral and anti-chiral superfield. The terms proportional to θ^2 are thus irrelevant provided that there is no supersymmetry breaking in the observable sector. This is a result of the celebrated holomorphy that underlies the spurion technique. The scalar masses are then read off from the $\theta^2\bar{\theta}^2$ component of (2.47). Use of (2.27) and the equation of motion for the auxiliary field F_η then leads to identification with (2.31).

The question remains, why do flat-space spurion techniques imply the vanishing of the Pauli-Villars tree level soft supersymmetry breaking parameters independent of the specific nature of the Kähler potential and superpotential? The answer can again be found in the special class of supergravity theories for which these techniques can be applied. Specifically, as mentioned above, a "sequestered" sector model is really nothing more than a model on an Einstein-Kähler manifold, of which the no-scale models are a particular subset [114]. These spaces are defined by the fact that the curvature is proportional to the metric. The constant of proportionality determines the normalization of the Einstein term in the supergravity Lagrangian. In flat space these are empty statements, but in curved space a properly normalized Einstein term in an Einstein-Kähler manifold will cause the scalar mass term $R + M_{3/2}^2$ in (2.15) to be proportional to $\widehat{V}$. Hence in a space with vanishing cosmological constant and Kähler potential given by (2.37) (which is equivalent to using the spurion technique in flat space) the PV tree level soft masses are identically zero. It follows that no one loop scalar masses will be generated in these theories by the conformal anomaly.

2.3 Explicit Form of the One Loop Soft Terms

In this section we imagine spontaneous supersymmetry breaking in the hidden sector as manifested by nonvanishing *vevs* for some set of chiral auxiliary fields F^n, as well as the supergravity auxiliary field M. We translate the results of Section 2.1 into a more useful form for phenomenological surveys, in which we assume the supersymmetry breaking is occurring in the moduli sector: $F^n \to F^S$, F^α. This procedure was laid out in the pioneering work of Brignole, Ibañez and Muñoz (BIM) [35, 36].

2.3.1 Gaugino Masses

The tree level expressions for the soft supersymmetry breaking terms are well known. The tree level contribution to the masses of canonically normalized gaugino fields simply reads:[6]

$$M_a^{(0)} = \frac{g_a^2}{2} F^n \partial_n f_a. \tag{2.49}$$

The full one loop anomaly-induced contribution was obtained in (2.32) and is transcribed here:

$$M_a^{(1)}|_{\text{an}} = \frac{g_a(\mu)^2}{2}\left[\frac{2b_a^0}{3}\overline{M} - \frac{1}{8\pi^2}\left(C_a - \sum_i C_a^i\right)F^n K_n - \frac{1}{4\pi^2}\sum_i C_a^i F^n \partial_n \ln \kappa_i\right], \tag{2.50}$$

where C_a, C_a^i are the quadratic Casimir operators for the gauge group $\mathcal{G}_a$ in the adjoint representation and in the representation of Z^i, respectively and b_a^0 is the one loop coefficient of the

[6] In this subsection we will suppress the brackets $\langle\cdots\rangle$ indicating vacuum expectation values. All expressions are to be understood to be in terms of *vevs* of the fields.

corresponding β-function:

$$b_a^0 = \frac{1}{16\pi^2}\left(3C_a - \sum_i C_a^i\right), \tag{2.51}$$

and the functions $\kappa_i(Z^n)$ have been defined in (1.23). The first term is the one generally quoted as the universal anomaly mediated piece [93, 131]: $-b_a^0 g_a^2 M_{3/2}$ using (1.3).

String threshold corrections may be interpreted as one loop corrections to the gauge kinetic functions. They read:

$$f_a^{(1)} = \frac{1}{16\pi^2}\sum_\alpha \ln\eta^2(T^\alpha)\left[\frac{\delta_{\rm GS}}{3} + C_a - \sum_i (1+2n_i^\alpha)C_a^i\right], \tag{2.52}$$

Combining contributions from the Green-Schwarz counterterm and string threshold corrections with the light loop contribution (2.50) yields a total one loop contribution:

$$\begin{aligned} M_a^{(1)} &= \frac{g_a(\mu)^2}{2}\left\{\sum_\alpha F^\alpha \frac{2}{3}\left[\frac{\delta_{\rm GS}}{16\pi^2} + b_a^0 - \frac{1}{8\pi^2}\sum_i C_a^i(1+3n_i^\alpha)\right]\left(2\zeta(t^\alpha) + \frac{1}{t^\alpha + \bar{t}^\alpha}\right)\right. \\ &\left. + \frac{2b_a^0}{3}\overline{M} + \frac{g_s^2}{16\pi^2}\left(C_a - \sum_i C_a^i\right)F^S\right\}. \end{aligned} \tag{2.53}$$

2.3.2 A-terms

A-terms are cubic terms in the scalar potential that generally arise when supersymmetry is broken:

$$V_A = \frac{1}{6}\sum_{ijk} A_{ijk}e^{K/2}W_{ijk}z^iz^jz^k + \text{ h.c. } = \frac{1}{6}\sum_{ijk} A_{ijk}e^{K/2}(\kappa_i\kappa_j\kappa_k)^{-\frac{1}{2}}W_{ijk}\hat{z}^i\hat{z}^j\hat{z}^k + \text{ h.c. }, \tag{2.54}$$

where $\hat{z}^i = \kappa_i^{-\frac{1}{2}}z^i$ is a normalized scalar field. At tree level we have

$$A_{ijk}^{(0)} = \left\langle F^n\partial_n \ln(\kappa_i\kappa_j\kappa_k e^{-K}/W_{ijk})\right\rangle. \tag{2.55}$$

The leading order A-term Lagrangian was given in (2.24); from the definition (2.54) we obtain for the one loop contribution:

$$\begin{aligned} A_{ijk}^{(1)} &= -\frac{1}{3}\gamma_i\overline{M} + \sum_a \gamma_i^a\left[2M_a^{(0)}\ln(|\hat{m}_i m_a|/\mu_R^2) + F^n\partial_n\ln(|\hat{m}_i m_a|)\right] \\ &+ \sum_{lm}\gamma_i^{lm}\left[A_{ilm}^{(0)}\ln(|m_l m_m|/\mu_R^2) + F^n\partial_n\ln(|m_l m_m|)\right] \\ &+ (i\to j) + (j\to k), \end{aligned} \tag{2.56}$$

where m_i and m_a are the PV masses of the supermultiplets Φ^i and Φ^a that regulate loop contributions of the light supermultiplets Z^i and W_a^α, respectively, and $\hat{m}_i$ is the PV mass of a field $\widehat{\Phi}^i$, in the gauge group representation conjugate to that of Φ^i (and of Z^i) needed

to complete the regularization of the gauge-dependent contribution to the one loop Kähler potential renormalization (2.2). The parameters γ_i^j determine the chiral multiplet wave function renormalization and were given in (2.7) and (2.8). Using (2.6) and (2.12) we obtain for the full A-term,

$$\begin{aligned} A_{ijk} &= \frac{1}{3}A_{ijk}^{(0)} - \frac{1}{3}\gamma_i\overline{M} - \sum_\alpha F^\alpha\left[\frac{1}{t^\alpha+\bar{t}^\alpha} + 2\zeta(t^\alpha)\right]\left(\sum_a \gamma_i^a p_{ia}^\alpha + \sum_{lm}\gamma_i^{lm}p_{lm}^\alpha\right) \\ &+F^S\frac{\partial}{\partial s}\left(\sum_a \gamma_i^a \ln(\tilde{\mu}_{ia}^2) + \sum_{lm}\gamma_i^{lm}\ln(\tilde{\mu}_{lm}^2)\right) \\ &-\sum_\alpha \ln\left[(t^\alpha+\bar{t}^\alpha)|\eta(t^\alpha)|^4\right]\left(2\sum_a \gamma_i^a p_{ia}^\alpha M_a^{(0)} + \sum_{lm}\gamma_i^{lm}p_{lm}^\alpha A_{ilm}^{(0)}\right) \\ &+2\sum_a \gamma_i^a M_a^{(0)}\ln(\tilde{\mu}_{ia}^2/\mu_R^2) + \sum_{lm}\gamma_i^{lm}A_{ilm}^{(0)}\ln(\tilde{\mu}_{lm}^2/\mu_R^2) + \text{cyclic (ijk)}, \end{aligned} \tag{2.57}$$

with the unknown dilaton dependence folded into the mass variables $\tilde{\mu}_A$ and the modular weight expressions p^α given by

$$\begin{aligned} p_{ij}^\alpha &= 1+\frac{1}{2}\left(n_i^\alpha+n_j^\alpha+q_i^\alpha+q_j^\alpha\right), \quad p_{ia}^\alpha = \frac{1}{2}\left(1+q_a^\alpha+\hat{q}_i^\alpha-n_i^\alpha\right), \\ \tilde{\mu}_{ij}^2 &= \mu_i\mu_j e^k(h_ih_j)^{-\frac{1}{2}}, \quad \tilde{\mu}_{ai}^2 = \mu_i\mu_a e^{k/2}g_a(h_a\hat{h}_i)^{-\frac{1}{2}}, \end{aligned} \tag{2.58}$$

where $\mu_i\mu_j$, $\mu_i\mu_a$ are constants. The tree level A-terms and gaugino masses are given from (2.55) and (2.49), using (1.26), by

$$\begin{aligned} A_{ijk}^{(0)} &= \sum_\alpha F^\alpha\left(n_i^\alpha+n_j^\alpha+n_k^\alpha+1\right)\left[\frac{1}{t^\alpha+\bar{t}^\alpha}+2\zeta(t^\alpha)\right] - k_S F^S, \\ M_a^{(0)} &= \frac{g_a^2(\mu)}{2}F^S = -\partial_s \ln g_a^2 F^S. \end{aligned} \tag{2.59}$$

2.3.3 B-terms

B-terms are quadratic terms in z^i and in $\bar{z}^{\bar{\imath}}$ that appear in the scalar potential after supersymmetry breaking if there are such quadratic terms in the superpotential and/or Kähler potential:

$$W(Z^i) = \frac{1}{2}\sum_{ij}\nu_{ij}(Z^n)Z^iZ^j + O[(Z^i)^3], \tag{2.60}$$

$$K(Z^i,\overline{Z}^{\bar{\imath}}) = \sum_i \kappa_i|Z^i|^2 + \frac{1}{2}\sum_{ij}\left[\alpha_{ij}(Z^n,\overline{Z}^{\bar{n}})Z^iZ^j + \text{ h.c. }\right] + O(|Z^i|^3). \tag{2.61}$$

These terms give rise to masses for the chiral supermultiplets Z^i:

$$\begin{aligned} \mathcal{L}_M &= -\sum_{ij}\left[\frac{1}{2}e^{K/2}\left(\psi^i\mu_{ij}\psi^j + \text{ h.c. }\right) + e^K|z^i|^2\kappa^j|\mu_{ij}|^2\right], \\ \mu_{ij} &= \nu_{ij} - e^{-K/2}\left(\frac{1}{3}M\alpha_{ij} - \overline{F}^{\bar{n}}\partial_{\bar{n}}\alpha_{ij}\right). \end{aligned} \tag{2.62}$$

The Lagrangian (2.62) is globally supersymmetric although the mass term arising from α_{ij} appears [94] only after local supersymmetry breaking: $M_{3/2} \neq 0$. The B-term potential takes the form

$$V_B = \frac{1}{2}\sum_{ij} B_{ij} e^{K/2} \mu_{ij} z^i z^j + \text{ h.c. } = \frac{1}{2}\sum_{ij} B_{ij} e^{K/2} (\kappa_i \kappa_j)^{-\frac{1}{2}} \mu_{ij} \hat{z}^i \hat{z}^j + \text{ h.c. }. \tag{2.63}$$

At tree level we have

$$B_{ij}^{(0)} = \left\langle F^n \partial_n \ln(\kappa_i \kappa_j e^{-K}/\mu_{ij}) + \frac{1}{3}\overline{M} \right\rangle. \tag{2.64}$$

The one loop contribution is easily extracted from the result for the leading order A-term Lagrangian given in Section 2.1.2; we obtain

$$\begin{aligned} B_{ij}^{(1)} &= -\frac{1}{3}\gamma_i \overline{M} + \sum_a \gamma_i^a \left[2M_a^{(0)} \ln(|\hat{m}_i m_a|/\mu_R^2) + F^n \partial_n \ln(|\hat{m}_i m_a|) \right] \\ &\quad + \sum_{lm} \gamma_i^{lm} \left[A_{ilm}^{(0)} \ln(|m_l m_m|/\mu_R^2) + F^n \partial_n \ln(|m_l m_m|) \right] + (i \to j). \end{aligned} \tag{2.65}$$

Using the assumptions and results of Section 2.3.2 we obtain for the full B-term in string-derived orbifold models

$$\begin{aligned} B_{ij} &= \frac{1}{2} B_{ij}^{(0)} - \frac{1}{3}\gamma_i \overline{M} - \sum_\alpha F^\alpha \left[\frac{1}{t^\alpha + \bar{t}^\alpha} + 2\zeta(t^\alpha) \right] \left(\sum_a \gamma_i^a p_{ia}^\alpha + \sum_{lm} \gamma_i^{lm} p_{lm}^\alpha \right) \\ &\quad + F^S \frac{\partial}{\partial s} \left(\sum_a \gamma_i^a \ln(\tilde{\mu}_{ia}^2) + \sum_{lm} \gamma_i^{lm} \ln(\tilde{\mu}_{lm}^2) \right) \\ &\quad - \sum_\alpha \ln\left[(t^\alpha + \bar{t}^\alpha) |\eta(t^\alpha)|^4 \right] \left(2\sum_a \gamma_i^a p_{ia}^\alpha M_a^{(0)} + \sum_{lm} \gamma_i^{lm} p_{lm}^\alpha A_{ilm}^{(0)} \right) \\ &\quad + 2\sum_a \gamma_i^a M_a^{(0)} \ln(\tilde{\mu}_{ia}^2/\mu_R^2) + \sum_{lm} \gamma_i^{lm} A_{ilm}^{(0)} \ln(\tilde{\mu}_{lm}^2/\mu_R^2) + (i \leftrightarrow j), \end{aligned} \tag{2.66}$$

with the various parameters defined in (2.58). Because we have assumed modular covariance for trilinear terms in the superpotential,[7] Eqs. (2.59) assure that the one loop contribution to the B-term reduces to the anomaly mediated term

$$B_{ij}^{\text{anom}} = -\frac{1}{3}\overline{M}\,(\gamma_i + \gamma_j) \tag{2.67}$$

if supersymmetry breaking is moduli mediated ($\langle F^S \rangle = 0$) with the moduli stabilized at self-dual points.

However tree level B-terms may not vanish in this case; they are sensitive to the origin of the "μ-term" (2.62). A modular invariant Kähler potential of the form (2.61) was constructed [5] for (2,2) orbifold compactifications of the heterotic string with both T-moduli and U-moduli. Here

[7] In fact we need only assume this for the dominant $T^c Q_3 H_u$ term; in making the approximation (2.8) we implicitly neglect the small Yukawa couplings that may themselves arise from higher dimension operators and/or loop corrections.

we restrict the moduli to T-moduli in which case modular invariance of the Kähler potential $K(Z^i, \overline{Z}^{\bar{i}})$ requires

$$\alpha_{ij}(Z^n, \overline{Z}^{\bar{n}}) = a_{ij}(S, \overline{S}) \prod_\alpha (T^\alpha + \overline{T}^\alpha)^{q^\alpha_{ij}} [\eta(T^\alpha)]^{2k^\alpha_{ij}} [\eta^*(\overline{T}^\alpha)]^{2q^\alpha_{ij}}, \quad k^\alpha_{ij} = q^\alpha_{ij} + n^\alpha_i + n^\alpha_j, \tag{2.68}$$

and modular covariance of the superpotential (2.60) requires

$$\nu_{ij}(Z^n) = n_{ij} \prod_\alpha [\eta(T^\alpha)]^{2w^\alpha_{ij}}, \quad w^\alpha_{ij} = 1 + n^\alpha_i + n^\alpha_j. \tag{2.69}$$

Bilinear terms in matter fields do not appear in the tree level superpotential in superstring-derived models, but they can be generated from higher dimension terms when some fields acquire *vev*'s. Bilinear terms in the Kähler potential could similarly be generated from higher dimension terms. These will be modular invariant if only modular invariant fields acquire *vev*'s. For example D-term induced breaking of an anomalous $U(1)$ above the scale of supersymmetry breaking preserves modular invariance. On the other hand if $\nu_{H_u H_d} \neq 0$, it is of the order of the electroweak scale: it presumably originates from the *vev* $\langle N \rangle$ of an electroweak singlet field N and there is no reason that modular invariance should still be operative at such low energy scales. In any case, the corresponding B-term is generated by an A-term in this instance.

To consider the case in which the μ-term is already present at the supersymmetry breaking scale, we can parameterize α_{ij}, ν_{ij} as in (2.68) and (2.69), but with the exponents $k^\alpha_{ij}, q^\alpha_{ij}, w^\alpha_{ij}$ left *a priori* arbitrary; the case of modular invariance is recovered when the last equalities in those equations are imposed. We also assume that Standard Model singlets N whose *vev*'s may generate quadratic terms in the superpotential or Kähler potential do not contribute to supersymmetry breaking: $F^N = 0$.

If the μ-term (2.62) is generated by a superpotential term (2.60), we obtain for the tree level B-term

$$\left[B^{(0)}_{ij}\right]_{\mathrm{W}} = \sum_\alpha F^\alpha \left[\left(1 + n^\alpha_i + n^\alpha_j\right) \frac{1}{t^\alpha + \bar{t}^\alpha} + 2\zeta(t^\alpha) w^\alpha_{ij}\right] - k_S F^S + \frac{1}{3}\overline{M}. \tag{2.70}$$

The coefficients of the moduli auxiliary fields vanish at the moduli self-dual points when modular invariance (2.69) is imposed, but the B-term does not vanish: $B^{(0)} = \frac{1}{3}\overline{M}$ for $F^S = 0$. Although it seems rather implausible that a hierarchically small value of $\nu_{ij} \leq$ TeV would be generated at the supersymmetry breaking scale $\Lambda_{\mathrm{SUSY}} \geq 10^{11}$ GeV, it could conceivably arise as a product of *vevs* in a superpotential term of very high dimension [91].

A more natural origin for a μ-term of the order of a TeV is a quadratic term in the Kähler potential as in (2.61). The expression for $B^{(0)}$ obtained from the general parameterization (2.68) is rather complicated and does not in general vanish when $\langle F^S \rangle = 0$ and modular invariance (2.68) is imposed. As an example, consider the simplifying assumptions that $a_{ij}(S, \overline{S}) =$ constant and $q^\alpha_{ij} = \langle \partial W / \partial t^\alpha \rangle = 0$, then for $\nu_{ij} = 0$

$$\begin{aligned} \mu_{ij} &= a_{ij} W [\eta(t^\alpha)]^{2k^\alpha_{ij}}, \quad F^\alpha = -\frac{1}{3}\left(t^\alpha + \bar{t}^\alpha\right), \\ \left[B^{(0)}_{ij}\right]_{\mathrm{K}} &= \sum_\alpha F^\alpha \left[\left(1 + n^\alpha_i + n^\alpha_j\right) \frac{1}{t^\alpha + \bar{t}^\alpha} + 2\zeta(t^\alpha) k^\alpha_{ij}\right] \\ &\quad - \left(k_S + \partial_S \ln W\right) F^S + \frac{1}{3}\overline{M}. \end{aligned} \tag{2.71}$$

In this case even the coefficients of the moduli auxiliary fields do not vanish at the moduli self-dual points when modular invariance is imposed, and under the above conditions we get $B_{ij}^{(0)} = -\frac{2}{3}\overline{M}$. It is possible that a comparison of $B_{H_u H_d}$ with A-terms might shed some light on the origin of the μ-term (2.62).

2.3.4 Scalar Masses

The expression "soft scalar masses" refers to mass terms in the scalar potential

$$V_M = \sum_i M_i^2 \kappa_i |z^i|^2 = \sum_i M_i^2 |\hat{z}^i|^2, \tag{2.72}$$

with no supersymmetric counterpart in the chiral fermion Lagrangian. The tree level soft scalar masses are given by

$$(M_i^{(0)})^2 = \frac{1}{9} M\overline{M} - F^n \overline{F}^{\bar{m}} \partial_n \partial_{\bar{m}} \ln \kappa_i. \tag{2.73}$$

Here and throughout the discussion of scalar masses, we drop terms proportional to the vacuum energy (1.4).

Denoting by N_A the soft mass of π^A, the one loop scalar masses can be written in the form

$$\begin{aligned}
(M_i^{(1)})^2 \;=\; & -\frac{1}{2}\Bigg[\sum_a \gamma_i^a \left(N_a^2 + \hat{N}_i^2 - (M_a^{(0)})^2 - (M_i^{(0)})^2\right) \\
& + \sum_{jk} \gamma_i^{jk} \left(N_j^2 + N_k^2 + (M_j^{(0)})^2 + (M_k^{(0)})^2\right)\Bigg] \\
& - \sum_a \gamma_i^a \left[3(M_a^{(0)})^2 - (M_i^{(0)})^2 + M_a^{(0)} \left(\overline{F}^{\bar{m}} \partial_{\bar{m}} + F^n \partial_n\right)\right] \ln(|\hat{m}_i m_a|/\mu_R^2) \\
& - \sum_{jk} \gamma_i^{jk} \left[(M_j^{(0)})^2 + (M_k^{(0)})^2 + (A_{ijk}^{(0)})^2 + \frac{1}{2} A_{ijk}^{(0)} \left(\overline{F}^{\bar{m}} \partial_{\bar{m}} + F^n \partial_n\right)\right] \ln(|m_j m_k|/\mu_R^2) \\
& + \frac{1}{3}(M + \overline{M}) \left[\sum_a \gamma_i^a M_a^{(0)} + \frac{1}{2} \sum_{jk} \gamma_i^{jk} A_{ijk}^{(0)}\right].
\end{aligned} \tag{2.74}$$

For orbifold compactifications of string theory, with the Kähler metrics given in (1.24), we obtain for the tree level scalar masses

$$(M_i^{(0)})^2 = \frac{1}{9} M\overline{M} + \sum_\alpha F^\alpha \overline{F}^\alpha n_i^\alpha (t^\alpha + \bar{t}^\alpha)^{-2}. \tag{2.75}$$

Note that if $\langle \partial W/\partial t \rangle = 0$, then $F^\alpha = -\frac{1}{3}\overline{M}(t^\alpha + \bar{t}^\alpha)$ and $M_i^{(0)} = 0$ in the no-scale case with $\sum_\alpha n_i^\alpha = -1$, as for the untwisted sector of orbifold models. The soft masses N_A are given by the standard formula (2.73) by just replacing κ_i by κ_A. The one loop contribution is then given

by

$$
\begin{aligned}
(M_i^{(1)})^2 \;=\;& \frac{1}{9}M\overline{M}\gamma_i - F^S\overline{F}^{\overline{S}}\partial_s\partial_{\overline{s}}\left(\sum_a \gamma_i^a \ln\tilde{\mu}_{ia}^2 + \sum_{jk}\gamma_i^{jk}\ln\tilde{\mu}_{jk}^2\right)\\
&-\sum_\alpha F^\alpha\overline{F}^\alpha(t^\alpha+\bar{t}^\alpha)^{-2}\left(\sum_a \gamma_i^a p_{ai}^\alpha + \sum_{jk}\gamma_i^{jk}p_{jk}^\alpha\right)\\
&+\frac{1}{3}\left(M+\overline{M}\right)\left[\sum_a \gamma_i^a M_a^{(0)} + \frac{1}{2}\sum_{jk}\gamma_i^{jk}A_{ijk}^{(0)}\right]\\
&+\left\{\sum_\alpha F^\alpha\left[\frac{1}{t^\alpha+\bar{t}^\alpha}+2\zeta(t^\alpha)\right]\left(\sum_a \gamma_i^a p_{ia}^\alpha M_a^{(0)} + \frac{1}{2}\sum_{jk}\gamma_i^{jk}p_{jk}^\alpha A_{jk}^{(0)}\right) + \text{h.c.}\right\}\\
&+\left\{F^S\frac{\partial}{\partial s}\left(\sum_a \gamma_i^a M_a^{(0)}\ln(\tilde{\mu}_{ia}^2) + \frac{1}{2}\sum_{jk}\gamma_i^{jk}A_{ijk}^{(0)}\ln(\tilde{\mu}_{jk}^2)\right) + \text{h.c.}\right\}\\
&-\sum_\alpha \ln\left[(t^\alpha+\bar{t}^\alpha)|\eta(t^\alpha)|^4\right]\left\{\sum_a \gamma_i^a p_{ia}^\alpha\left[3(M_a^{(0)})^2-(M_i^{(0)})^2\right]\right.\\
&\qquad\left.+\sum_{jk}\gamma_i^{jk}p_{jk}^\alpha\left[(M_j^{(0)})^2+(M_k^{(0)})^2+(A_{ijk}^{(0)})^2\right]\right\}\\
&+\sum_a \gamma_i^a\left[3(M_a^{(0)})^2-(M_i^{(0)})^2\right]\ln(\tilde{\mu}_{ia}^2/\mu_R^2)\\
&+\sum_{jk}\gamma_i^{jk}\left[(M_j^{(0)})^2+(M_k^{(0)})^2+(A_{ijk}^{(0)})^2\right]\ln(\tilde{\mu}_{jk}^2/\mu_R^2).
\end{aligned}
\tag{2.76}
$$

Chapter 3

Orbifold Models

Following [35, 36], we will consider models where the supersymmetry breaking arises through non-vanishing expectation values of the auxiliary fields F^S, F^α and M and we write:

$$F^S = \frac{1}{\sqrt{3}}\overline{M}K_{S\bar{S}}^{-1/2}\sin\theta e^{-i\gamma_S}, \tag{3.1}$$

$$F^\alpha = \frac{1}{\sqrt{3}}\overline{M}K_{\alpha\bar{\alpha}}^{-1/2}\cos\theta\ \Theta_\alpha e^{-i\gamma_\alpha}, \tag{3.2}$$

with $\sum_\alpha \Theta_\alpha^2 = 1$. In the case where one considers a single common modulus T (the overall radius of compactification), (3.2) simply reads:

$$F^T = \frac{1}{\sqrt{3}}\overline{M}K_{T\overline{T}}^{-1/2}\cos\theta e^{-i\gamma_T}. \tag{3.3}$$

Recall that the *vev* of M is related to the gravitino mass through (1.3) and that these auxiliary fields automatically satisfy the constraint that the potential $\widehat{V}$ in (1.4) vanishes at the ground state.

In the orbifold models that we consider, *i.e.* with gauge kinetic function (1.14) and Kähler potential given by (1.19) and (1.24), the tree level soft terms have simple expressions:

$$\begin{aligned}
M_a^{(0)} &= \frac{g_a^2}{2\sqrt{3}}\overline{M}k_{s\bar{s}}^{-1/2}\sin\theta e^{-i\gamma_S} \\
A_{ijk}^{(0)} &= \frac{\overline{M}}{\sqrt{3}}\left\{\cos\theta\sum_\alpha(t^\alpha+\bar{t}^\alpha)G_2^\alpha\Theta_\alpha(n_i^\alpha+n_j^\alpha+n_k^\alpha+1)e^{-i\gamma_\alpha} - \frac{k_s}{k_{s\bar{s}}^{1/2}}\sin\theta e^{-i\gamma_S}\right\} \\
B_{ij}^{(0)} &= \frac{\overline{M}}{\sqrt{3}}\left\{\frac{1}{\sqrt{3}} - \frac{\sin\theta}{k_{s\bar{s}}^{1/2}}\left[k_s+\partial_s\ln\mu_{ij}\right]e^{-i\gamma_S} + \cos\theta\sum_\alpha\Theta_\alpha\left[(n_i^\alpha+n_j^\alpha+1)-\partial_{t_\alpha}\ln\mu_{ij}\right]e^{-i\gamma_\alpha}\right\} \\
(M_i^{(0)})^2 &= \frac{M\overline{M}}{9}\left\{1+3\sum_\alpha n_i^\alpha\Theta_\alpha^2\cos^2\theta\right\}
\end{aligned} \tag{3.4}$$

The one loop contributions to (3.4) are decidedly more cumbersome and the complete expressions are given in Appendix B. Below we consider the phenomenological implications of some specific cases in which the soft supersymmetry breaking terms are simpler. In all of the following $G_2^\alpha = (2\zeta(T^\alpha) + 1/(T^\alpha + \overline{T}^\alpha))$, which is proportional to the Eisenstein function (1.30).

The expressions in Section 2.1 require some further assumptions regarding the Pauli-Villars sector if we are to extract predictions from the models. We will choose two possible scenarios

for the PV masses and modular weights in what follows. First, if the PV masses m_i, m_a, and $\hat{m}^i$ in (2.13) are constant (as well as μ_A)[1] we have from (2.13)

$$(A) \qquad \begin{aligned} n_i^\alpha + q_i^\alpha &= -1, \\ n_i^\alpha - \hat{q}_i^\alpha &= 1, \\ q_a^\alpha &= 0, \end{aligned} \tag{3.5}$$

and thus $p_{ij}^\alpha = p_{ia}^\alpha = 0$, from (2.58) with $\tilde{\mu}_{ij}^2$ and $\tilde{\mu}_{ai}^2$ constants.

A commonly (though often implicitly) made assumption in the literature is instead that Π^A has the same Kähler metric as Φ^A, as was discussed in Section 2.2:

$$(B) \qquad \begin{aligned} q_i^\alpha &= n_i^\alpha, \\ \hat{q}_i{}^\alpha &= -n_i^\alpha, \\ q_a^\alpha &= -1; \end{aligned} \tag{3.6}$$

this gives $\tilde{\mu}_{ij}^2$ constant, $\tilde{\mu}_{ia}^2 = g_a^2$, $p_{ij}^\alpha = 1 + n_i^\alpha + n_j^\alpha$ and $p_{ai}^\alpha = -n_i^\alpha$. Distinguishing among the possibilities from the theoretical point of view requires string loop calculations similar to those used to fix the moduli dependence of the gauge kinetic function [6, 59]. We now apply these relations to a range of orbifold models

3.1 Anomaly Dominated Scenarios

The analysis of the preceding sections indicates a very specific situation which turns out to give quasi-model independent contributions. It is the case of moduli mediated supersymmetry breaking ($F^S = 0$ or $\theta = 0$) where the moduli fields lie at a self-dual point ($t^\alpha = 1$ or $e^{i\pi/6}$, and thus $G_2^\alpha = 0$). Assuming (1.14), we have vanishing tree level gaugino masses and A-terms and from (2.53), (2.57) and (2.67) we obtain:

$$\begin{aligned} M_a &= g_a(\mu)^2 \, \frac{b_a^0}{3} \overline{M}, \\ A_{ijk} &= -\frac{1}{3}\overline{M}(\gamma_i + \gamma_j + \gamma_k). \\ B_{ij} &= -\frac{1}{3}\overline{M}(\gamma_i + \gamma_j) \end{aligned} \tag{3.7}$$

Further assuming that $\Theta_\alpha^2 = \frac{1}{3}$ (as in the case of a single modulus T, see (3.3)), $\gamma_\alpha = 0$ and $\sum_\alpha n_i^\alpha = -1$ (as in the untwisted sector), we have vanishing tree level scalar masses and

$$M_i^2 = \frac{1}{9} M\overline{M} \left[\gamma_i - \sum_{\alpha,a} \gamma_i^a p_{ai}^\alpha - \sum_{\alpha,jk} \gamma_i^{jk} p_{jk}^\alpha \right]. \tag{3.8}$$

For the choice (A) of PV weights (3.5), one finds $M_i^2 = M\overline{M}\gamma_i/9$ whereas for the choice (B) in (3.6), one obtains $M_i^2 = 0$. This shows very clearly how dependent the scalar masses are on

[1] It was shown in [77, 78, 79] that the Kähler potential for the untwisted sector from orbifold compactification can be made modular invariant with the relevant masses constant. Since the tree level Kähler potential for the twisted sector is not known beyond quadratic order in twisted sector fields, the one loop corrections to it cannot be calculated.

Scalar Mass	$\Lambda_{\rm UV} = 1 \times 10^{11}$ GeV	$\Lambda_{\rm UV} = 2 \times 10^{16}$ GeV
$M^2_{Q_3}$	$1.4 \leq \tan\beta \leq 45$	$1.7 \leq \tan\beta \leq 44$
$M^2_{U_3}$	$1.8 \leq \tan\beta \leq 48$	$1.9 \leq \tan\beta \leq 44$
$M^2_{D_3}$	$1.3 \leq \tan\beta \leq 42$	$1.6 \leq \tan\beta \leq 41$
$M^2_{L_3}$	$1.3 \leq \tan\beta \leq 46$	$1.6 \leq \tan\beta \leq 44$
$M^2_{E_3}$	$1.3 \leq \tan\beta \leq 39$	$1.6 \leq \tan\beta \leq 41$
$M^2_{H_u}$	always negative	$3.6 \leq \tan\beta \leq 33$
$M^2_{H_d}$	$1.3 \leq \tan\beta \leq 33$	$1.6 \leq \tan\beta \leq 37$

Table 3.1: Regions of Positive Squared-Mass in the Anomaly Dominated Scenario. Range of $\tan\beta$ for which scalar squared-masses are positive at the boundary scale $\Lambda_{\rm UV}$ using the PV scenario (A). The value of $\tan\beta$ was varied over the range for which the third generation Yukawa couplings remain perturbative up to the scale $\Lambda_{\rm UV}$. This corresponds to the range $1.3 \leq \tan\beta \leq 44$ for $\Lambda_{\rm UV} = 1 \times 10^{11}$ GeV and $1.6 \leq \tan\beta \leq 48$ for $\Lambda_{\rm UV} = 2 \times 10^{16}$ GeV.

the regularization scheme forced upon us by the underlying theory. Case (B) corresponds to the anomaly mediated scenario, as in Section 2.2, in which scalar squared-masses arise at two loops but are negative for sleptons, thus implying an unacceptable phenomenology without further *ad hoc* assumptions. As discussed in Section 2.3.3, if the μ-term (2.62) has a low energy origin through the *vev* of a standard model singlet in a superpotential term, we would expect that in this scenario the B-term would also be dominated by the anomaly mediated contribution (2.67). On the other hand if it arises from Planck scale physics, we do not expect the tree level contribution to vanish.

Let us note moreover that any departure from our hypothesis (*i.e.* a small value for F^S or a departure from the self-dual point in moduli space) generates tree level values for the soft terms which tend to overcome the one loop anomaly-induced contributions considered here, as we will see in the next subsection. Therefore if gaugino masses and/or A-terms are measured to be significantly larger than the "anomaly mediated" values in the string context of assumed modular invariance this would quite generally suggest dilaton dominated supersymmetry breaking and/or moduli *vevs* far from the self-dual points.

When (3.8) represents the leading contribution to scalar masses we can see from (2.8) that the positivity of scalar squared masses depends on the size of the Yukawa couplings (which themselves are a function of the value of $\tan\beta$ and of the scale $\Lambda_{\rm UV}$ at which the soft terms are determined) and the values of the high-scale parameters p^α_{ia} and p^α_{ij} of (2.58). In the simple case of scenario (A) (3.5) mentioned above, the sign of the scalar squared mass depends on the sign of the anomalous dimensions. Keeping all third generation Yukawa couplings and taking the running masses of the third generation fermions at the Z-mass to be $\{m_t, m_b, m_\tau\} = \{165\text{ GeV}, 4.1\text{ GeV}, 1.78\text{ GeV}\}$, we investigated the range in $\tan\beta$ for which the scalar masses are positive for a GUT-inspired boundary scale of $\Lambda_{\rm UV} = 2 \times 10^{16}$ GeV as well as an intermediate scale of $\Lambda_{\rm UV} = 1 \times 10^{11}$ GeV. As can be seen from Table 3.1 the problem of tachyonic scalar masses for the matter fields is eased considerably in this scenario relative to the previously studied anomaly mediated scenario represented by case (B) (3.6).

Let us now investigate the pattern of soft terms as the parameters p^α_{ia} and p^α_{ij} are varied by assuming that $p^\alpha_{ia} = p^\alpha_{ij} \equiv p$ with p a constant. If the scale at which the soft terms emerge is taken to be $\Lambda_{\rm UV} = 1 \times 10^{11}$ GeV then the spectrum of soft terms as a function of p is displayed in Figure 3.1. In general gaugino masses are an order of magnitude smaller than scalar masses,

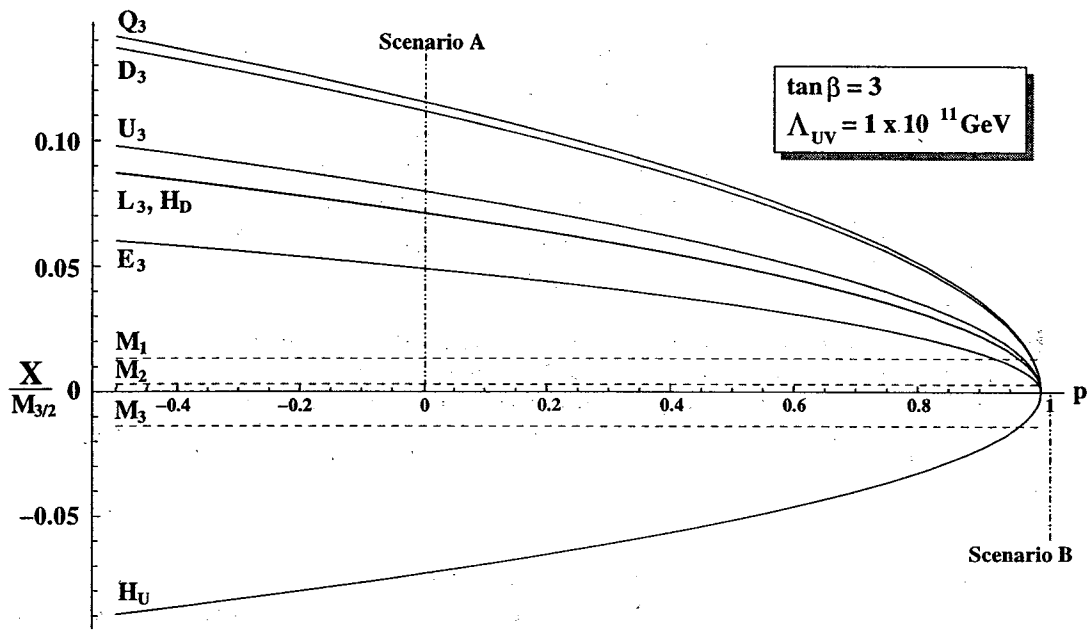

Figure 3.1: Soft Term Spectrum for Anomaly Dominated Scenario. Soft term magnitudes for third generation scalars, Higgs fields and gaugino masses are given as a function of universal PV parameter p as a fraction of gravitino mass $M_{3/2}$. Scalar particles are generally much heavier than gauginos except for the limiting case of $p \to 1$.

except for values of p approaching the limiting case of $p = 1$ (which is equivalent to scenario (B) given by (3.6)) where scalar masses go through zero. It is important to note that all of the possibilities of Figure 3.1 represent "anomaly mediated" scenarios. However, it is only the extreme case of $p = 1$ that was studied previously in the particular model of Randall and Sundrum [131].

One final aspect of these soft term patterns relevant to low energy phenomenology is the relative size of the scalar masses and A-terms. It is well known that for any generation of matter with non-negligible Yukawa couplings the relation

$$|A_{ijk}|^2 \lesssim 3(M_i^2 + M_j^2 + M_k^2), \tag{3.9}$$

evaluated at the scale of supersymmetry breaking, is a good indicator that the minimum of the scalar potential will yield proper electroweak symmetry breaking: when the bound is not satisfied it is typical to develop minima away from the electroweak symmetry breaking point in a direction in which one of the scalars masses of a field carrying electric or color charge becomes negative. Since the "anomaly mediated" A-term and the scalar *squared* mass both have a single loop factor of $1/16\pi^2$ the condition (3.9) is generally satisfied. For example, in scenario (A) discussed above

$$(M_i^2 + M_j^2 + M_k^2) = M_{3/2} A_{ijk}, \tag{3.10}$$

and since A_{ijk} is loop-suppressed relative to the gravitino mass, as seen from (3.7), this scenario is phenomenologically acceptable. Scenario (B) with its vanishing scalar masses at one loop is problematic, however, and the two loop contributions are relevant to the determination of its viability.

3.2 BIM O-II Models

This class of orbifold models discussed in [35, 36] has matter fields in the untwisted sector with weights $(n_i^1, n_i^2, n_i^3) = (-1,0,0)$ $(0,-1,0)$ or $(0,0,-1)$. Then, taking for simplicity the same common value T for the T^α fields[2], one obtains from (B.1):

$$M_a^{tot} = \frac{g_a^2(\mu)}{2\sqrt{3}}\overline{M}\left\{\frac{2}{\sqrt{3}}\cos\theta(t+\bar{t})G_2\left[\frac{\delta_{\rm GS}}{16\pi^2}+b_a^0\right]+\frac{2b_a^0}{\sqrt{3}}+\frac{\sin\theta}{k_{s\bar{s}}^{1/2}}\left[1+\frac{g_s^2}{16\pi^2}\left(C_a-\sum_i C_a^i\right)\right]\right\}. \tag{3.11}$$

The above form suggests a closer investigation of the relative magnitude of the contributions to gaugino masses arising from the dilaton sector (proportional to $\sin\theta$), the moduli sector (proportional to $\cos\theta$) and the anomaly-induced piece (independent of the Goldstino angle). As mentioned in the previous section, any tree level contribution (from the dilaton sector) will likely dominate the gaugino mass, particularly when the Green-Schwarz coefficient is smaller than $-3C_{E_8}$. The anomaly-induced piece is typically quite small and will only be relevant in the case of moduli domination ($\sin\theta = 0$) with moduli stabilized very near their self-dual points and/or very small Green-Schwarz coefficient. This behavior is demonstrated for the case of the $U(1)_Y$ gaugino mass M_1 in Figure 3.2. We have taken $k = -\ln(S+\overline{S})$ and set $g_s^2 = g_{\rm STR}^2 = 1/2$ here.

In Figure 3.3 we look at the relative sizes of the three gaugino mass terms for the case of moduli domination ($\theta = 0$) and a mixed case ($\theta = \pi/3$) for real moduli vacuum values $\langle \mathrm{Re}\, t\rangle$ at a boundary scale of $\Lambda_{\rm UV} = 2\times 10^{16}$ GeV. Note that there is always a particular value of the moduli *vev* such that a nearly degenerate gaugino mass spectrum is recovered. As $\cos\theta \to 0$ this value gets ever larger as we approach the limiting case in which the gaugino masses are independent of the value of $\langle \mathrm{Re}\, t\rangle$. At the GUT scale where $g_2^2 \approx g_1^2 \approx 1/2$ the difference in SU(2) and U(1) gaugino masses is given by

$$M_2 - M_1 \approx -\frac{M_{3/2}}{40\pi^2}\left\{7\left[1+\cos\theta\left(1-\frac{\pi}{3}\mathrm{Re}\, t\right)\right]+2\sqrt{3}\sin\theta\right\}, \tag{3.12}$$

where we have used the fact that for $\mathrm{Re}\, t > 1$, $\zeta(t) \approx -\pi/12$. For $\theta = 0$ equation (3.12) indicates that $M_1 = M_2$ at $\mathrm{Re}\, t \approx 6/\pi$ while for $\theta = \pi/3$ this occurs when $\mathrm{Re}\, t \approx 3.7$.

When $\theta \neq 0$ (3.12) implies that $|M_2| \geq |M_1|$ (the gaugino masses in this regime are negative) whenever

$$\mathrm{Re}\, t \leq \frac{3}{\pi}\left\{\frac{2\sqrt{3}}{7}\tan\theta + \sec\theta + 1\right\}. \tag{3.13}$$

In the case where $\theta = 0$ so that there is no tree level contribution to gaugino masses we see from Figure 3.3 that $|M_1| \geq |M_2|$ in nearly all of the $\langle \mathrm{Re}\, t\rangle$ parameter space. This relationship between the boundary values of the SU(2) and U(1) gaugino masses is crucial to the low energy phenomenology of the model in that it determines whether the lightest neutralino is predominantly bino-like, predominantly wino-like or a mixed state. Thus a lightest neutralino with a significant wino content *need not necessarily imply that supersymmetry breaking is due to pure anomaly mediation.* We will return to this point when we investigate sample spectra in Section 3.4.

[2]All the expressions given in this and the following sections will assume zero phases $\gamma_S = \gamma_T = 0$

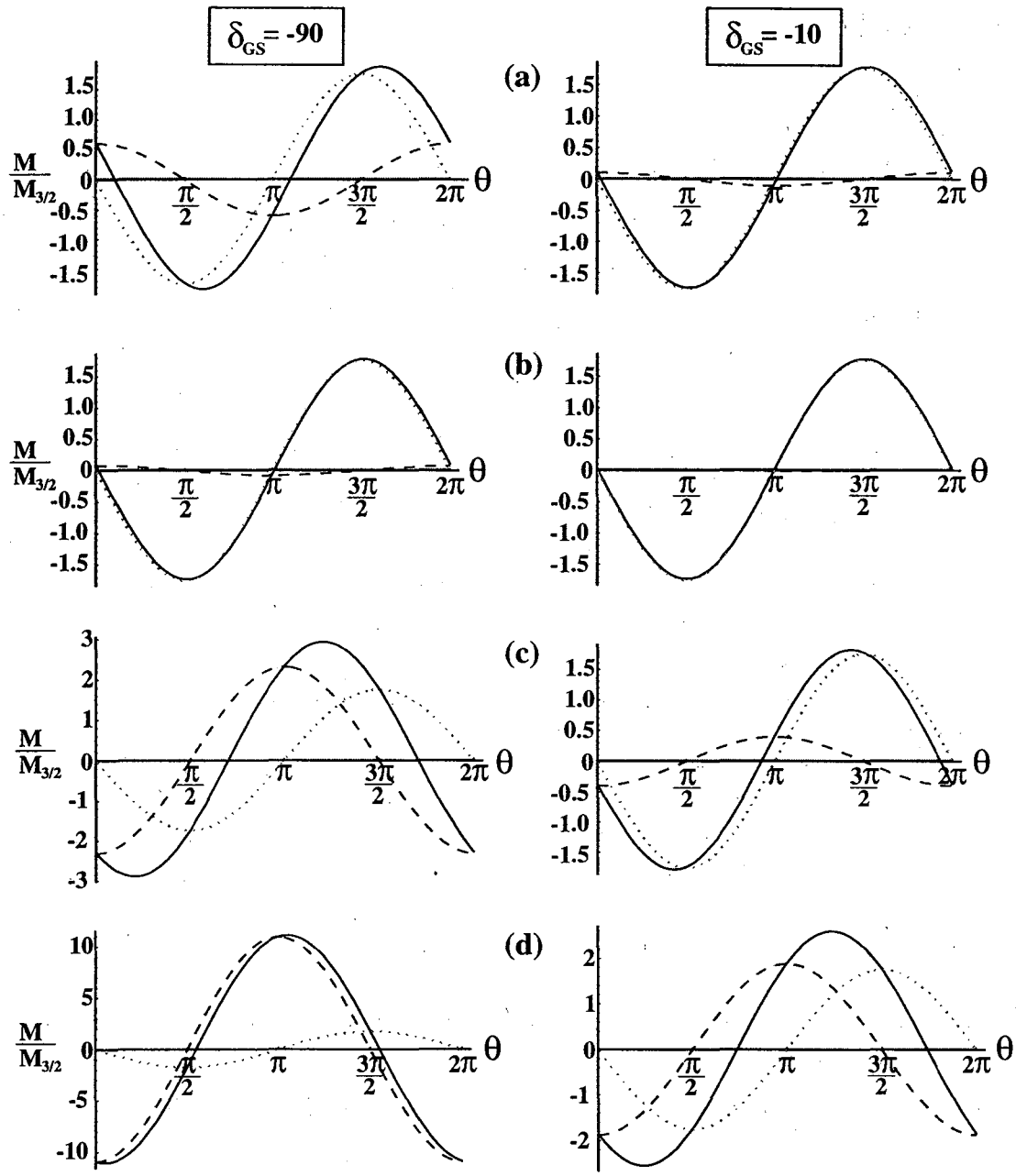

Figure 3.2: $U(1)_Y$ Gaugino Mass in the BIM O-II Model. Contributions to the value of M_1 from F^T (dashed) and F^S (dotted) as well as total M_1 (solid) are given as a function of Goldstino angle for two values of δ_{GS} and four T-modulus *vevs*: $\langle \mathrm{Re}\, t \rangle = 0.5$ (a), $\langle \mathrm{Re}\, t \rangle = 0.9$ (b), $\langle \mathrm{Re}\, t \rangle = 5$ (c), and $\langle \mathrm{Re}\, t \rangle = 20$ (d). All values are given as a fraction of the gravitino mass $M_{3/2}$.

The scale at which the soft masses emerge is particularly important: the largest contributions to gaugino masses generically arise from the tree level piece and the piece proportional to the Green-Schwarz coefficient δ_{GS}. These terms cancel in (3.12), however, when the difference is evaluated at the GUT scale. Thus the location of the crossover point is independent of the choice of δ_{GS} in Figure 3.3.

An immediate consequence of the above is that measurement of the properties of the lightest

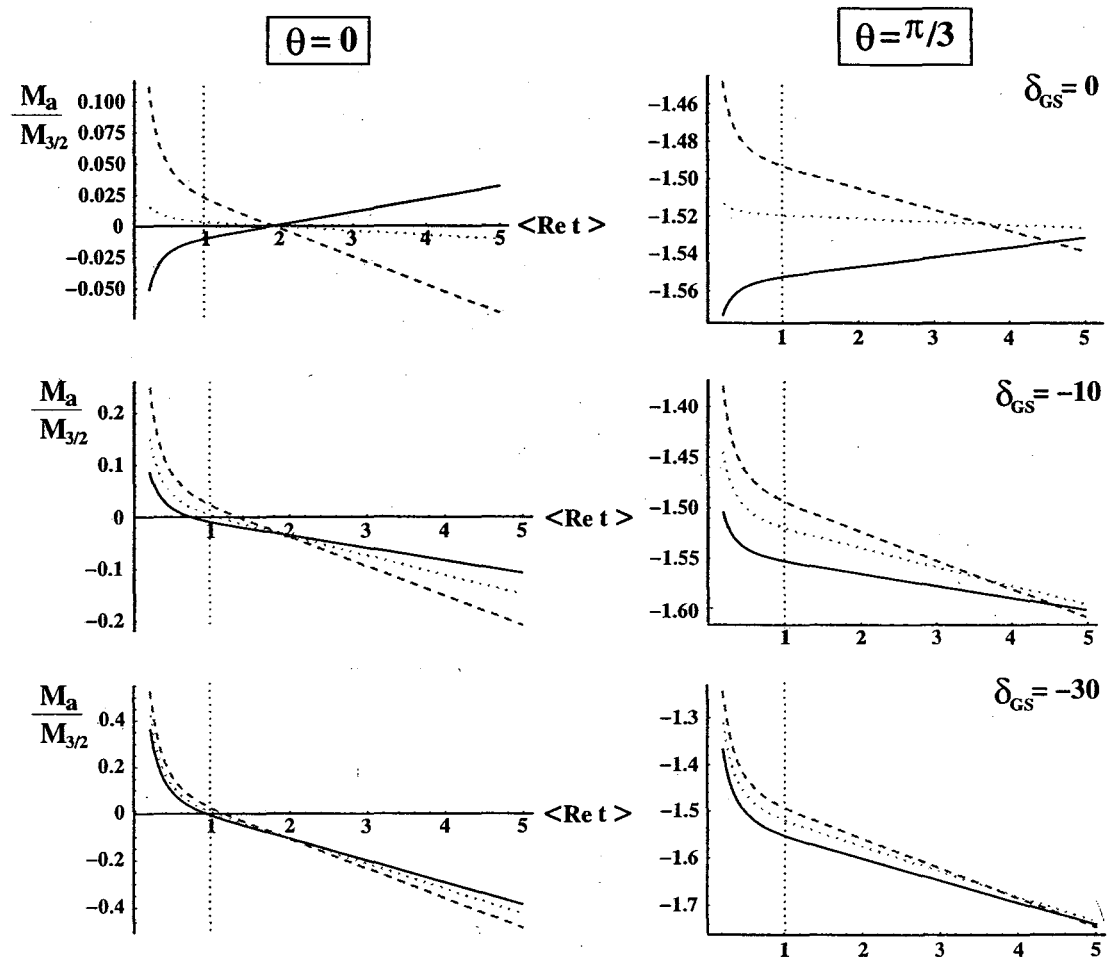

Figure 3.3: Relative Gaugino Masses vs. $\langle \mathrm{Re}\, t \rangle$ in the BIM O-II Model with $\Lambda_{\mathrm{UV}} = 2 \times 10^{16}$ GeV. Relative sizes of the three gaugino masses M_1 (dashed), M_2 (dotted) and M_3 (solid) are displayed as a function of $\langle \mathrm{Re}\, t \rangle$ for two values of the Goldstino angle θ and three representative values of δ_{GS}. The vertical dotted line at $\langle \mathrm{Re}\, t \rangle = 1$ indicates the moduli self-dual point where gaugino masses become independent of δ_{GS}. When $\sin\theta = 0$ this point represents the case of leading anomaly contributions discussed in Section 3.1. All masses are relative to the gravitino mass $M_{3/2}$.

neutralinos may reveal information on the nature of the scale of ultraviolet physics. In particular the region of parameter space for which the lightest neutralino is predominantly wino-like becomes increasingly small as the scale of supersymmetry breaking is lowered. This is illustrated in Figure 3.4 where we plot the ratio of gaugino masses M_1/M_2 for two different boundary scales: $\Lambda_{\mathrm{UV}} = 2 \times 10^{16}$ GeV and $\Lambda_{\mathrm{UV}} = 1 \times 10^{11}$ GeV, for which $g_2^2 \approx (7/5) g_1^2$. As the gauge couplings run farther apart the shaded areas in which $M_1/M_2 \geq 1$ (and hence where a wino-like lightest neutralino is possible) grow steadily smaller. When $\delta_{\mathrm{GS}} = 0$ the ratio M_1/M_2 diminishes as the Goldstino angle θ increases until M_2 begins to approach its vanishing value and the ratio passes through a discontinuity before increasing rapidly as $\theta \to \pi$. When the Green-Schwarz coefficient δ_{GS} is increased the location of this discontinuity, as indicated in Figure 3.4 by a heavy arrow, moves to smaller values of θ.

The trilinear A-terms for these orbifold models are given by (B.3); for scenario (A) as defined

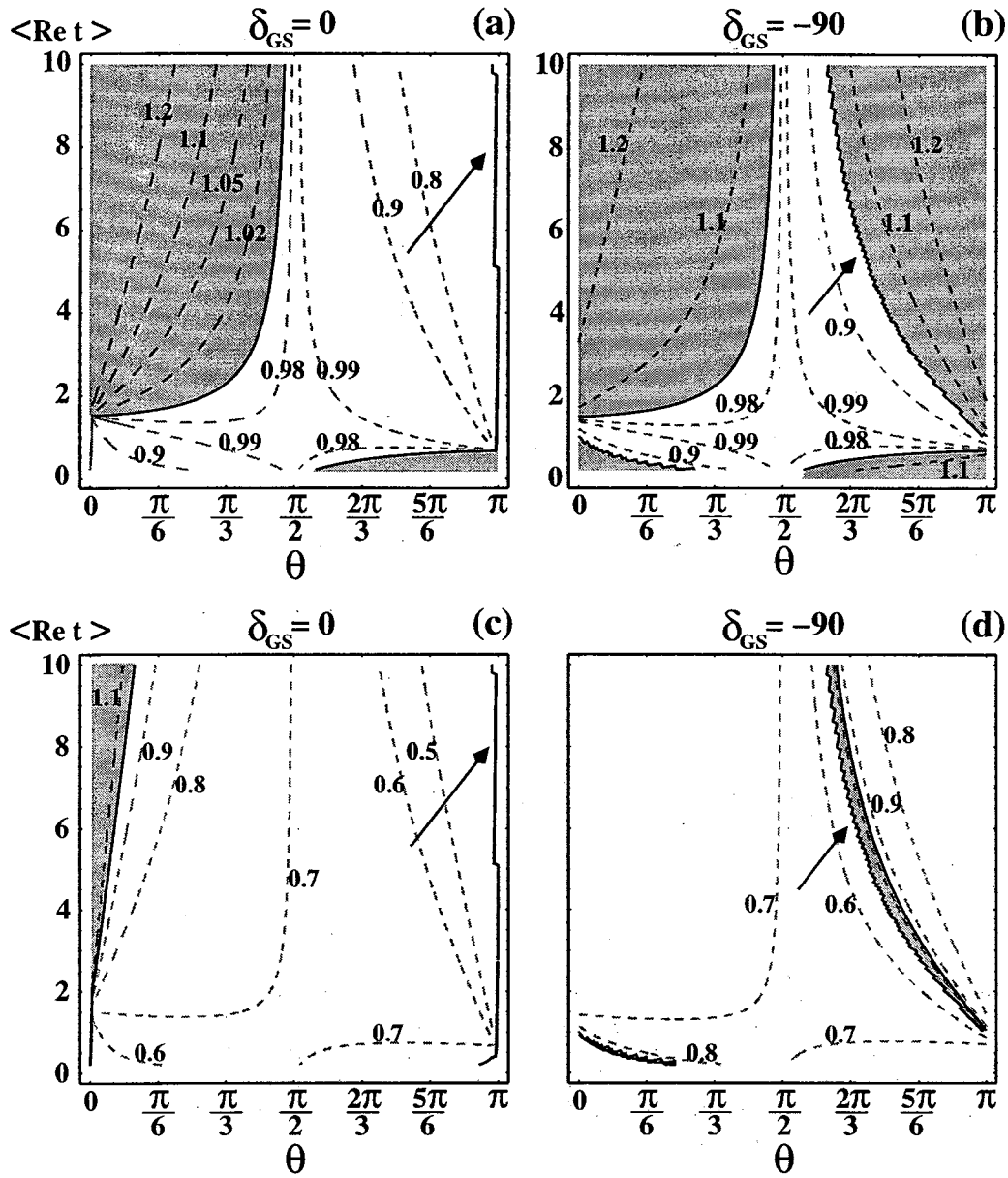

Figure 3.4: Ratio M_1/M_2 in BIM O-II Model. Contours of the absolute value of the ratio of U(1) to SU(2) gaugino masses are given for boundary scales of $\Lambda_{UV} = 2 \times 10^{16}$ GeV for panels (a) and (b), and $\Lambda_{UV} = 1 \times 10^{11}$ GeV for panels (c) and (d). The shaded area is the region of parameter space for which $|M_1| \geq |M_2|$. The arrow indicates the direction of smallest ratios as the discontinuity $M_2 = 0$ is approached. The contour $M_1 = M_2$ is given by the heavy solid line.

by (3.5), this expression is particularly simple

$$A_{ijk}^{tot} = \frac{\overline{M}}{\sqrt{3}} \left\{ \frac{\sin\theta}{k_{s\bar{s}}^{1/2}} \left[-\frac{k_s}{3} + \sum_a \gamma_i^a \frac{g_a^2}{2} \ln(\tilde{\mu}_{ia}^2/\mu_R^2) \right] - \frac{\gamma_i}{\sqrt{3}} \right\} + \text{cyclic (ijk)}. \tag{3.14}$$

It is worth noting that, with such a scenario for the PV metrics, this pattern for A-terms goes beyond the BIM O-II model. Any of the following conditions: (i) $\sum_\alpha (n_i^\alpha + n_j^\alpha + n_k^\alpha + 1) = 0$ with identical vacuum values for all T-moduli (as in the BIM O-II model), (ii) $\cos\theta = 0$ (dilaton

domination) or (iii) $G_2^\alpha = 0$ (moduli stabilized at self-dual point), yields the A-terms given by (3.14) above.

By contrast, for scenario (B) defined by (3.6) the A-terms take the form

$$\begin{aligned} A_{ijk}^{tot} &= \frac{\overline{M}}{\sqrt{3}}\left\{-\frac{\gamma_i}{\sqrt{3}}\left[1+\cos\theta(t+\bar{t})G_2\right]+\frac{\sin\theta}{k_{s\bar{s}}^{1/2}}\left[-\frac{k_s}{3}+\sum_a \frac{g_a^2}{2}\gamma_i^a(\ln(g_a^2)-1)\right.\right. \\ &\left.\left.-\ln\left[(t+\bar{t})|\eta(t)|^4\right]\left(\sum_a g_a^2\gamma_i^a-\sum_{lm}k_s\gamma_i^{lm}\right)\right]\right\}+\text{cyclic (ijk)}. \end{aligned} \tag{3.15}$$

This scenario also allows for the recovery of an "anomaly mediated-like" result of A-terms proportional to anomalous dimensions in the moduli dominated limit ($\sin\theta = 0$). Expression (3.15) differs from the situation in Section 3.1 in that for moduli domination this scenario can accommodate proper electroweak symmetry breaking provided the moduli are stabilized *away* from their self-dual points: in particular, using the fact that for Re $t > 1$, $\zeta(t) \approx -\pi/12$ we have $\langle(t+\bar{t})G_2\rangle \approx -1$ for $\langle t\rangle \approx 6/\pi \approx 2$ leading to $A \approx 0$ from (3.15).

The expressions for the bilinear B-terms are similar, but with added model dependence at the tree level involving the origin of bilinear terms in the Kähler potential or superpotential. For the case of scenario (A) the general form given in (B.4) yields

$$\begin{aligned} B_{ij}^{tot} &= \frac{\overline{M}}{\sqrt{3}}\frac{\sin\theta}{k_{s\bar{s}}^{1/2}}\left[-k_s-\partial_s\ln\mu_{ij}+\sum_a\gamma_i^a\left(\frac{g_a^2}{2}\right)\ln(\tilde{\mu}_{ia}^2)\right. \\ &\left.+\frac{\overline{M}}{6}\cos\theta\left[1-\sum_\alpha\partial_{t^\alpha}\ln\mu_{ij}\right]+\frac{\overline{M}}{3}\left(\frac{1}{2}-\gamma_i\right)\right]+(i\leftrightarrow j), \end{aligned} \tag{3.16}$$

while for case (B) the corresponding expression is

$$\begin{aligned} B_{ij}^{tot} &= \frac{\overline{M}}{\sqrt{3}}\frac{\sin\theta}{k_{s\bar{s}}^{1/2}}\left[-k_s-\partial_s\ln\mu_{ij}+\sum_a\gamma_i^a\frac{g_a^2}{2}\left(\ln(g_a^2)-1\right)\right. \\ &\left.-\ln\left[(t+\bar{t})|\eta(t)|^4\right]\left(\sum_a\gamma_i^a g_a^2-\sum_{lm}\gamma_i^{lm}k_s\right)\right]+\frac{\overline{M}}{3}\left(\frac{1}{2}-\gamma_i\right) \\ &+\frac{\overline{M}}{6}\cos\theta\left[1-\sum_\alpha\partial_{t^\alpha}\ln\mu_{ij}-2(t+\bar{t})G_2\gamma_i\right]+(i\leftrightarrow j). \end{aligned} \tag{3.17}$$

Finally, the scalar masses in the BIM O-II model are found from equation (B.7) of Appendix B. Under the assumptions of scenario (A) this reduces to

$$\begin{aligned} (M_i^{tot})^2 &= |M|^2\left\{\frac{1}{9}\gamma_i+\frac{1}{k_{s\bar{s}}^{1/2}}\frac{\sin\theta}{3\sqrt{3}}\left[\sum_a\gamma_i^a g_a^2-\frac{1}{2}\sum_{jk}\gamma_i^{jk}(k_s+k_{\bar{s}})\right]\right. \\ &+\frac{\sin^2\theta}{9}\left[1-\sum_a\gamma_i^a\ln(\tilde{\mu}_{ia}^2)+2\sum_{jk}\gamma_i^{jk}\ln(\tilde{\mu}_{jk}^2)\right] \\ &\left.+\frac{\sin^2\theta}{k_{s\bar{s}}}\left[-\frac{1}{4}\sum_a g_a^4\gamma_i^a\ln(\tilde{\mu}_{ia}^2)-\frac{1}{3}\sum_{jk}\gamma_i^{jk}\left(k_sk_{\bar{s}}+2k_{s\bar{s}}\right)\ln(\tilde{\mu}_{jk}^2)\right]\right\} \end{aligned} \tag{3.18}$$

and for scenario (B) the scalar masses are given by

$$
\begin{aligned}
(M_i^{tot})^2 \;=\; & |M|^2 \left\{ \frac{1}{3\sqrt{3}} \frac{\sin\theta}{k_{s\bar{s}}^{1/2}} \left[1+\cos\theta(t+\bar{t})G_2\right] \left[\sum_a g_a^2 \gamma_i^a - \frac{1}{2}\sum_{jk} \gamma_i^{jk}\left(k_s + k_{\bar{s}}\right)\right] \right. \\
& + \frac{\sin^2\theta}{9} \left[1 + \gamma_i + \ln\left[(t+\bar{t})|\eta(t)|^4\right] \left(\sum_a \gamma_i^a - 2\sum_{jk} \gamma_i^{jk} \right) \right. \\
& \left. - \sum_a \gamma_i^a \ln(g_a^2) + 2\sum_{jk} \gamma_i^{jk} \ln(\tilde{\mu}_{jk}^2) \right] \\
& - \frac{\sin^2\theta}{k_{s\bar{s}}} \left[\sum_a \gamma_i^a \left(\frac{g_a^4}{4}\right) \left(\ln(g_a^2) + \frac{5}{3}\right) + \frac{1}{3}\sum_{jk} \gamma_i^{jk} \left(k_s k_{\bar{s}} + 2k_{s\bar{s}}\right) \ln(\tilde{\mu}_{jk}^2) \right. \\
& \left. \left. + \ln\left[(t+\bar{t})|\eta(t)|^4\right] \left(\sum_a \gamma_i^a \left(\frac{g_a^4}{4}\right) + \frac{1}{3}\sum_{jk} \gamma_i^{jk} k_s k_{\bar{s}} \right) \right] \right\}. \qquad (3.19)
\end{aligned}
$$

The pattern of soft supersymmetry breaking terms that arise in this orbifold model with uniform modular weights $n_i = -1$ and with the same Kähler metric for the Π^A and the Φ^A, as in scenario (3.6), will produce a low energy phenomenology very similar to that of the recently proposed "gaugino mediation" scenario [108, 134] if the Green-Schwarz coefficient is sufficiently large, the supersymmetry breaking is moduli dominated and the moduli are stabilized at $\langle \mathrm{Re}\, t \rangle \approx 2$. Such a situation gives rise to exactly vanishing scalar masses and nearly vanishing A-terms and the gaugino masses in such a regime are very nearly universal, as can be seen from the lower panels of Figure 3.3. However, as the Green-Schwarz coefficient is reduced the gaugino masses become negligible at the point $\langle \mathrm{Re}\, t \rangle \approx 2$, eventually coming into conflict with direct search results at LEP and the Tevatron. Specific spectra for the O-II model will be presented with spectra for orbifold models with large threshold corrections in Section 3.4.

3.3 BIM O-I Models

Models of this type were proposed with the goal of obtaining coupling constant unification at the string scale, as opposed to the extrapolated unification scale of $\Lambda_{\mathrm{GUT}} \approx 2 \times 10^{16}$ GeV which is typically a factor of twenty or so lower than the string scale. This is achieved through large string threshold corrections and the requirement of both particular sets of modular weights for the massless fields and relatively large values of $\langle \mathrm{Re}\, t \rangle$ far from the self-dual points. Other solutions to this discrepancy of scales have been proposed since but because the O-I models have often been discussed in the literature we include them in the present discussion.

To investigate the phenomenological consequences of such models we will assume a common vacuum value for all three moduli and take $\Theta_\alpha = 1/\sqrt{3}$ as before. We shall investigate two scenarios: (A) the original "O-I" scenario of Brignole et al. [35, 36] with modular weights $n_Q = n_D = -1$, $n_U = -2$, $n_L = n_E = -3$, $n_{H_d}, n_{H_u} = -4$ and (B) a $Z_3 \times Z_6$ compactification studied by Love and Stadler [116] with modular weights $n_Q = n_D = 0$, $n_U = -2$, $n_L = -4$, $n_E = -1$, $n_{H_d} = n_{H_u} = -1$. In what follows let us assume that the soft terms emerge at a

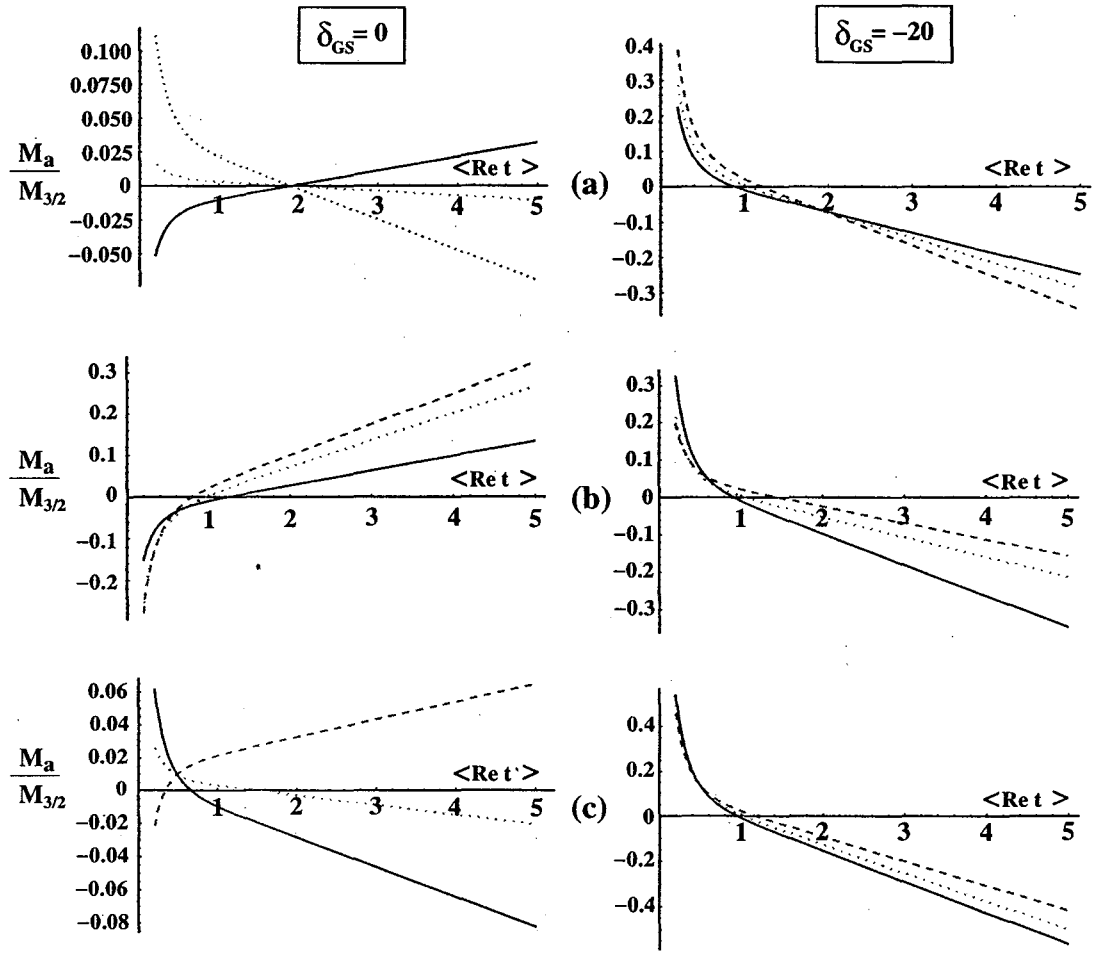

Figure 3.5: Relative Gaugino Masses in the BIM O-II and BIM O-I Models with $\theta = 0$. Relative sizes of the three gaugino masses M_1 (dashed), M_2 (dotted) and M_3 (solid) are displayed as a function of $\langle \mathrm{Re}\, t \rangle$ for two values of the Green-Schwarz coefficient δ_{GS} and $\Lambda_{\mathrm{UV}} = 2 \times 10^{16}$ GeV. The top panels (a) represent the BIM O-II model from Section 3.2, the middle panels (b) represent the BIM O-I model and the bottom panels (c) represent the Love & Stadler case from [116]. All masses are relative to the gravitino mass $M_{3/2}$.

scale for which logarithms such as $\ln(\tilde{\mu}^2_{ia})$ and $\ln(\tilde{\mu}^2_{jk})$ are negligible and assume PV case (A) for simplicity. In this approximation the general expressions of Appendix B take a simplified form. The gaugino masses, given by

$$\begin{aligned} M_a^{tot} &= g_a^2(\mu)\frac{\overline{M}}{3}\left\{ b_a^0 + \cos\theta(t+\bar{t})G_2\left[\frac{\delta_{\mathrm{GS}}}{16\pi^2} + b_a^0 - \frac{1}{8\pi^2}\sum_i C_a^i(1+n_i)\right]\right. \\ &\quad \left. + \frac{\sqrt{3}\sin\theta}{2k_{s\bar{s}}^{1/2}}\left[1 + \frac{g_s^2}{16\pi^2}\left(C_a - \sum_i C_a^i\right)\right]\right\}, \end{aligned} \tag{3.20}$$

are displayed in Figure 3.5 with the value $\theta = 0$ (where the impact of the differing modular weights is the greatest) for three models: the BIM O-II case of Section 3.2, the original BIM O-I case and the Love & Stadler case. The boundary scale is taken to be $\Lambda_{\mathrm{UV}} = 2 \times 10^{16}$ GeV.[3]

[3]Though these models are designed to allow for unification of gauge couplings at the string scale $\Lambda_{\mathrm{STR}} \approx$

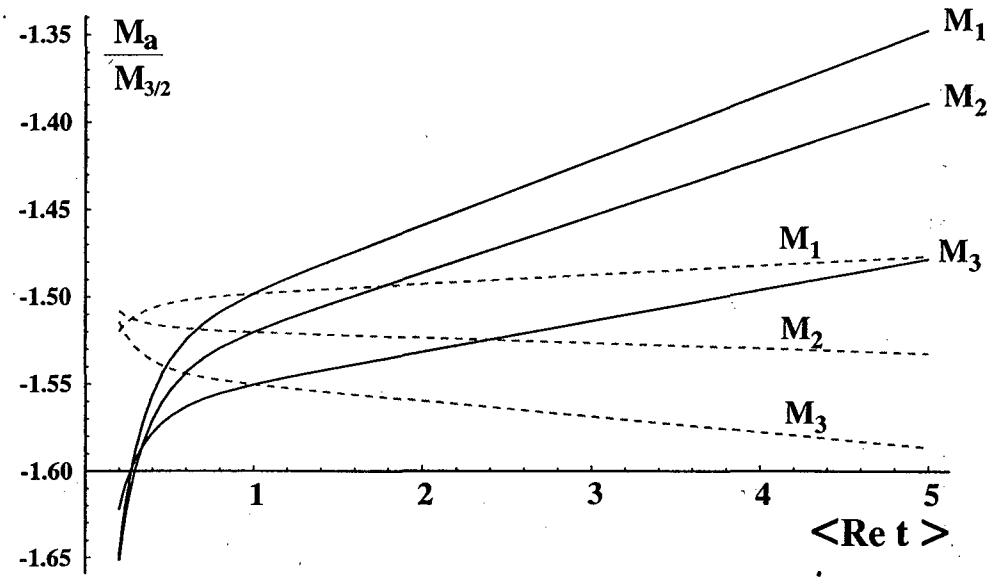

Figure 3.6: Relative Gaugino Masses in the BIM O-I Models with $\theta = \pi/3$ and $\delta_{GS} = 0$. Relative sizes of the three gaugino masses are displayed as a function of $\langle \mathrm{Re}\, t \rangle$ for the BIM O-I model (solid) and the Love & Stadler model (dashed) at $\Lambda_{UV} = 2 \times 10^{16}$ GeV. All masses are relative to the gravitino mass $M_{3/2}$.

It is clear from Figure 3.5 that the modular weights of the matter fields play a crucial role in determining the gaugino mass spectrum provided the Green-Schwarz coefficient is sufficiently small. As this parameter is increased it will quickly come to dominate the other terms in (3.20).

However, looking at the tree level expressions for the scalar masses (3.4) it is apparent that when $\cos\theta = 1$ any field with a modular weight such that $n_i < -1$ will have a negative tree level squared scalar mass, as was noted in [35, 36]. Thus, to accommodate these large threshold models proper electroweak symmetry breaking (*i.e.* positive squared scalar masses) will generally require a Goldstino angle such that $\sin\theta$ is large and the tree level terms in (3.20) are dominant. Models with a viable low energy vacuum will therefore be models for which the impact of the matter fields' modular weights on the gaugino spectrum is considerably muted. This is displayed in Figure 3.6 where gaugino masses in the BIM O-I model and the Love & Stadler model are displayed for $\theta = \pi/3$ and $\delta_{GS} = 0$. We see that in these realistic cases the differences in gaugino mass spectra between these models is small, making them hard to distinguish experimentally.

The trilinear A-terms for scenario (A) are

$$A_{ijk}^{tot} = \frac{\overline{M}}{3}\left\{-\gamma_i + \frac{\cos\theta}{3}(t+\bar{t})G_2(n_i+n_j+n_k+3) - \frac{\sin\theta}{\sqrt{3}}\frac{k_s}{k_{s\bar{s}}^{1/2}}\right\} + \text{cyclic (ijk)}, \tag{3.21}$$

5×10^{17} GeV, we will investigate the pattern of soft supersymmetry breaking terms at the GUT scale to allow for comparison with other models.

Model	Anomaly (3.1)	O-II (3.2)					O-I (3.3)	L&S (3.3)
θ	0	0	0	0	0	$\pi/3$	$\pi/3$	$\pi/3$
δ_{GS}	N/A	0	0	0	-90	-90	-90	-90
$\langle \mathrm{Re}\, t \rangle$	1	$6/\pi$	5	20	$6/\pi$	$6/\pi$	16	14.5
$M_{3/2}$	1.9×10^4	1.9×10^4	1.6×10^4	4500	1600	450	150	150
$m_{\tilde{N}_1}$	51.81	0.32	152.53	248.97	332	313	287	297
$m_{\tilde{N}_2}$	168	3.7	462	759	615	599	557	581
$\tilde{B}$ %	0.01	80.9	0.001	0.001	99.9	99.9	99.9	99.9
$\tilde{W}_3$ %	99.7	19.1	99.7	99.7	0.001	0.001	0.001	0.001
$m_{\tilde{\chi}_1^\pm}$	51.83	3.1	152.55	249.00	615	599	557	581
$m_{\tilde{g}}$	623	3.6	1468	2245	2156	2164	2106	2128
m_h	114	114	114	114	114	114	114	114
m_A	2237	2217	1992	1357	1447	1387	1810	1568
$m_{\tilde{t}_R}$	860	796	1142	1597	1521	1610	1373	1532
$m_{\tilde{t}_L}$	1842	1810	1818	1820	1804	1866	1709	1793
$m_{\tilde{b}_R}$	1805	1765	1802	1769	1782	1847	1701	1773
$m_{\tilde{b}_L}$	1810	1770	1824	1908	1883	1945	1881	1871
$m_{\tilde{\tau}_R}$	1191	1180	1076	514	329	302	198	290
$m_{\tilde{\tau}_L}$	1193	1182	1078	515	330	303	281	301
A_{top}	391	71	-815	-1423	1696	1541	560	1607
A_{bot}	973	463	-999	-1827	2819	2200	-405	4650
A_{tau}	220	273	376	305	466	-184	-7417	-2734
μ	1617	1592	1501	1281	1341	1302	1577	1297

Table 3.2: Sample Spectra (in GeV) for Typical Models of Sections 3.1, 3.2 and 3.3. All cases are for PV scenario (A), $\tan\beta = 3$ and $\Lambda_{\mathrm{UV}} = 2 \times 10^{16}$ GeV ($\tilde{B}$ % and $\tilde{W}_3$ % represent the content of the lightest neutralino in per cents). The first O-II case considered, while clearly ruled out experimentally, is presented as an illustrative example.

and the scalar masses are determined from

$$
\begin{aligned}
(M_i^{tot})^2 &= \frac{|M|^2}{9}\Bigg\{(1+\gamma_i) + \cos\theta(t+\bar{t})G_2 \sum_{jk} \gamma_i^{jk}(n_i+n_j+n_k+3) + n_i\cos^2\theta \\
&\quad + \frac{\sqrt{3}\sin\theta}{k_{s\bar{s}}^{1/2}}\left(\sum_a \gamma_i^a g_a^2 - \frac{1}{2}\sum_{jk}\gamma_i^{jk}\,(k_s + k_{\bar{s}})\right)\Bigg\}, \qquad (3.22)
\end{aligned}
$$

With these expressions we are now in a position to compare the typical spectra of these O-I large threshold models with the models of Section 3.1 and Section 3.2.

3.4 Comparisons

In Tables 3.2 and 3.3 we give some representative sample spectra for Pauli-Villars scenario (A) defined by (3.5) and $\tan\beta = 3$ and $\tan\beta = 10$, respectively. The spectra for scenario (B) are very similar and these values vary only minimally when Λ_{UV} is varied. To obtain these spectra at the electroweak scale the renormalization group equations (RGEs) were run from the boundary scale to the electroweak scale. All gauge and Yukawa couplings as well as gaugino masses and A-terms were run with one loop RGEs while scalar masses were run at two loops to capture the possible effects of heavy scalars on the evolution of third generation squarks and sleptons. We chose to keep only the top, bottom and tau Yukawas and the corresponding A-terms. The

gravitino mass has been scaled in each case to obtain a Higgs mass of 114 GeV, which can be considered either as a limiting case or as an experimental requirement, depending on what happens next at LEP.

At the electroweak scale the one loop corrected effective potential $V_{1-\text{loop}} = V_{\text{tree}} + \Delta V_{\text{rad}}$ is computed and the effective μ-term $\bar{\mu}$ is calculated

$$\bar{\mu}^2 = \frac{\left(m_{H_d}^2 + \delta m_{H_d}^2\right) - \left(m_{H_u}^2 + \delta m_{H_u}^2\right)\tan^2\beta}{\tan^2\beta - 1} - \frac{1}{2}M_Z^2. \tag{3.23}$$

In equation (3.23) the quantities δm_{H_u} and δm_{H_d} are the second derivatives of the radiative corrections ΔV_{rad} with respect to the up-type and down-type Higgs scalar fields, respectively. These corrections include the effects of all third generation particles. If the right hand side of equation (3.23) is positive then there exists some initial value of μ at the condensation scale which results in correct electroweak symmetry breaking with $M_Z = 91.187$ GeV.[4]

Note that the gravitino mass varies greatly over the models considered in Tables 3.2 and 3.3. For the anomaly case (which is equivalent to the BIM O-II model with $\sin\theta = 0$ and $\langle \text{Re } t\rangle = 1$) there is a large hierarchy between scalars and gauginos, as noted in Section 3.1, which necessitates a large value of the gravitino mass to yield neutralinos with masses near the current LEP limits. Having normalized our scales to yield Higgs masses of 114 GeV we find chargino masses (for PV scenario (A) and thus $p = 0$ in Figure 3.1) below the recently reported bounds of $m_{\chi^\pm} \geq 86.1$ GeV for the case of a chargino which is nearly degenerate with a wino-like lightest neutralino [113]. As the PV scenario assumed is modified, however, this relation between the chargino mass and Higgs mass varies. In particular as the value of p approaches larger, positive values the gauginos steadily become heavier for a fixed Higgs mass, eventually satisfying the experimental constraints. For the large threshold models, by contrast, the large values of $\langle \text{Re } t\rangle$ necessary to ensure gauge coupling unification at the string scale make the gauginos typically *heavier* than the gravitino at the boundary scale Λ_{UV}, due to the large value of $(t + \bar{t})G_2$, and have a smaller degree of hierarchy between gauginos and scalars.

The O-II models can interpolate between these two extremes. When $\theta = 0$ and $\delta_{\text{GS}} = 0$ the pattern of physical masses shows the anomaly mediated feature of a wino-like lightest supersymmetric particle (LSP). As the value of $\langle \text{Re } t\rangle$ increases from $\langle \text{Re } t\rangle = 1$ (the pure anomaly mediated case) it first passes through the experimentally excluded values where $\langle \text{Re } t\rangle \approx 6/\pi$ and the gaugino masses are nearly zero. Thereafter the hierarchy between gauginos and scalars steadily decreases until the spectra of masses is very similar to that of the more typical supergravity spectra to the right of Table 3.2. However, as mentioned at the end of the previous section the feature of a wino-like LSP persists. Once $\theta \neq 0$ and/or $\delta_{\text{GS}} \neq 0$ the pattern of soft terms immediately becomes relatively insensitive to the value of $\langle \text{Re } t\rangle$ and the LSP once again becomes predominantly bino-like. The properties of the LSP are of paramount importance to the question of neutralino dark matter, as we will see in Section 4.

The models with large threshold corrections also tend to have very light staus. In fact, as the value of $\tan\beta$ increases the stau mass $m_{\tilde{\tau}_R}$ eventually becomes negative. The limiting value of $\tan\beta$ for which these models are phenomenologically viable depends slightly on the value of δ_{GS}: for $\theta = \pi/3$ the model of Love & Stadler requires $\tan\beta < 9.1$ when $\delta_{\text{GS}} = -90$ and $\tan\beta < 4.8$

[4]Note that for these tables we do not try to specify the origin of this μ-term (nor its associated B-term) and merely leave them as free parameters in the theory – ultimately determined by the requirement that the Z-boson receive the correct mass.

Model	Anomaly (3.1)	O-II (3.2)					O-I (3.3)	L&S (3.3)
θ	0	0	0	0	0	$\pi/3$	$\pi/3$	$\pi/3$
δ_{GS}	N/A	0	0	0	-90	-90	-90	-90
$\langle \mathrm{Re}\, t \rangle$	1	$6/\pi$	5	20	$6/\pi$	$6/\pi$	16	14.5
$M_{3/2}$	8000	8000	6500	1800	1200	200	N/A	N/A
$m_{\tilde{N}_1}$	20.20	0.17	62.11	98.72	139	129		
$m_{\tilde{N}_2}$	70	3.11	187	301	260	244		
$\tilde{B}$ %	0.08	79.2	0.002	1.9×10^{-7}	99.3	99.1		
$\tilde{W}_3$ %	98.0	20.8	97.8	97.4	0.001	0.002		
$m_{\tilde{\chi}_1^\pm}$	20.21	2.5	62.14	98.75	260	244		
$m_{\tilde{g}}$	280	1.85	644	978	1020	979		
m_h	114	114	114	114	114	114		
m_A	797	790	689	485	560	497		
$m_{\tilde{t}_R}$	449	427	527	658	663	667		
$m_{\tilde{t}_L}$	797	782	774	806	849	819		
$m_{\tilde{b}_R}$	739	720	727	737	792	771		
$m_{\tilde{b}_L}$	763	744	753	799	838	812		
$m_{\tilde{\tau}_R}$	493	490	431	206	147	121		
$m_{\tilde{\tau}_L}$	503	499	440	211	156	132		
A_{top}	190	47	-336	-596	796	668		
A_{bot}	398	187	-403	-858	1223	893		
A_{tau}	83	108	153	130	190	100		
μ	578	565	529	495	559	499		

Table 3.3: Sample Spectra (in GeV) for Typical Models of Sections 3.1, 3.2 and 3.3. The same as in Table 3.2 but for $\tan\beta = 10$. Neither of the large threshold models are viable at this value of $\tan\beta$.

when $\delta_{GS} = 0$, while the original BIM O-I model requires $\tan\beta < 3.1$ when $\delta_{GS} = -90$ and is not allowed at all for $\delta_{GS} = 0$. This is reflected in the empty columns in Table 3.3. This problem is slightly ameliorated when the Goldstino angle is increased. For $\theta = 2\pi/5$, for example, the model of Love & Stadler requires $\tan\beta < 12.7$ when $\delta_{GS} = -90$ and $\tan\beta < 9.6$ when $\delta_{GS} = 0$, while the original BIM O-I model requires $\tan\beta < 4.9$ when $\delta_{GS} = -90$ and $\tan\beta < 2.1$ when $\delta_{GS} = 0$.

The pattern of masses exhibited in Tables 3.2 and 3.3 suggests that the hierarchy between gauginos and scalars in any potential observation of supersymmetry will be a key to understanding the nature of the underlying physics giving rise to supersymmetry breaking. The observation of a lightest neutralino with significant wino content will not be enough to distinguish between the pure anomaly mediated cases and the BIM O-II type models but *will* indicate that supersymmetry breaking is moduli dominated within this class of models. The presence of a large hierarchy between scalars and gauginos and large mixing in the stop sector will point towards moduli stabilized at or near their self-dual values, while the absence of such effects would suggest the moduli are stabilized far from these values.

Chapter 4

Dark Matter Constraints

It has long been held that one of the prime virtues of supersymmetry as an explanation of the hierarchy problem is that it tends to also provide a solution to the dark matter problem as a nearly automatic consequence of R-parity conservation. The lightest supersymmetric particle (LSP) is then stable and, as it tends to be a neutral gaugino, it will typically have the right mass and annihilation rate in the early universe to provide sufficient mass density today to account for observations suggesting $\rho_{\rm tot} \simeq \rho_{\rm crit}$ [69, 96, 141].

This section initially investigates the dark matter implications of the most widely studied benchmark in supersymmetric phenomenology, the constrained Minimal Supersymmetric Standard Model (cMSSM). As we are primarily interested in a gaugino-like LSP we will restrict ourselves to low values of $\tan\beta$ for which the Higgsino content of the lightest neutralino is negligibly small. We emphasize that the cMSSM in this context typically fails to solve the dark matter problem over most of its parameter space, with the exception of certain very special patterns of soft supersymmetry breaking terms. These patterns must constrain the neutralino (a fermion) to have a very specific mass relationship to an unrelated boson such as the lightest Higgs or the stau. Barring these relationships, the cMSSM tends to predict too much dark matter – thus bringing it into conflict with direct measurements of the age of the universe [50, 60, 104, 126]. We find this failure to be due, in part, to the cMSSM constraint on the gaugino mass ratio M_2/M_1. Eliminating this assumption of universal gaugino masses uncovers new regions of parameter space that allow for cosmologically allowed, and often experimentally preferred, values of the neutralino relic density.

This chapter is organized as follows: in Section 4.1 we present our methodology in the context of the cMSSM with its standard minimal supergravity (mSUGRA) universal soft supersymmetry breaking terms. Subsequently, in Section 4.2, we relax our assumption of universal gaugino masses. While the relic density implications of nonuniversal gaugino masses, and in particular the role of M_2/M_1 in dark matter phenomenology, have been explored previously these past studies have either focused on specific models or have not included the important effects of coannihilation between the LSP and the lightest chargino [44, 49, 99].[1]

Later, in Section 5.4 we consider a specific class of supergravity models derived from heterotic string theory which implement supersymmetry breaking through gaugino condensation in a

[1] A noteworthy exception is Ref. [122] though it focuses primarily on a purely wino-like LSP scenario with LSP masses below M_W.

hidden sector [27, 28, 29, 84] as an example of how the general results of Section 4.2 can be applied on a model-by-model basis. Requiring a cosmologically relevant thermal LSP relic density will imply very specific conclusions about the content of the hidden sector of these models.

4.1 Universal Gaugino Masses

The phenomenological consequences of the cMSSM have been studied extensively [19, 51, 106, 107], including the cosmological implications of its (presumed stable) LSP [10, 20, 63, 70, 98, 115, 132, 133]. In such a regime the entire low energy phenomenology is specified by five parameters: a common gaugino mass $M_{1/2}$, a common scalar mass M_0, a common trilinear scalar A-term A_0, the value of $\tan\beta$ and the sign of the μ-parameter in the scalar potential. These values are defined at some high energy scale, which we will take here to be the scale of gauge coupling unification $\Lambda_{\rm UV} \sim 2 \times 10^{16}$ GeV.

To obtain the superpartner spectrum at the electroweak scale the renormalization group equations are run in the manner described in 3.4 from the boundary scale to the electroweak scale. The neutralino states and their masses are calculated using the neutralino mass matrix

$$\begin{pmatrix} M_1 & 0 & -\sin\theta_W \cos\beta M_Z & \sin\theta_W \sin\beta M_Z \\ 0 & M_2 & \cos\theta_W \cos\beta M_Z & -\cos\theta_W \sin\beta M_Z \\ -\sin\theta_W \cos\beta M_Z & \cos\theta_W \cos\beta M_Z & 0 & -\mu \\ \sin\theta_W \sin\beta M_Z & -\cos\theta_W \sin\beta M_Z & -\mu & 0 \end{pmatrix}, \tag{4.1}$$

where M_1 is the mass of the hypercharge U(1) gaugino at the electroweak scale and M_2 is the mass of the SU(2) gauginos at the electroweak scale. The matrix (4.1) is given in the $(\tilde{B}, \tilde{W}_3, \tilde{H}_d^0, \tilde{H}_u^0)$ basis, where $\tilde{B}$ represents the bino, $\tilde{W}_3$ represents the neutral wino and $\tilde{H}_d^0$ and $\tilde{H}_u^0$ are the down-type and up-type Higgsinos, respectively.[2] More generally the content of the LSP can be parametrized by writing the lightest neutralino as:

$$\chi_1^0 = N_{11}\tilde{B} + N_{12}\tilde{W}_3 + N_{13}\tilde{H}_d^0 + N_{14}\tilde{H}_u^0, \tag{4.2}$$

which is normalized to $N_{11}^2 + N_{12}^2 + N_{13}^2 + N_{14}^2 = 1$. Thus by saying that the bino content of the lightest neutralino is high, we mean $N_{11} \simeq 1$.

The lightest eigenvalue of this matrix is then typically the LSP and it is overwhelmingly bino-like in content over most of the parameter space when $\tan\beta$ is low. This is because the cMSSM universality constraint on gaugino masses at the high scale of the theory implies $M_1 \simeq \frac{1}{2}M_2$ when the masses are evolved to the electroweak scale via the RGEs. Provided $|M_1|, |M_2| \ll |\mu|$, which is the case for low $\tan\beta$, the LSP mass is then dominated by M_1 and has a typical bino content of $\gtrsim 99\%$. We will restrict ourselves to this low $\tan\beta$ regime and adopt a value of $\tan\beta = 3$ for the remainder of the chapter. The dark matter prospects of the high $\tan\beta$ limit, and in particular the possibility of heavy scalars in such a regime, have been studied recently by Feng et al. [73].

Given the particle spectrum we compute the thermal relic LSP density with a modified version of the software package *neutdriver* [105]. This program includes all of the annihilation processes

[2] Loop corrections at next-to-leading order [90] to this mass matrix have been incorporated and found to have little effect on the results that follow.

computed by Drees and Nojiri [61] which are used to compute a thermally averaged cross section $\langle\sigma v\rangle_{\rm ann}$ and freeze-out temperature $x_F = T_F/m_{\chi_1^0}$. From knowledge of the mass of the lightest neutralino $m_{\chi_1^0}$ (assumed to be the LSP), $\langle\sigma v\rangle_{\rm ann}$ and T_F, a relic abundance can be computed using the standard approximation [105]

$$\Omega_\chi h^2 = \frac{1.07\times 10^9 x_F}{g_*^{1/2} M_{\rm Pl}\left(a_{\rm eff} + 3\left(b_{\rm eff} - a_{\rm eff}/4\right)/x_F\right)}\ {\rm GeV}^{-1}, \tag{4.3}$$

where we have expressed the thermally averaged annihilation cross section as an expansion in powers of the relative velocity:

$$\langle\sigma v\rangle_{\rm ann} = a_{\rm eff} + b_{\rm eff} v^2 + \cdots \tag{4.4}$$

A proper determination of relic LSP densities requires that the above computation be amended to include the possible effects of coannihilation [97, 100, 123]. This occurs when another particle is only slightly heavier than the lightest neutralino so that both particles freeze out of equilibrium at approximately the same temperature. The neutralino can now not only deplete its relic abundance through annihilation processes such as $\chi_1^0\chi_1^0 \to e^+e^-$, but also through interactions with the coannihilator such as $\chi_1^\pm\chi_1^0 \to e^\pm\nu_e$. The extreme importance of including relevant coannihilation channels has recently been emphasized for the case of the cMSSM [64, 65, 66, 67, 68], and in that spirit we have added a number of coannihilation channels which are relevant for both the universal gaugino mass case [64, 66, 67] as well as the case of nonuniversal gaugino masses to be considered in Section 4.2.

The program *neutdriver* includes $\chi^\pm\chi_1^0$ coannihilation to $W^\pm\gamma$ [44] and two (massless) fermions $f\bar{f}'$ which we recalculated to account for non-zero fermion masses. We have also included a calculation of the process $\chi^\pm\chi_1^0 \to W^\pm Z$, and found this channel to often dominate when kinematically accessible. Additionally, we have inserted the results of [65, 68] for $\chi_1^0\tilde{\tau}$ coannihilation to $Z\tau$, $\gamma\tau$, $h\tau$, and $H\tau$ final states.

The region of cMSSM parameter space that gives rise to acceptable levels of bino-like LSP relic density is given in Figure 4.1 where we have plotted contours of $\Omega_\chi h^2 = 0.1$, 0.3 and $\Omega_\chi h^2 = 1$. Here Ω_χ is the fractional LSP matter density relative to the critical density and h is the reduced Hubble parameter: $h \simeq 0.65$ [130]. We have chosen $M_{1/2}$ and M_0 as free parameters in the manner of Ellis, Falk & Olive [64, 66, 67] with $\tan\beta = 3$, $A_0 = 0$ and positive μ-term.[3]

This plot is similar to the ones presented in [64, 66, 67] and we reproduce it here to draw attention to two important facts. First, observations suggest that the preferred values for cold dark matter densities are in the range $0.1 \le \Omega_\chi h^2 \le 0.3$ [15, 76], though including the latest evidence of a cosmological constant [126] may shift this to $0.06 \lesssim \Omega_\chi h^2 \lesssim 0.2$. This experimental data points to a region of the cMSSM parameter space in which both the universal scalar mass and the universal gaugino mass are small, on the order of 200 GeV for each (see, for example, the region around point A in Figure 4.1). In fact, heavy scalars can only be accommodated cosmologically if nature was kind enough to arrange the soft-supersymmetry breaking parameters so that the mass of the LSP is about half of the mass of the lightest Higgs boson. In that case, though t-channel scalar fermion exchange may be suppressed and the annihilation rate into two fermions is not sufficient to deplete the LSP density adequately, the annihilation through

[3] In our conventions this is the sign of μ least constrained by the measurement of the branching ratio for $b \to s\gamma$ events. This is the opposite convention used by the *neutdriver* package.

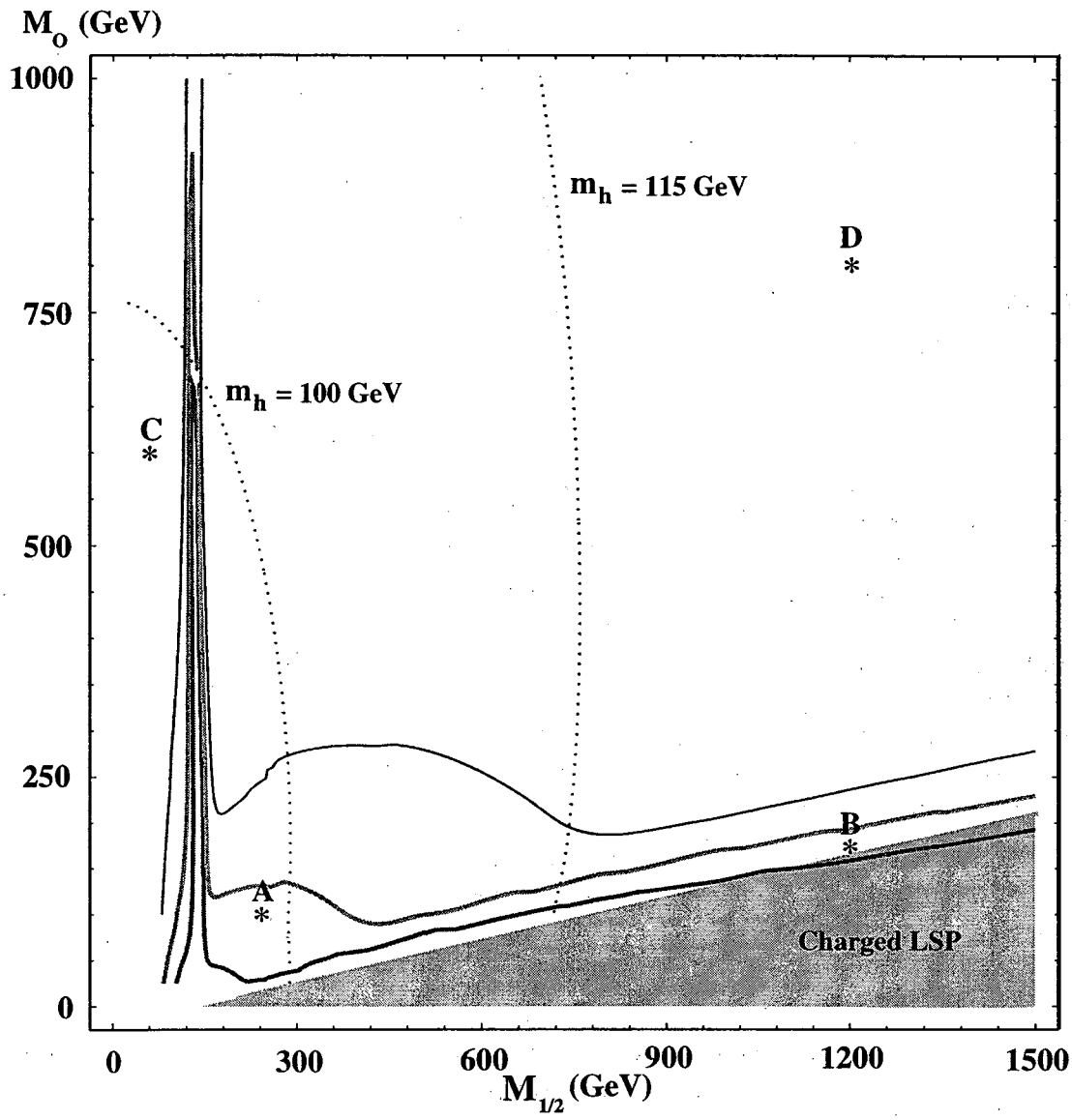

Figure 4.1: Preferred Dark Matter Region for the cMSSM. Contours of $\Omega_\chi h^2$ of 0.1 (bottom-most contour), 0.3 and 1.0 (top-most contour) are given. The shaded region is ruled out by virtue of having the stau as the LSP. The Higgs pole region and stau coannihilation tail are clearly discernible. We have also added contours of constant Higgs mass for $m_h = 100$ GeV and $m_h = 115$ GeV. The four labeled points are examined in Figure 4.2.

resonant s-channel exchange of the lightest Higgs is efficient enough to provide an acceptable dark matter region insensitive to the scalar mass.

Once we begin to impose constraints arising from Higgs searches at LEP, the preferred low mass region in Figure 4.1 begins to be ruled out. The only region which then remains in the $\{M_0, M_{1/2}\}$ plane for $\tan\beta = 3$ is that which is due to coannihilation between the LSP and the lightest stau. Being in this region requires a very specific relationship between the gaugino mass parameter and the unrelated scalar mass parameter. We have allowed our M_0 value to range to as much as a TeV, in contrast to [64, 66, 67], to accentuate the point that most of the cMSSM parameter space with moderate to heavy scalar masses predicts far *too much* neutralino relic

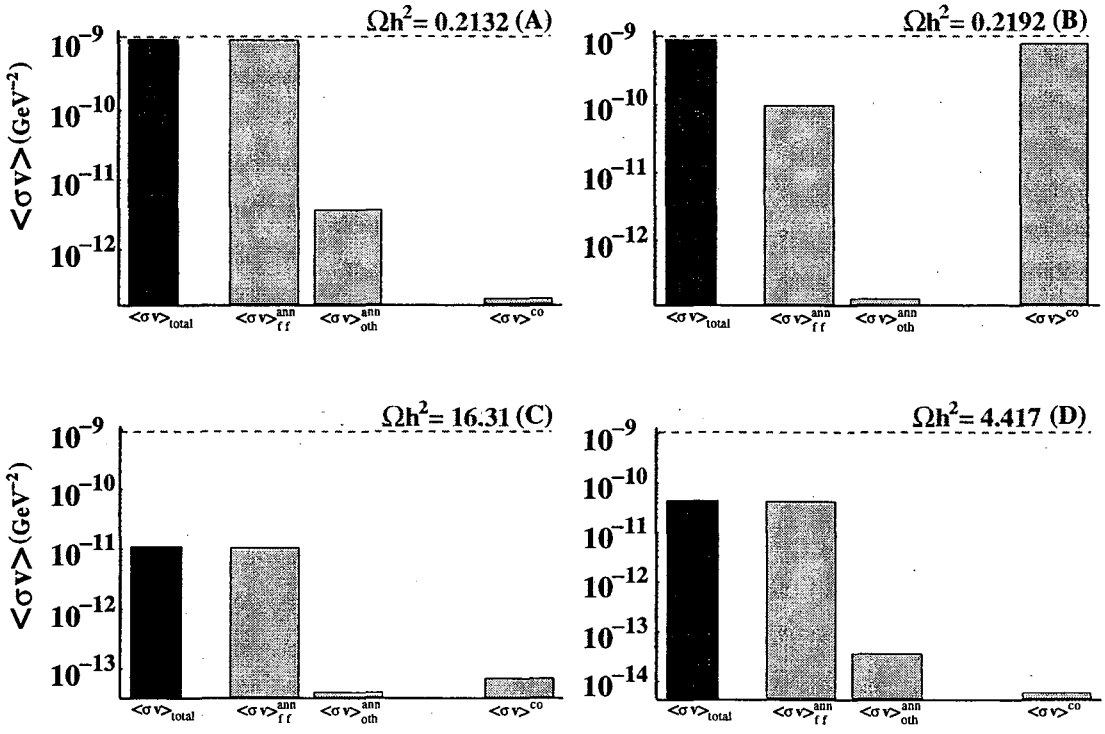

Figure 4.2: Annihilation Cross Sections for Selected Points from Figure 4.1. These graphs detail the composition of the neutralino depletion cross section. The total depletion cross section is on the far left. The next two columns divide the normal annihilation channels by final state into two fermions or all other annihilation channels. The final column is the sum of all coannihilation channels. The total relic density is given at the top of each plot and the dashed horizontal line illustrates the ideal total depletion cross section for a $\Omega_\chi h^2 = 0.2$.

density. Every point in Figure 4.1 above the $\Omega_\chi h^2 = 0.3$ line is already excluded by astrophysical measurements of the dark matter density.

To better illustrate the physics behind Figure 4.1 and to serve as a comparison for our subsequent analysis we have chosen four representative points from the parameter space for deeper investigation. Both points A and B fall within the cosmologically preferred region. Point B is in the coannihilation "tail," so we would expect most of the annihilation cross section to come from coannihilation. As we can see in Figure 4.2 the annihilation cross section of point B is indeed dominated by coannihilation. We can also see the importance of t-channel scalar fermion exchange to $\chi^0\chi^0 \to f\bar{f}$ in points A and B, which is due to the universal scalar mass being relatively light so that this channel is open. Referring back to Figure 4.1, both points C and D are in regions where there is too much relic density. Figure 4.2 shows that, indeed, the annihilation is too inefficient to eliminate enough dark matter. The annihilation channels to two fermions still dominate but now scalar fermion exchange is too suppressed to provide the critical annihilation rate (indicated by the dashed line). As with points C and D, most of the parameter space of the cMSSM is experimentally excluded since there is no efficient way of depleting the relic density.

It is a generic result of the low $\tan\beta$ cMSSM scenario that, excluding stau coannihilation, cosmological viability depends almost solely on the t-channel exchange of scalar fermions. This strict dependence causes most of the presumed parameter space with heavy scalars to be ex-

perimentally excluded, leaving the dark matter prospects of the cMSSM at low $\tan\beta$ in serious jeopardy.[4]

4.2 Nonuniversal Gaugino Masses

The reason for the failure of the low $\tan\beta$ cMSSM with heavy scalars to solve the dark matter problem is the low annihilation cross section for the neutralino. The only channel capable of providing a suitable cross section is the aforementioned t-channel scalar fermion exchange which is only efficient in a small region of parameter space. If we relax the GUT relationship between the gaugino masses but still remain in the large $|\mu|$ limit (low $\tan\beta$) then we will continue to have a predominantly *gaugino-like* LSP ($N_{11}^2 + N_{12}^2 \simeq 1$) with the relative values of N_{11} and N_{12} governed by the relative values of M_1 and M_2. Decreasing M_2 relative to M_1 at the electroweak scale increases the wino content of the LSP until ultimately $M_1 \gg M_2$ and $N_{11} \simeq 0$, $N_{12} \simeq 1$.

The bino component of the neutralino couples with a U(1) gauge strength whereas the wino component couples with the larger SU(2) gauge strength, thus enhancing its annihilation cross section and thereby lowering its relic density. As N_{12} is increased more parameter space should open up for dark matter until annihilation becomes too efficient in the pure wino-like limit and we are left with no neutralino dark matter at all [122]. This is evident in Figure 4.3 where we plot contours of $\Omega_\chi h^2$ as a function of scalar mass and the ratio (M_2/M_1) at the boundary condition scale $\Lambda_{\rm GUT}$. Allowing the gaugino masses to vary independently introduces two new degrees of freedom. We have chosen to vary the ratio (M_2/M_1) while fixing the value of $M_{1/2} \equiv \min(M_1, M_2)$ and M_3 at the high scale. In practice we use our choice of $M_{1/2}$ to determine the value of the smaller of the pair (M_1, M_2) at the high scale and then use the ratio (M_2/M_1) to determine the larger of (M_1, M_2). In Figure 4.3 we have set $M_{1/2} = 200$ GeV and $M_3 = M_{1/2}$.

Particular values of (M_2/M_1) which deviate from the universal cMSSM case allow for cosmologically interesting relic densities which are almost independent of the scalar mass. To see how dark matter physics changes as one departs from the cMSSM we have analyzed the six labelled points from Figure 4.3 in Figure 4.4. Starting with the two cMSSM points, E and F, the importance of the process $\chi_1^0\chi_1^0 \to f\bar{f}$ is again demonstrated. Point F has scalars that are too heavy for the two fermion final state to sufficently deplete the LSP relic density while point E has much lighter scalars, allowing efficient annihilation to two fermions and resulting in an appropriate amount of dark matter. Given the value of $M_{1/2} = 200$ GeV for this plot point E would lie a little to the left of point A in Figure 4.1.

Points C and D sit at much lower values of (M_2/M_1), resulting in a lightest chargino that is much more degenerate with the lightest neutralino. This enhances the importance of coannihilation channels, leading them to dominate the annihilation cross section. The main channels for coannihilation are $\chi^\pm\chi_1^0 \to f\bar{f}'$, making up the left-hand coannihilation column in Figure 4.4, and $\chi^\pm\chi_1^0 \to W^\pm Z$, which is the main contributor to the right-hand coannihilation column. Chargino-neutralino coannihilation has become so efficient here that the relic density is now not enough to account for observations. It should be noted that point D gives almost the cosmologically preferred relic density – its relic density is higher than that of point C for two reasons.

[4] At high values of $\tan\beta$ in the cMSSM, for which the LSP has a significant Higgsino component, heavy scalars can be accommodated and may even be preferred [73].

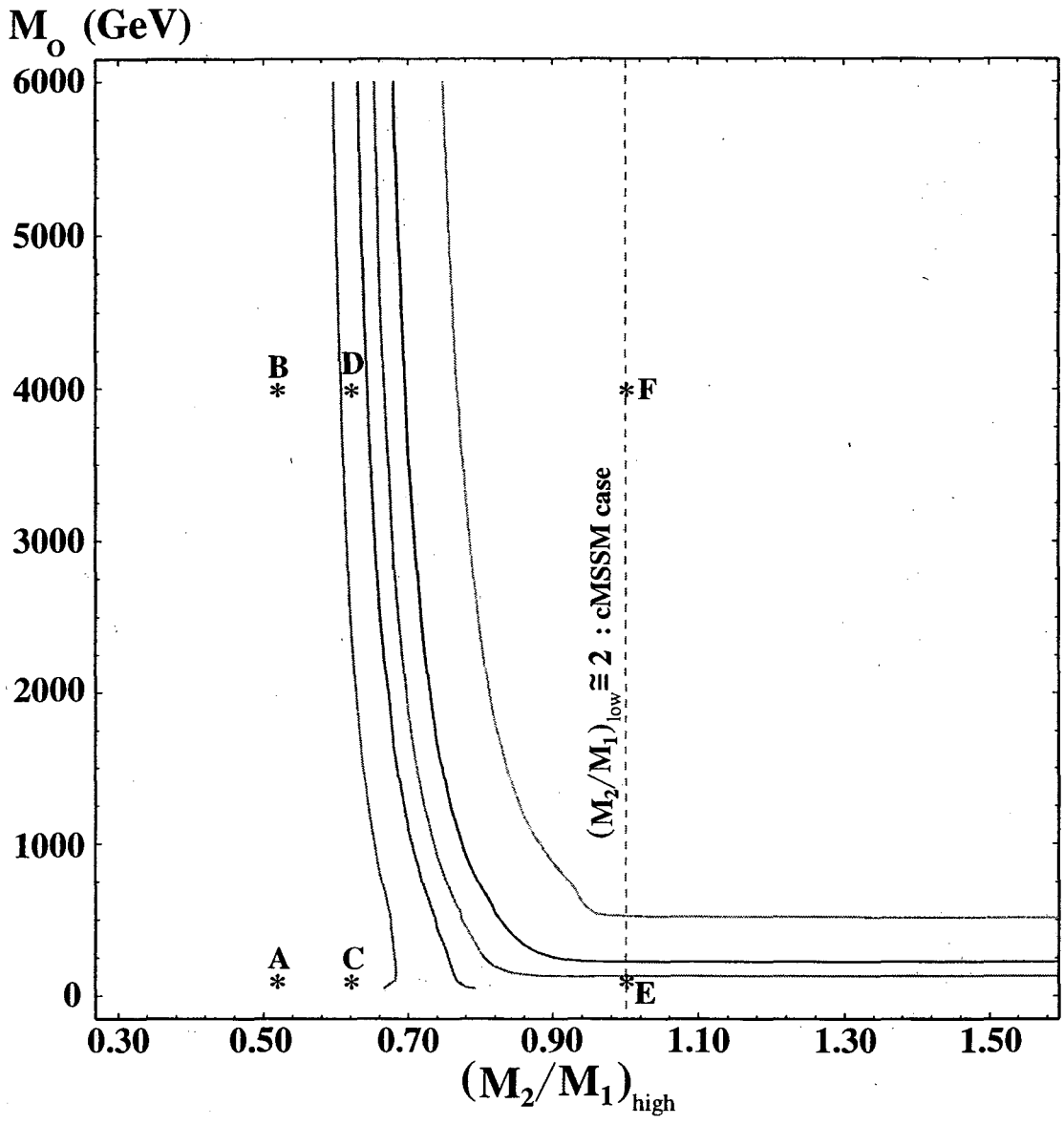

Figure 4.3: Preferred Dark Matter Region for Nonuniversal Gaugino Masses. Contours of $\Omega_\chi h^2$ of 0.01, 0.1, 0.3, 1.0 and 10.0 from left to right, respectively, are given as a function of the ratio of SU(2) to U(1) gaugino masses M_2/M_1 at the high scale. The cMSSM is recovered where the two masses are equal at the high scale, as has been indicated by the dashed line. The six labeled points are examined in Figure 4.4.

First, the mass of the lightest neutralino drops slightly in going from point D ($\sim$ 122 GeV) to point C ($\sim$ 112 GeV). Second, the lower scalar mass at point C allows t-channel exchange of scalar fermions to go unsuppressed. This is important in one of the diagrams contributing to $\chi^\pm\chi_1^0 \to f\bar{f}'$. The wino content of the lightest neutralino is also increased by lowering (M_2/M_1), causing the standard annihilation channel to two fermions to become relatively unimportant. This increase in efficiency continues through points A and B, now making the neutralino relic density cosmologically irrelevant.

The irrelevance of scalar masses above 1 TeV can be simply understood. Above 1 TeV the

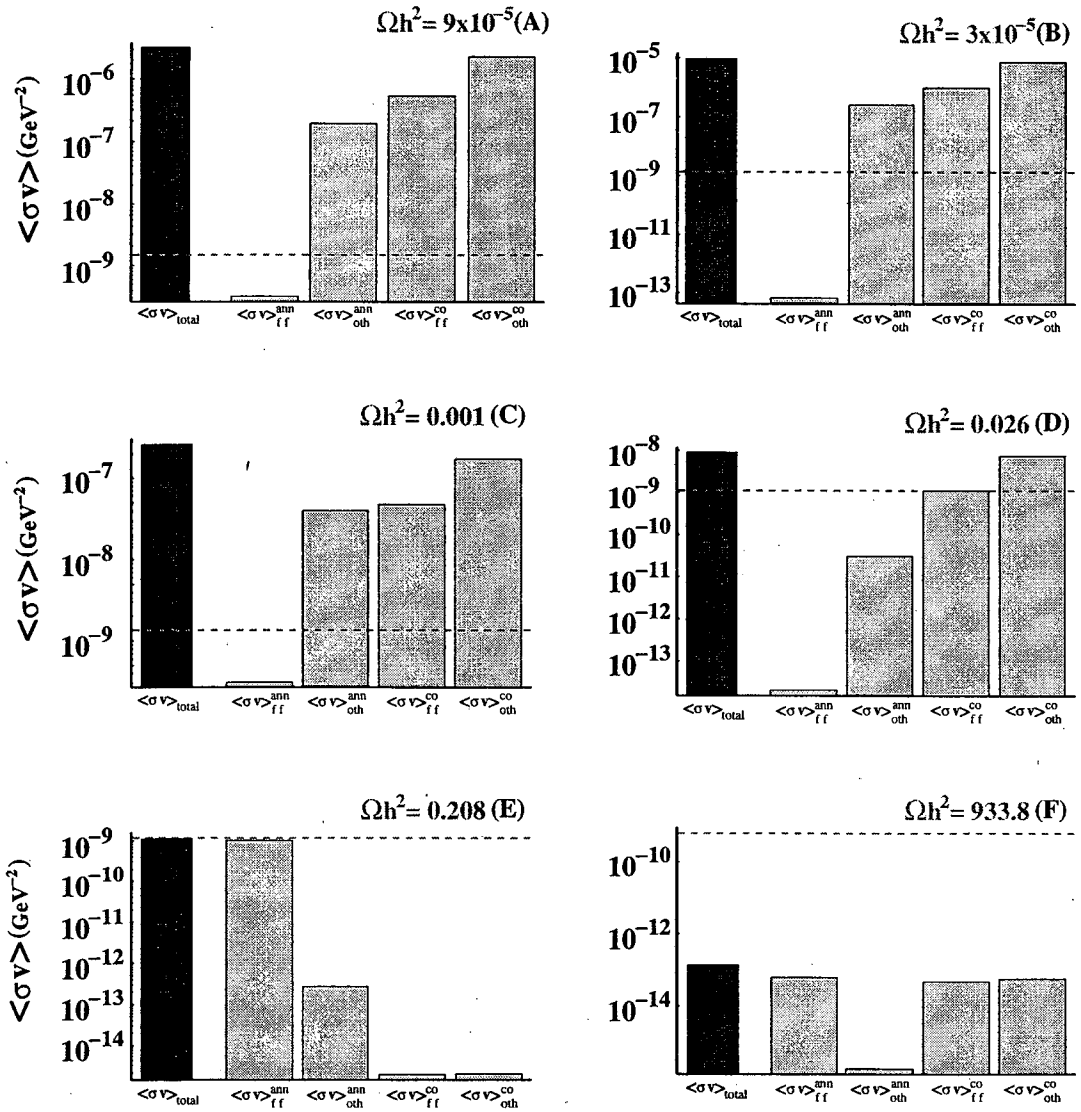

Figure 4.4: Annihilation Cross Sections for Selected Points from Figure 4.3. These graphs are identical in layout to those of Figure 4.2, except now the coannihilation channels are split into two columns: two-fermion final states and everything else.

t-channel scalar exchange contribution to $\chi_1^0\chi_1^0 \to f\bar{f}$ is suppressed due to the scalar mass. With enhanced wino content, however, channels that were previously suppressed are now more efficient, such as $\chi_1^0\chi_1^0 \to W^+W^-$. More importantly, we can also see from Figure 4.3 that much of the parameter space in the $\{M_0, (M_2/M_1)\}$ plane is not ruled out: an $\Omega_\chi h^2 \leq 0.1$ is not experimentally excluded, it just does not completely explain all of the needed dark matter.

Figure 4.5 examines the effect of changing the boundary scale value of M_3 on the cosmologically preferred parameter space of Figure 4.3. In Figure 4.5 and subsequent plots we impose the constraint that the LSP be electrically neutral and that the resulting spectrum at the electroweak scale satisfies the search limits of Table 4.1. The shaded region in panel (A) of Figure 4.5 is excluded by the gluino mass bound while the shaded region in panels (C) and (D) are excluded by the constraint on the stau mass. As the value of the gluino mass M_3 is increased relative to the other gaugino masses the cosmologically preferred range of the ratio (M_2/M_1) moves to

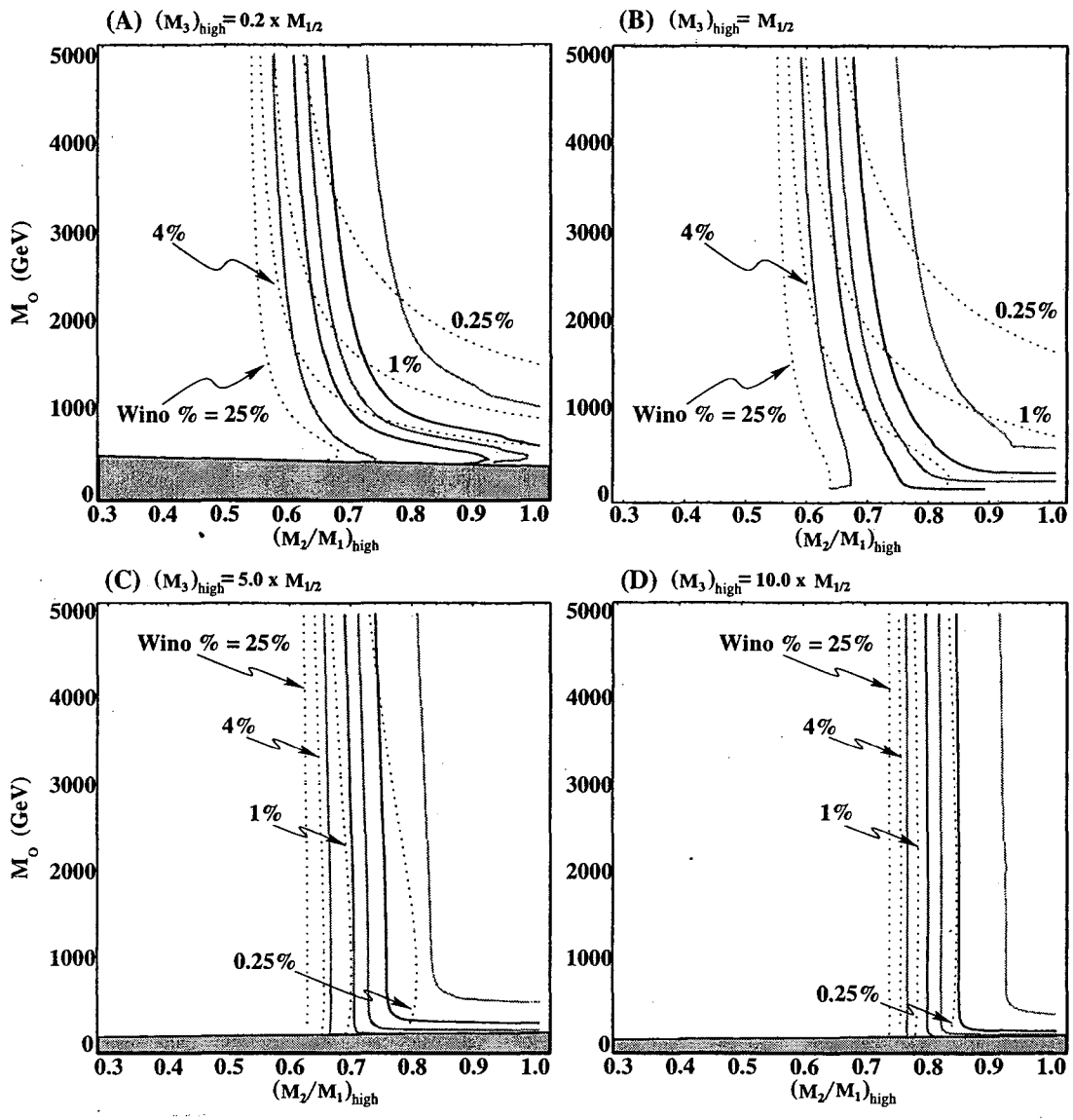

Figure 4.5: Preferred Dark Matter Region with Nonuniversal Gaugino Masses for Various M_3 Values [I]. Contours of constant relic density are given by the solid lines for $\Omega_\chi h^2 = 0.01$, 0.1, 0.3, 1, and 10 from left to right. The dotted lines are curves of constant wino content for $N_{12}^2 = 0.25$, 0.04, 0.01 and 0.025 from left to right. The value of the high-scale gluino mass M_3 is given in terms of the universal gaugino mass $M_{1/2}$ at the top of each plot. This plot uses a value of $M_{1/2} = 200$ GeV except for panel (A) where $M_{1/2} = 250$ GeV. The shaded region is excluded by the constraints of Table 4.1.

slightly higher values.

It is apparent from Figure 4.6 that the crucial variable in the determination of the LSP relic density is the value of the ratio (M_2/M_1) at the electroweak scale. The region of preferred relic density $0.1 \leq \Omega_\chi h^2 \leq 0.3$ consistently asymptotes to the region between the values $(M_2/M_1)_{\rm low} = 1.15$ and $(M_2/M_1)_{\rm low} = 1.25$ independent of the value of M_3, with the influence of the universal scalar mass M_0 most pronounced for small values of M_3. Most of the reason for this behavior is the composition of the low-scale squark masses. For large values of M_3 the RG evolution of the squark masses is dominated by M_3 which drives scalar masses to higher values

Gluino Mass	$m_{\tilde{g}}$	$>$	190 GeV
Lightest Neutralino Mass	$m_{\chi_1^0}$	$>$	32.5 GeV
Lightest Chargino Mass	$m_{\chi_1^\pm}$	$>$	75 GeV
Lightest Squark Masses	$m_{\tilde{q}}$	$>$	90 GeV
Lightest Slepton Masses	$m_{\tilde{l}}$	$>$	87 GeV
Light Higgs Mass	m_h	$>$	95.3 GeV
Pseudoscalar Higgs Mass	m_A	$>$	84.1 GeV
Charged Higgs Mass	$m_{H^\pm}$	$>$	69.0 GeV

Table 4.1: Superpartner and Higgs mass constraints imposed [125, 53].

and further suppresses the t-channel slepton and squark exchange diagrams. This causes the asymptotic approach to scalar-mass-independence to saturate for much lower values of M_0 than in the low M_3 case, where the value of squark and slepton masses is largely independent of M_3 and merely a function of the boundary value M_0 at the high scale.

These results are robust under changes in the relative sign between the soft supersymmetry breaking values of $M_{1,2}$ and M_3, as well as changes in the overall gaugino mass scale $M_{1/2}$, as is demonstrated in Figure 4.7. [5] For low values of M_3 there is little difference between the positive and negative values, though for high values of M_3 the entire plot moves from right to left when the sign is reversed. Nonetheless, the cosmologically preferred region falls between the same values of $(M_2/M_1)_{\text{low}}$ (denoted by dashed lines), regardless of the sign of M_3: it is only the preferred region of $(M_2/M_1)_{\text{high}}$ that changes with the sign flip. Both the effects of the magnitude of M_3 as well as its relative sign can be understood from the effect M_3 has on the running of M_2 and M_1, starting at two loops. The two loop running of the gaugino masses, in the conventions of [120], is partially given by

$$\frac{d}{dt}M_a \ni \frac{2g_a^2}{(16\pi^2)^2}\sum_{b=1}^{3} B_{ab}^{(2)} g_b^2 \left(M_a + M_b\right), \tag{4.5}$$

where $B_{ab}^{(2)}$ is a matrix of positive entries. Therefore the higher the value of $|M_3|$ the greater the impact on the gaugino masses M_1 and M_2. Furthermore, this effect is felt more strongly by the SU(2) gaugino mass than the U(1) gaugino mass. Thus for a given value of $(M_2/M_1)_{\text{high}}$ changing the sign of M_3 drives the value of M_2 higher at the electroweak scale to a greater degree than it does M_1, resulting in a higher value of $(M_2/M_1)_{\text{low}}$. This in turn leads to an increased relic density as can be seen by comparing the right and left sets of panels in Figure 4.7.

We have seen that relaxing the GUT constraint on the gaugino masses allows for significant improvement in the dark matter arena. This relaxation only requires a slight increase in the wino content of the LSP on the order of 0.1% to 5% (see Figure 4.5): the LSP is still predominantly bino-like and is not in the unappealling wino-dominated scenario which must rely on other mechanisms to generate supersymmetric dark matter [124]. The observations made in this section indicate that models which allow control over (M_2/M_1) at the boundary scale may be more suitable to providing supersymmetric dark matter than the unified cMSSM paradigm. In fact, requiring a cosmologically relevant relic LSP density may in turn shed light on the nature of physics at the GUT scale in models of supersymmetry breaking. We will carry out an example of

[5] For the effect of changing the relative sign between M_1 and M_2 see [122].

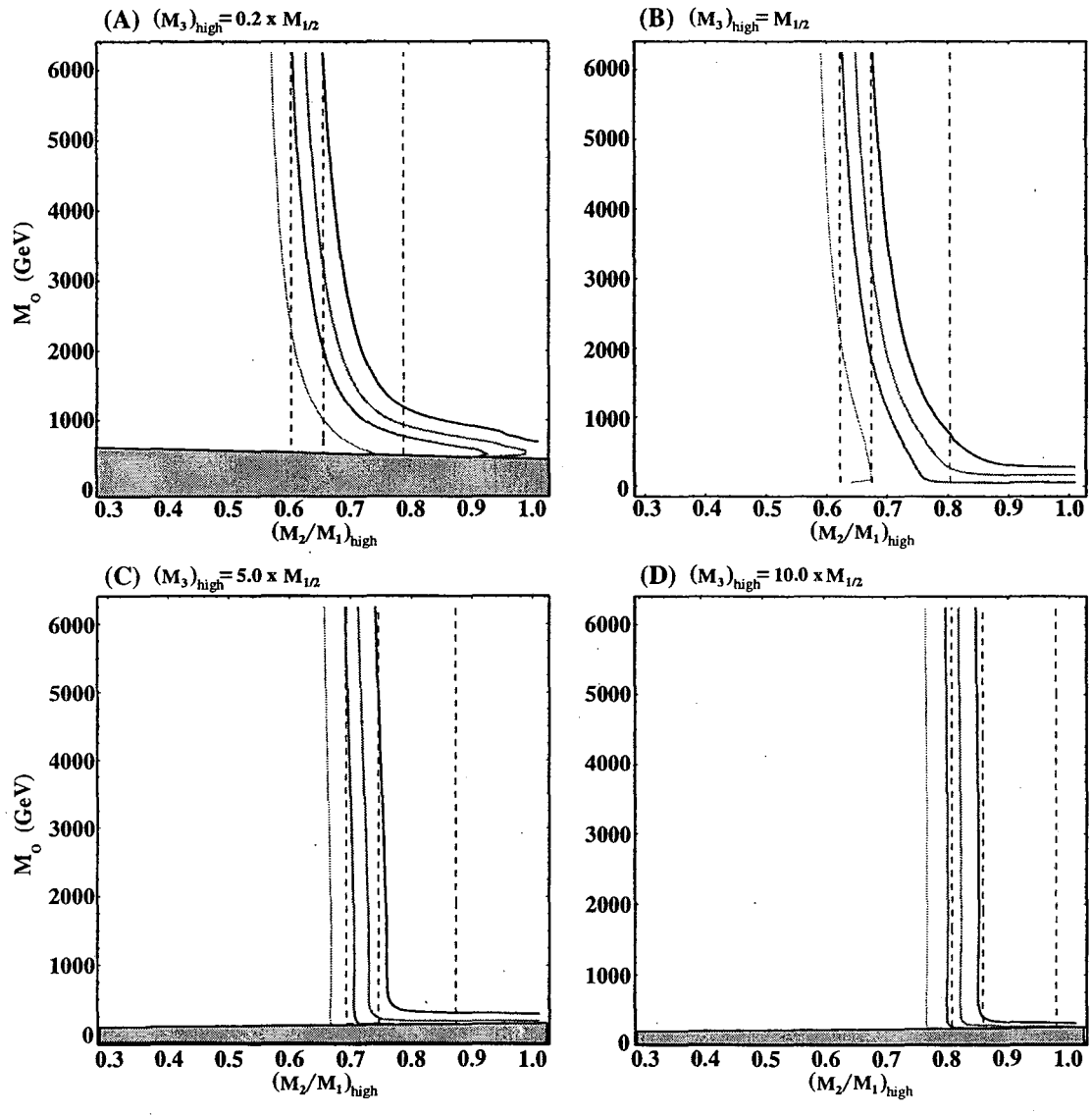

Figure 4.6: Preferred Dark Matter Region with Nonuniversal Gaugino Masses for Various M_3 Values [II]. Contours of constant relic density are given by the solid lines for $\Omega_\chi h^2 = 0.01$, 0.1, 0.3, and 1.0 from left to right. The value of the ratio $(M_2/M_1)_{\rm low}$ is indicated by the dashed lines for the values $(M_2/M_1)_{\rm low} = 1.15$, 1.25 and 1.50 from left to right. The shaded regions are ruled out because of a stau LSP.

just such an investigation in Section 5.4 on a class of supergravity models derived from heterotic string theory.

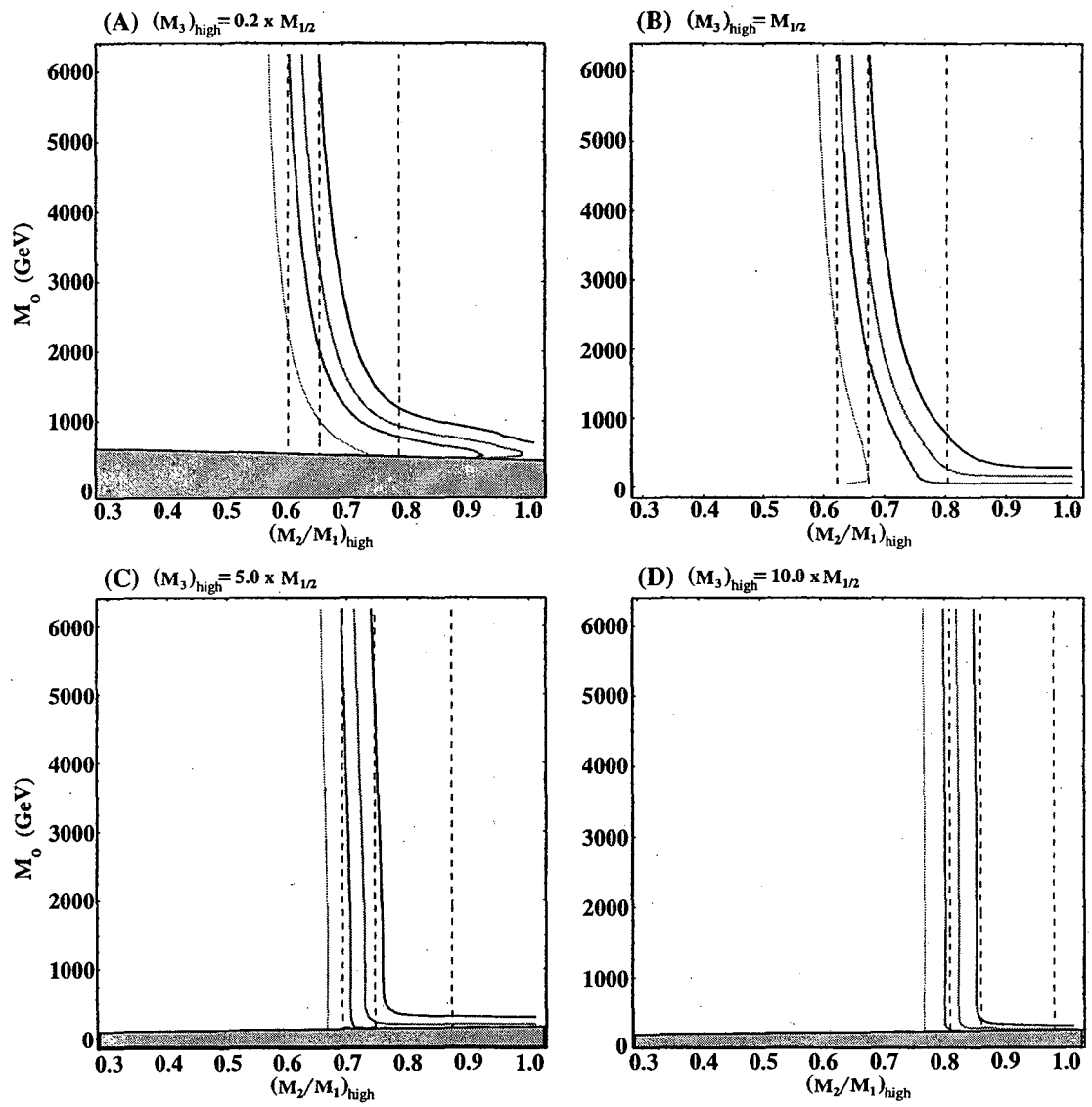

Figure 4.7: Preferred Dark Matter Region with Nonuniversal Gaugino Masses for Differing Signs of M_3. The solid lines are lines of constant $\Omega_\chi h^2$ and the dashed lines represent values of $(M_2/M_1)_{low} = 1.15$, 1.25 and 1.50 as in Figure 4.6. The shaded regions are excluded by virtue of having a stau for the LSP. We have indicated the Higgs mass constraint in panels (A) and (B). Here $M_{1/2}$ is taken to be 500 GeV in all panels.

Chapter 5

Phenomenology of Gaugino Condensation Models

Section 5.1 is a condensation of theoretical material more fully presented in [27, 28, 84] and aims to bring together the key points necessary for the subsequent discussion in Sections 5.2- 5.4 of the phenomenological consequences of a large class of string-derived models in which gaugino condensation [26, 38] occurs in a hidden sector with modular invariant couplings. The Kähler $U(1)$ superspace formalism of Section 1.2 is used throughout.

5.1 Models of Gaugino Condensation

Supersymmetry breaking is implemented via condensation of gauginos charged under the hidden sector gauge group $\mathcal{G}_{\text{hid}} = \prod_a \mathcal{G}_a$, which is taken to be a subgroup of E_8. For each gaugino condensate a vector superfield V_a is introduced and the gaugino condensate superfields $U_a \simeq (W^\alpha W_\alpha)_a$ are then identified as the (anti-)chiral projections of the vector superfields:

$$U_a = -\left(\overline{\mathcal{D}}^2 - 8R\right) V_a, \quad \overline{U}_a = -\left(\mathcal{D}^2 - 8\overline{R}\right) V_a. \tag{5.1}$$

The components of $V = \sum_a V_a$ include those of the linear multiplet L from Section 1.3, and the dilaton field is the lowest component of the vector superfield $\ell = V|_{\theta=\bar{\theta}=0}$. Note that none of the individual lowest components $V_a|_{\theta=\bar{\theta}=0}$ will appear in the effective theory component Lagrangian. With this construction the superfield U_a has the correct Kähler $U(1)$ weight as well as the correct constraint, that is, the counterpart of the Bianchi identity (1.13). When both the condensate and the weakly coupled, unconfined Yang-Mills sectors are included, the linearity condition (1.12) takes the modified form

$$\begin{aligned} -(\overline{\mathcal{D}}^2 - 8R)V &= U + \sum_a (W^\alpha W_\alpha)_a, \\ -(\mathcal{D}^2 - 8\overline{R})V &= \overline{U} + \sum_a (\overline{W}_{\dot{\alpha}} \overline{W}^{\dot{\alpha}})_a, \end{aligned} \tag{5.2}$$

Note that we will not introduce kinetic terms for the condensate superfield; that is, we are treating the condensate as static. A dynamical condensate has been studied [144] in the case of

an E_8 gauge group, and it was found that the bound state masses are above the condensation scale; when these states are integrated out the theory reduces to the static case considered here.

We consider the class of orbifold compactifications with three untwisted moduli chiral superfields described in Section 1.3. We will now label the three moduli by the superscript I (T^I) and we reserve the label α for matter condensates to be introduced below. The kinetic energy terms for the dilaton, chiral moduli, chiral matter, gravity fields and Yang-Mills fields are contained in the Lagrangian term (1.16) with L replaced by V:

$$\mathcal{L}_{\rm KE} = \int \mathrm{d}^4\theta\, E\,[-2 + f(V)]\,, \quad k(V) = \ln V + g(V), \tag{5.3}$$

with

$$Vg'(V) = f - Vf'(V), \quad g(0) = f(0) = 0, \tag{5.4}$$

as before (1.17). The relevant part of the complete effective Lagrangian is then

$$\mathcal{L}_{\rm eff} = \mathcal{L}_{\rm KE} + \mathcal{L}_{\rm VY} + \mathcal{L}_{\rm pot} + \sum_a \mathcal{L}_{\rm a} + \mathcal{L}_{\rm GS}, \tag{5.5}$$

with Kähler potential for the moduli sector and chiral matter superfields Φ^A:

$$K = k(V) + \sum_I g^I + \sum_A e^{q_I^A}|\Phi^A|^2 + \mathcal{O}(\Phi^4), \quad g^I = -\ln(T^I + \overline{T}^I), \tag{5.6}$$

where the parameters q_I^A are the modular weights of Φ^A.

The second term in (5.5) is a generalization to supergravity [23, 138] of the original Veneziano-Yankielowicz superpotential term [140],

$$\mathcal{L}_{\rm VY} = \frac{1}{8}\sum_a \int \mathrm{d}^4\theta\, \frac{E}{R} U_a \left[b'_a \ln\left(e^{-K/2}U_a\right) + \sum_\alpha b_a^\alpha \ln\left[(\Pi^\alpha)^{p_\alpha}\right]\right] + \text{ h.c. }, \tag{5.7}$$

which involves the gauge condensates U_a as well as possible gauge-invariant matter condensates described by chiral superfields $\Pi^\alpha \sim \prod_A (\Phi^A)^{n_\alpha^A}$ [117, 139]. The coeffecients b'_a, b_a^α and p_α are determined by demanding the correct transformation properties of the expression in (5.7) under chiral and conformal transformations [28, 87] and yield the following relations:

$$b'_a = \frac{1}{8\pi^2}\left(C_a - \sum_A C_a^A\right), \quad \sum_{\alpha,A} b_a^\alpha n_\alpha^A p_\alpha = \sum_A \frac{C_a^A}{4\pi^2}, \quad p_\alpha \sum_A n_\alpha^A = 3 \quad \forall\alpha. \tag{5.8}$$

The final condition amounts to choosing the value of p_α so that the effective operator $(\Pi^\alpha)^{p_\alpha}$ has mass dimension three. Given the above relations it is also convenient to define the combination

$$b_a \equiv b'_a + \sum_\alpha b_a^\alpha = \frac{1}{8\pi^2}\left(C_a - \frac{1}{3}\sum_A C_a^A\right) \tag{5.9}$$

which is proportional to the one-loop β-function coefficient for the condensing gauge group $\mathcal{G}_a$.

The third term in (5.5) is a superpotential term for the matter condensates consistent with the symmetries of the underlying theory

$$\mathcal{L}_{\text{pot}} = \frac{1}{2}\int \mathrm{d}^4\theta\, \frac{E}{R} e^{K/2} W\left[(\Pi^\alpha)^{p_\alpha}, T^I\right] + \text{ h.c.}\,. \tag{5.10}$$

We will adopt the same set of simplifying assumptions taken up in [28] for this superpotential, namely that for fixed α, $b_a^\alpha \neq 0$ for only one value of a. Then $u_a = 0$ unless $W_\alpha \neq 0$ for every value of α for which $b_a^\alpha \neq 0$. We next assume that there are no unconfined matter fields charged under the hidden sector gauge group and ignore possible dimension-two matter condensates involving vector-like pairs of matter fields. This allows a simple factorization of the superpotential of the form

$$W\left[(\Pi^{p_\alpha}), T\right] = \sum_\alpha W_\alpha(T)\,(\Pi^\alpha)^{p_\alpha}\,, \tag{5.11}$$

where the form of the functions W_α are partially dictated by the requirement of modular invariance and are given by

$$W_\alpha(T) = c_\alpha \prod_I \left[\eta\left(T^I\right)\right]^{2\left(p_\alpha q_I^\alpha - 1\right)}\,. \tag{5.12}$$

Here $q_I^\alpha = \sum_A n_\alpha^A q_I^A$ and the Yukawa coefficients c_α, while *a priori* unknown variables, are taken to be of $\mathcal{O}(1)$.

The remaining terms in (5.5) include the quantum corrections from light field loops to the unconfined Yang-Mills couplings and the Green-Schwarz counterterm introduced to ensure modular invariance.[1] The latter is given by (1.32) with the notation change $p_i \to p_A$ here. The operators $\mathcal{L}_{\text{a}}$ in (5.5) are the quantum corrections from the light field loops to the *unconfined* Yang-Mills couplings that give rise to the loop corrections found in Section 2.3.1. They are given by

$$\mathcal{L}_{\text{a}} = \frac{1}{64\pi^2}\int \mathrm{d}^4\theta\, \frac{E}{R}\left(W_\alpha P_\chi\left[f_a(\Box_\chi) - B_a\right] W^\alpha\right)_a + \text{ h.c.}\,, \tag{5.13}$$

where $\Box_\chi^{-1}$ is the chiral superfield propagator [89]:

$$\langle \Box_\chi \rangle = \left\langle \Box + \frac{1}{2} R\mathcal{D}^2 + \mathcal{O}(R\overline{R}) \right\rangle, \tag{5.14}$$

in our notation,[2] and P_χ is the chiral projection operator: $P_\chi W^\alpha = W^\alpha$, that reduces in the flat space limit to $(16\Box)^{-1}\overline{\mathcal{D}}^2\mathcal{D}^2$. The function [87]

$$B_a = C\sum_I g^I + \left(C^a - C_M^a\right) k(V) + 2\sum_A C_A^a \ln\left(1 + p_A V\right) \tag{5.15}$$

[1]Not included in this section are the string loop corrections ($\mathcal{L}_{\text{th}}$) of (1.33) which vanish for orbifold compactifications with no $\mathcal{N} = 2$ supersymmetry sector [6]. We tacitly assume such orbifold compactifications for the rest of this section.

[2]We set the background space-time curvature scalar r to zero throughout this paper. A term proportional to $r\lambda\lambda$ would result in a contribution to the gaugino mass through a Weyl rescaling, but we find that such terms are suppressed by powers of μ^{-2} or m^{-2} where m is the Pauli-Villars mass.

determines the renormalized coupling constant [29, 138, 110] $g_a(\Lambda_{\rm STR})$ at the string scale $\Lambda_{\rm STR}$:

$$g_a^{-2}(\Lambda_{\rm STR}) = \left\langle \frac{1+f}{2\ell} - b'_a k(\ell) + \sum_A \frac{C_a^A}{8\pi^2} \ln(1+\ell p_A) \right\rangle, \tag{5.16}$$

$$\Lambda_{\rm STR} = \left\langle e^{\frac{1}{2}(k-1)} \right\rangle, \tag{5.17}$$

and the functions

$$\frac{1}{8\pi^2} f_a(\mu^2) = g_a^2(\mu^2) - g_a^2(\Lambda_{\rm STR}^2) \tag{5.18}$$

govern the running of the gauge couplings from the string scale to the normalization scale.

5.2 Preliminary Issues

5.2.1 Condensation and Dilaton Stabilization

The Lagrangian in (5.5) can be expanded into component form using the standard techniques of the Kähler superspace formalism of supergravity from Section 1.2. In reference [28] the bosonic part of the Lagrangian relevant to dilaton stabilization and gaugino condensation was presented and the equations of motion for the nonpropagating fields were solved. In particular, the equations of motion for the auxiliary fields of the condensates F^a give

$$\rho_a{}^2 = e^{-2\frac{b'_a}{b_a}} e^K e^{-\frac{(1+f)}{b_a \ell}} e^{-\frac{b}{b_a}\sum_I g^I} \prod_I \left|\eta\left(t^I\right)\right|^{\frac{4(b-b_a)}{b_a}} \prod_\alpha \left|b_a^\alpha / 4c_\alpha\right|^{-2\frac{b_a^\alpha}{b_a}}, \tag{5.19}$$

where $t_I \equiv T_I|_{\theta=\bar\theta=0}$ and $u_a = U_a|_{\theta=\bar\theta=0} \equiv \rho_a e^{i\omega_a}$.

Upon substituting for the gauge coupling via the relation (1.18) we recognize the expected one-instanton form for gaugino condensation. Expression (5.19) encodes more information, however, than simply the one loop running of the gauge coupling. In [87] the loop corrections to the gauge coupling constants were computed using a manifestly supersymmetric Pauli-Villars regularization. The (moduli independent) corrections were identified with the renormalization group invariant [136]

$$\delta_a = \frac{1}{g_a^2(\mu)} - \frac{3b_a}{2} \ln \mu^2 + \frac{2C_a}{16\pi^2} \ln g_a^2(\mu) + \frac{2}{16\pi^2} \sum_a C_a^A \ln Z_a^A(\mu). \tag{5.20}$$

Using the above expression it is possible to solve for the scale at which the $1/g^2(\mu)$ term becomes negligible relative to the $\ln g^2(\mu)$ term – effectively looking for the "all loop" Landau pole for the coupling constant. This scale is related to the string scale by the relation

$$\mu_L{}^2 \sim \mu_{\rm STR}{}^2 e^{-\frac{2}{3b_a g_a^2(\mu)}} \prod_A \left[Z_a^A(\mu_{\rm STR}) / Z_a^A(\mu_L)\right]^{\frac{C_a^A}{12\pi^2 b_a}}. \tag{5.21}$$

Now comparing the effective Lagrangian given in Section 5.1 with the field theory loop calculation given in [87] shows that the two agree provided we identify the wave function renormalization coefficients Z_a^A with the quantity $|4W_\alpha/b_a^\alpha|^2$. This is precisely what is needed to produce the

final product in the condensate expression given in (5.19), indicating that the condensation scale represents the scale at which the coupling becomes strong as would be computed using the so-called "exact" β-function.

Note that this final factor introduces the unknown Yukawa coefficients c_α into the scale of supersymmetry breaking. Such dependence of the gaugino condensate on the parameters of the superpotential is not unexpected, and has in fact been demonstrated in the case of supersymmetric QCD as well as certain models of supersymmetric Yang-Mills theories coupled to chiral matter [4]. This last Yukawa-related factor has the virtue of allowing two different hidden sector configurations which result in the same β-function to condense at widely different scales.

In order to go further and make quantitative statements about the scale of gaugino condensation (and hence supersymmetry breaking) it is necessary to specify some form for the nonperturbative effects represented by the functions f and g. The parameterization adopted in [29] was originally motivated by Shenker [135] and was of the form $\exp\left(-1/g_{\text{STR}}\right)$ where g_{STR} is the string coupling constant. A consensus seems to be forming [16, 127, 137, 143] around this characterization for string nonperturbative effects and the function $f\left(V\right)$ in (5.3) will be taken to be of the form

$$f\left(V\right) = \left[A_0 + A_1/\sqrt{V}\right] e^{-B/\sqrt{V}}, \tag{5.22}$$

which was shown [29] to allow dilaton stabilization at weak to moderate string coupling with parameters that are all of $\mathcal{O}\left(1\right)$. The benefits of invoking string-inspired nonperturbative effects of the form of (5.22) have recently been explored by others in the literature [21, 41].

The scalar potential for the moduli t_I is minimzed at the self-dual points $\langle t_I \rangle = 1$ or $\langle t_I \rangle = \exp\left(i\pi/6\right)$, where the corresponding F-components F^I of the chiral superfields T^I vanish. At these points the dilaton potential is given by

$$V(\ell) = \frac{1}{16\ell^2}\left(1 + \ell\frac{\mathrm{d}g}{\mathrm{d}\ell}\right)\left|\sum_a \left(1 + b_a\ell\right) u_a\right|^2 - \frac{3}{16}\left|\sum_a b_a u_a\right|^2. \tag{5.23}$$

As an example, the potential (5.23) can be minimized with vanishing cosmological constant and $\alpha_{\text{STR}} = 0.04$ for $A_0 = 3.25, A_1 = -1.70$ and $B = 0.4$ in expression (5.22).

5.2.2 Scale of Supersymmetry Breaking

With the adoption of (5.22) the scale of gaugino condensation can be obtained once the following are specified:

(1) the condensing subgroup(s) of the original hidden sector gauge group E_8;

(2) the representations of the matter fields charged under the condensing subgroup(s);

(3) the Yukawa coefficients in the superpotential for the hidden sector matter fields;

(4) the value of the string coupling constant at the compactification scale, which in turn determines the coefficients in (5.22) necessary to minimize the scalar potential (5.23).

A great deal of simplification in the above parameter space can be obtained by making the ansatz that all of the matter in the hidden sector which transforms under a given subgroup $\mathcal{G}_a$ is of the same representation, such as the fundamental representation. Then the sum of the coefficients b_a^α over the number of condensate fields labeled by α ($\alpha = 1, \ldots, N_c$), can be replaced by one effective variable

$$\sum_\alpha b_a^\alpha \longrightarrow (b_a^\alpha)_{\text{eff}} \quad (b_a^\alpha)_{\text{eff}} = N_c b_a^{\text{rep}}. \tag{5.24}$$

In the above equation b_a^{rep} is proportional to the quadratic Casimir operator for the matter fields in the common representation and the number of condensates, N_c, can range from zero to a maximum value determined by the condition that the gauge group presumed to be condensing must remain asymptotically free. The redefinition in (5.24) essentially takes the coefficients b_a^α, which we are free to choose in our effective Lagrangian up to the conditions given in (5.8), and assigns the same value to each condensate.

The variable b_a^α can then be eliminated in (5.19) in favor of $(b_a^\alpha)_{\text{eff}}$ provided the simultaneous redefinition $c_\alpha \longrightarrow (c_\alpha)_{\text{eff}}$ is made so as to keep the product in (5.19) invariant:

$$\langle \rho_+^2 \rangle \sim \left| \frac{(b_a^\alpha)_{\text{eff}}}{4\,(c_\alpha)_{\text{eff}}} \right|^{-2(b_a^\alpha)_{\text{eff}}/b_a}. \tag{5.25}$$

With the assumption of universal representations for the matter fields, this implies

$$(c_\alpha)_{\text{eff}} \equiv N_c \left(\prod_{\alpha=1}^{N_c} c_\alpha \right)^{\frac{1}{N_c}} \tag{5.26}$$

which we assume to be an $\mathcal{O}(1)$ number, if not slightly smaller.

From a determination of the condensate value ρ using (5.19) the supersymmetry-breaking scale can be found by solving for the gravitino mass, given by

$$M_{3/2} = \frac{1}{3} \langle |M| \rangle = \frac{1}{4} \left\langle \left| \sum_a b_a u_a \right| \right\rangle. \tag{5.27}$$

In [28] it was shown that in the case of multiple gaugino condensates the scale of supersymmetry breaking was governed by the condensate with the largest one loop β-function coefficient. Hence in the following it is sufficient to consider the case with just one condensate with β-function coefficient denoted b_+ for gauge group $\mathcal{G}_a = \mathcal{G}_+$:

$$M_{3/2} = \frac{1}{4} b_+ \langle |u_+| \rangle. \tag{5.28}$$

As an illustration of this point, the gravitino mass for the case of pure supersymmetric Yang-Mills $SU(5)$ condensation (no hidden sector matter fields) would be 4000 GeV. The addition of an additional condensation of pure supersymmetric Yang-Mills $SU(4)$ gauginos would only add an additional 0.004 GeV to the mass.

Now for given values of $(c_\alpha)_{\text{eff}}$ and g_{STR} the condensation scale

$$\Lambda_{\text{COND}} = (M_{\text{PL}}) \langle \rho_+^2 \rangle^{1/6} \tag{5.29}$$

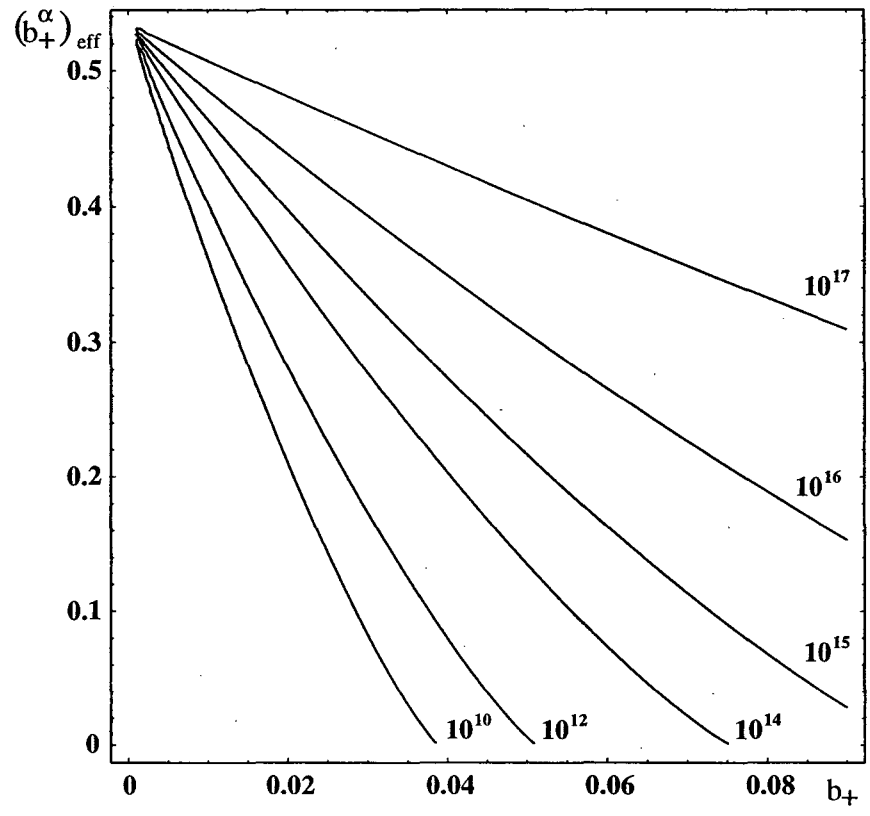

Figure 5.1: Condensation Scale as a Function of Hidden Sector Gauge Configuration. Contours give the scale of gaugino condensation in GeV for $(c_\alpha)_{\rm eff} = 3$.

and gravitino mass (5.28) can be plotted in the $\{b_+, (b_+^\alpha)_{\rm eff}\}$ plane. The sharp variation of the condensate value with the parameters of the theory, as anticipated by the functional form in (5.19), is apparent in the contour plot of Figure 5.1. The dependence of the gravitino mass on the group theory parameters is even more profound. Figure 5.2 gives contours for the gravitino mass between 100 GeV and 100 TeV. Clearly, the region of parameter space for which a phenomenologically preferred value of the supersymmetry breaking scale occurs is a rather limited slice of the entire space available.

The variation of the gravitino mass as a function of the Yukawa parameters c_α is shown in Figure 5.3. On the horizontal axis there are no matter condensates ($b_a^\alpha = 0,\ \forall\alpha$) so there is no dependence on the variable $(c_\alpha)_{\rm eff}$. For values of $(c_\alpha)_{\rm eff} \lesssim 0.1$ the contours of gravitino mass in the TeV region lie beyond the limiting value of $b_+ \simeq 0.09$ and are thus in a region of parameter space which is inaccessible to a model in which the unified coupling at the string scale is $\alpha_{\rm STR} = 0.04$ or larger. For very large values of the effective Yukawa parameter the gravitino mass contours approach an asymptotic value very close to the case shown here for $(c_\alpha)_{\rm eff} = 50$. We might therefore consider the shaded region between the two sets of contours as roughly the maximal region of viable parameter space for a given value of the unified coupling at the string scale.

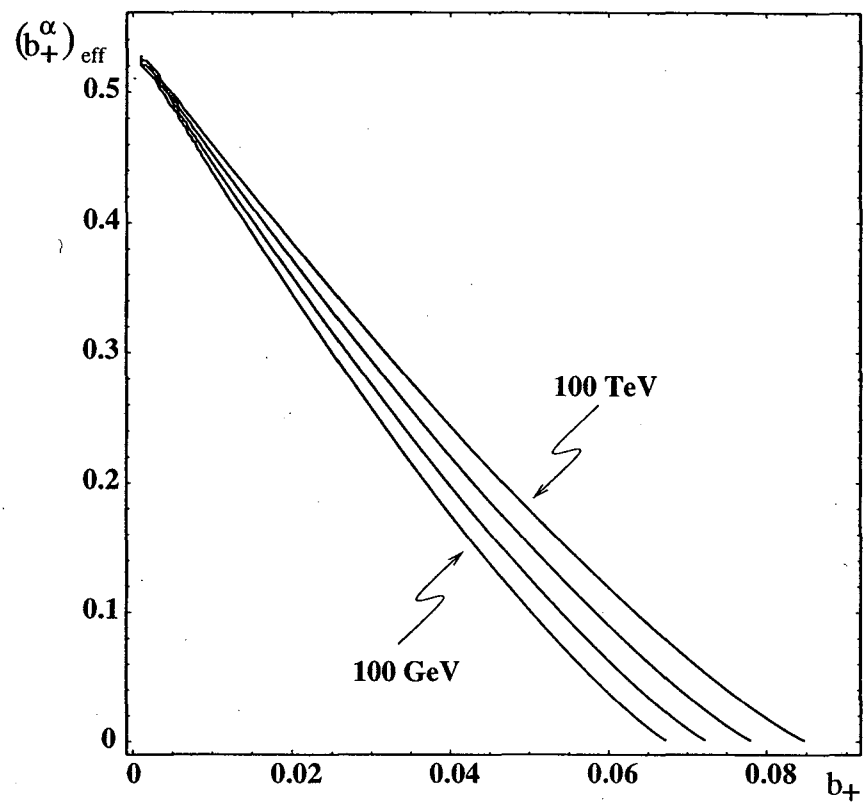

Figure 5.2: Gravitino Mass as a Function of Hidden Sector Gauge Configuration. Contours of gravitino mass for 10^2 GeV through 10^5 GeV are given for $(c_\alpha)_{\text{eff}} = 3$.

5.2.3 Implications for the Hidden Sector

Having examined some of the universal constraints placed on any string-derived model proposing to describe low energy physics it is natural to ask whether the region of phenomenological viability (roughly the shaded area in Figure 5.3) can be used to constrain the matter content of the hidden sector.

Upon orbifold compactification the E_8 gauge group of the hidden sector is presumed to break to some subgroup(s) of E_8 and the set of all such possible breakings has been computed for Z_N orbifolds [111]. Under the working assumption that only the subgroup with the largest β-function coefficient enters into the low energy phenomenology, there are then a finite number of possible groups to consider:

$$\begin{cases} E_7,\, E_6 \\ SO\,(16)\,,\, SO\,(14)\,,\, SO\,(12)\,,\, SO\,(10)\,,\, SO\,(8) \\ SU\,(9)\,,\, SU\,(8)\,,\, SU\,(7)\,,\, SU\,(6)\,,\, SU\,(5)\,,\, SU\,(4)\,,\, SU\,(3) \end{cases} \tag{5.30}$$

For each of the above gauge groups equations (5.8) and (5.9) define a line in the $\{b_+, (b_+^\alpha)_{\text{eff}}\}$ plane. These lines will all be parallel to one another with horizontal intercepts at the β-function coefficient for a pure Yang-Mills theory. The vertical intercept will then indicate the amount of matter required to prevent the group from being asymptotically free, thereby eliminating it as a candidate source for the supersymmetry breaking described in Section 5.2.2.

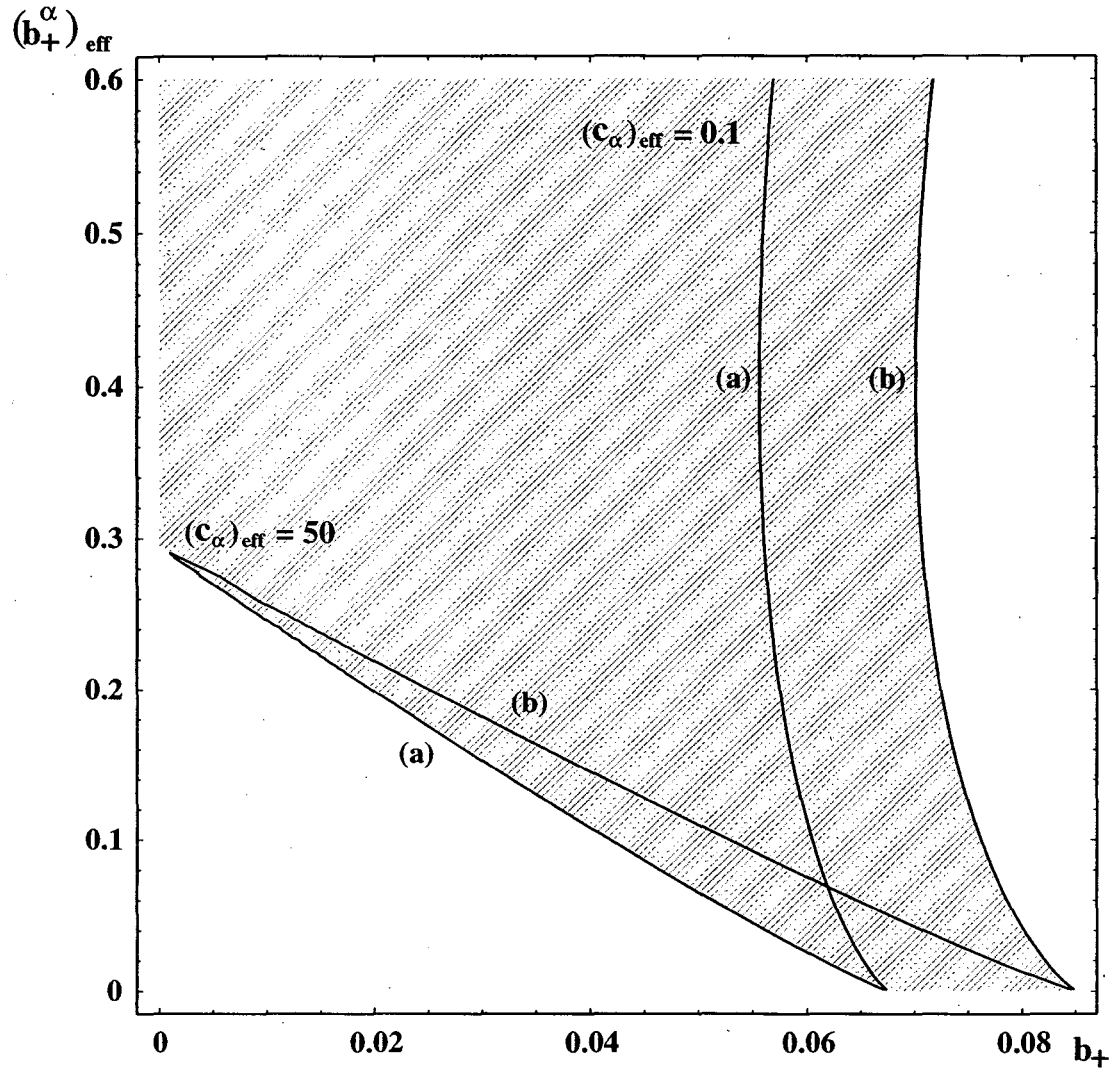

Figure 5.3: Gravitino Mass Regions as a Function of Yukawa Parameter. Gravitino mass contours for (a) 100 GeV and (b) 10 TeV are shown for $(c_\alpha)_{\text{eff}} = 50$ and $(c_\alpha)_{\text{eff}} = 0.1$ with $\alpha_{\text{STR}} = 0.04$. The region between the two sets of curves can be considered roughly the region of phenomenological viability.

In Figure 5.4 we have overlaid these gauge lines on a plot similar to Figure 5.3. We restrict the Yukawa couplings of the hidden sector to the more reasonable range of $1 \leq (c_\alpha)_{\text{eff}} \leq 10$ and give three different values of the string coupling at the string scale. The choice of string coupling constant is made when specifying the boundary conditions for solving the dilaton scalar potential, as described in Section 5.2.1. Changing this boundary condition will affect the scale of gaugino condensation through equation (5.19), altering the supersymmetry breaking scale for a fixed point in the $\{b_+, (b_+^\alpha)_{\text{eff}}\}$ plane. Demanding larger values of g_{STR} will result in the shifting of the contours of fixed gravitino mass towards the origin, as in Figure 5.4. Such large values of α_{STR} have recently been invoked as part of a mechanism for stabilizing the dilaton and/or as a consequence of reconciling the apparent scale of gauge unification in the MSSM with the scale predicted by string theory [16, 112]. We will return to such issues in Section 5.3.3.

A typical matter configuration would be represented in Figure 5.4 by a point on one of the

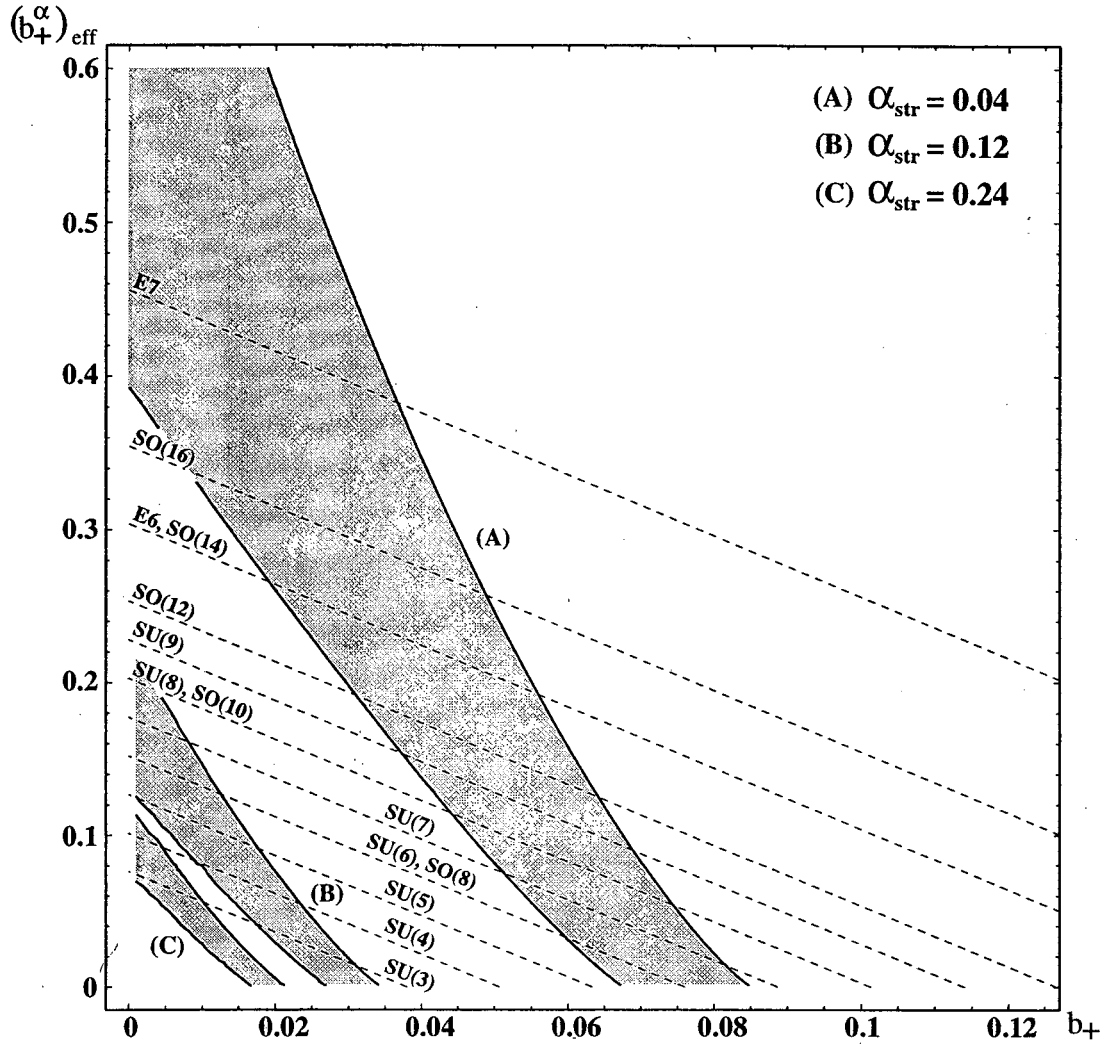

Figure 5.4: Constraints on the Hidden Sector. The shaded regions give three different "viable" regions depending on the value of the unified coupling strength at the string scale. The upper limit in each case represents a 10 TeV gravitino mass contour with $(c_\alpha)_{\text{eff}} = 1$, while the lower bound represents a 100 GeV gravitino mass contour with $(c_\alpha)_{\text{eff}} = 10$.

gauge group lines. As each field adds a discrete amount to $(b_a^\alpha)_{\text{eff}}$ and the fields must come in gauge-invariant multiples, the set of all such possible hidden sector configurations is necessarily a finite one.[3] The number of possible configurations consistent with a given choice of $\{\alpha_{\text{STR}}, (c_\alpha)_{\text{eff}}\}$ and supersymmetry breaking scale $M_{3/2}$ is quite restricted. For example, Figure 5.4 immediately rules out hidden sector gauge groups smaller than SU(6) for weak coupling at the string scale $\left(g_{\text{STR}}^2 \simeq 0.5\right)$. Furthermore, even moderately larger values of the string coupling at unification become increasingly difficult to obtain as it is necessary to postulate a hidden sector with very small gauge group and particular combinations of matter to force the beta-function coefficient to small values.

[3]For example, one cannot obtain values of b_+ arbitrarily close to zero in practical model building.

5.3 Low Energy Physics Signatures

5.3.1 Soft Supersymmetry Breaking Terms

Simply requiring that the scale of supersymmetry breaking be in a reasonable range of energy values (*i.e.* within an order of magnitude of 1 TeV) can put significant constraints on the dynamics of the hidden sector. Requiring further that the *pattern* of supersymmetry breaking be consistent with observed electroweak symmetry breaking and direct experimental bounds on superpartner masses can restrict the parameter space even more. This pattern of supersymmetry breaking is determined by the appearance of soft scalar masses, gaugino masses and trilinear couplings at the condensation scale. In order to investigate nonuniversal soft terms we would like to make use of the one loop results for soft terms found in Section 2 where supersymmetry breaking was confined to the (chiral) dilaton and/or the chiral moduli fields.

As was mentioned at the end of Section 5.2.1, modular-invariant gaugino condensation models are "dilaton-dominated" in that the T-moduli are stabilized at self-dual points where their F-term auxiliary fields vanish identically. We are thus led to consider models with an effective nonzero F^S and $\sin\theta = 1$, but we must develop a lexicon for converting results obtained in the linear multiplet formalism of gaugino condensation to those of Section 2. As was noted in Appendix A the scalar potential can be written as in (A.3)

$$\begin{aligned} V &= \sum_\alpha \frac{1}{(t^\alpha + \bar{t}^\alpha)^2} F^\alpha \overline{F}^\alpha + \frac{\ell}{k'(\ell)} F^2 - \frac{1}{3} M \overline{M}, \\ F &= \frac{k'(\ell)}{4\ell} f(\ell, t^\alpha, z^i), \end{aligned} \tag{5.31}$$

where comparison with (5.23) gives

$$f(\ell, t^\alpha, z^i) = -\sum_a (1 + \ell b_a)\bar{u}_a \approx -(1 + \ell b_+)\bar{u}_+. \tag{5.32}$$

Now our lexicon can be completed by identifying the expressions in (A.13), to give the following

$$M = \frac{1}{2} b_+^0 u = -3M_{3/2}, \quad F^S = -\frac{1}{4} K_{S\overline{S}}^{-1} \left(1 + \frac{g_{\rm STR}^2}{3} b_+^0\right) \bar{u}, \quad K_S = -\frac{1}{2} g_{\rm STR}^2, \tag{5.33}$$

Vanishing of the vacuum energy (1.4) now requires

$$K_{S\overline{S}} |F^S|^2 = \frac{1}{3} |M^2|, \quad K_{S\overline{S}}^{-1} = \frac{(2b_+^0)^2}{3(1 + \frac{1}{3} g_{\rm STR}^2 b_+^0)^2}, \quad \left|\frac{F^S}{M}\right| = \frac{2b_+^0}{3(1 + \frac{1}{3} g_{\rm STR}^2 b_+^0)}, \tag{5.34}$$

Using the expressions in Appendix B, together with (5.33) and (5.34) the pattern of soft supersymmetry breaking terms can be obtained as a function of the condensing group β-function coefficient b_+ and the modular weights of the fields with $\langle \mathrm{Re}\, t \rangle = 1$ or $\langle \mathrm{Re}\, t \rangle = e^{i\pi/6}$ and $\sin\theta = 1$. From Figure 5.1 the condensation scale in these models is typically of the order of 1×10^{14} GeV and we take this to be the boundary condition scale $\Lambda_{\rm UV}$ in what follows.

The gaugino masses in the one-condensate approximation, including the contribution from the quantum effects of light fields arising at one loop from the superconformal anomaly, are

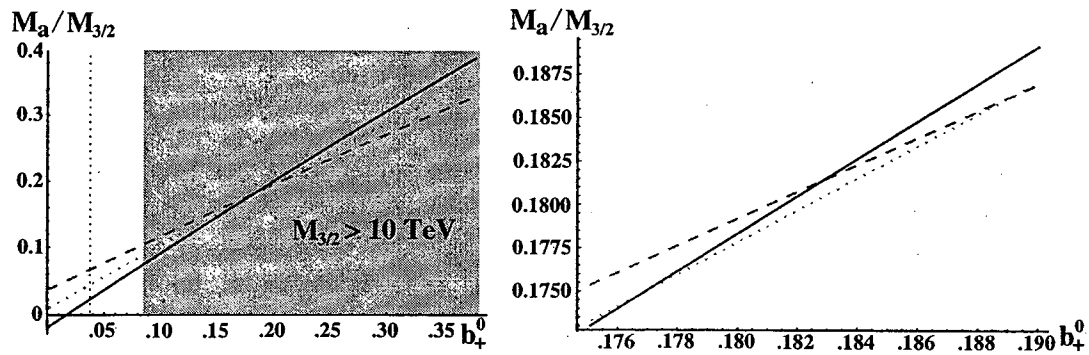

Figure 5.5: Gaugino Masses in the Model of Section 5.1. Gaugino masses M_1 (dashed), M_2 (dotted) and M_3 (solid) are given at a scale $\Lambda_{UV} = 1 \times 10^{14}$ GeV as a function of the condensing group β-function coefficient b_+^0. The vertical dotted line in the left panel is the benchmark case of E_6 condensation in the hidden sector with 9 **27**s of hidden sector matter studied in [84]. The right panel focuses on the region where the three masses are approximately unified.

given by

$$M_{\lambda_a}|_{\mu=\Lambda_{\rm COND}} = -\frac{g_a^2(\mu)}{2}\left[\frac{3b_+(1+b'_a\ell)}{1+b_+\ell} - 3b_a + \sum_A \frac{C_a^A p_A(1+b_+\ell)}{4\pi^2 b_+(1+p_A\ell)}\right] M_{3/2}. \tag{5.35}$$

In Figure 5.5 the gaugino masses are displayed as a function b_+ relative to the gravitino mass. In reference to Figure 5.4 in Section 5.2 we noted that a reasonable scale of supersymmetry breaking (*i.e.* gravitino masses less than 10 TeV) generally requires $b_+ \lesssim 0.085$. The region with gravitino mass larger than 10 TeV is shaded in Figure 5.5. Also indicated in Figure 5.5 is a benchmark scenario consisting of an E_6 gaugino condensate in the hidden sector together with 9 **27**s of matter and having a beta function coefficient of $b_+ = 0.038$. The spectrum of gaugino masses will typically be similar to that of the "anomaly mediated" cases with $M_1 \gtrsim M_2$ and a lightest neutralino with substantial wino-like content provided $b_+ \lesssim 0.19$. The location of the approximate unification of gaugino masses near this value of b_+ is expanded in the right panel of Figure 5.5.

We next turn our attention to the entire set of soft supersymmetry breaking parameters at one loop in the gaugino condensate models. In Figure 5.6 we plot the relative sizes of all third generation scalar masses and A-terms, Higgs masses and gaugino masses as a fraction of the gravitino mass for $\tan\beta = 3$, assuming $n_i = -1$ for all fields. As was the case in Sections 3.1 – 3.3, the gauginos are typically an order of magnitude smaller than scalars (note the change in vertical scale in Figure 5.6). Figure 5.6 displays an important feature of the always-present one loop contributions arising from the conformal anomaly: when tree level scalar masses are present and universal the nonuniversality arising from the anomaly pieces is negligible (here averaging less than a 1% correction). However, the corrections to the gaugino masses may significantly alter the gaugino spectrum *provided the tree level contributions are absent or suppressed*, as in the models considered here. Neglecting these one loop anomaly-induced contributions to soft terms is an approximation whose validity needs to be assessed on a model-by-model basis. For the remainder of this section we will neglect the loop corrections to the soft scalar masses and trilinear A-terms. This will allow us to use exact expressions for the soft terms as derived in the linear multiplet formulation.

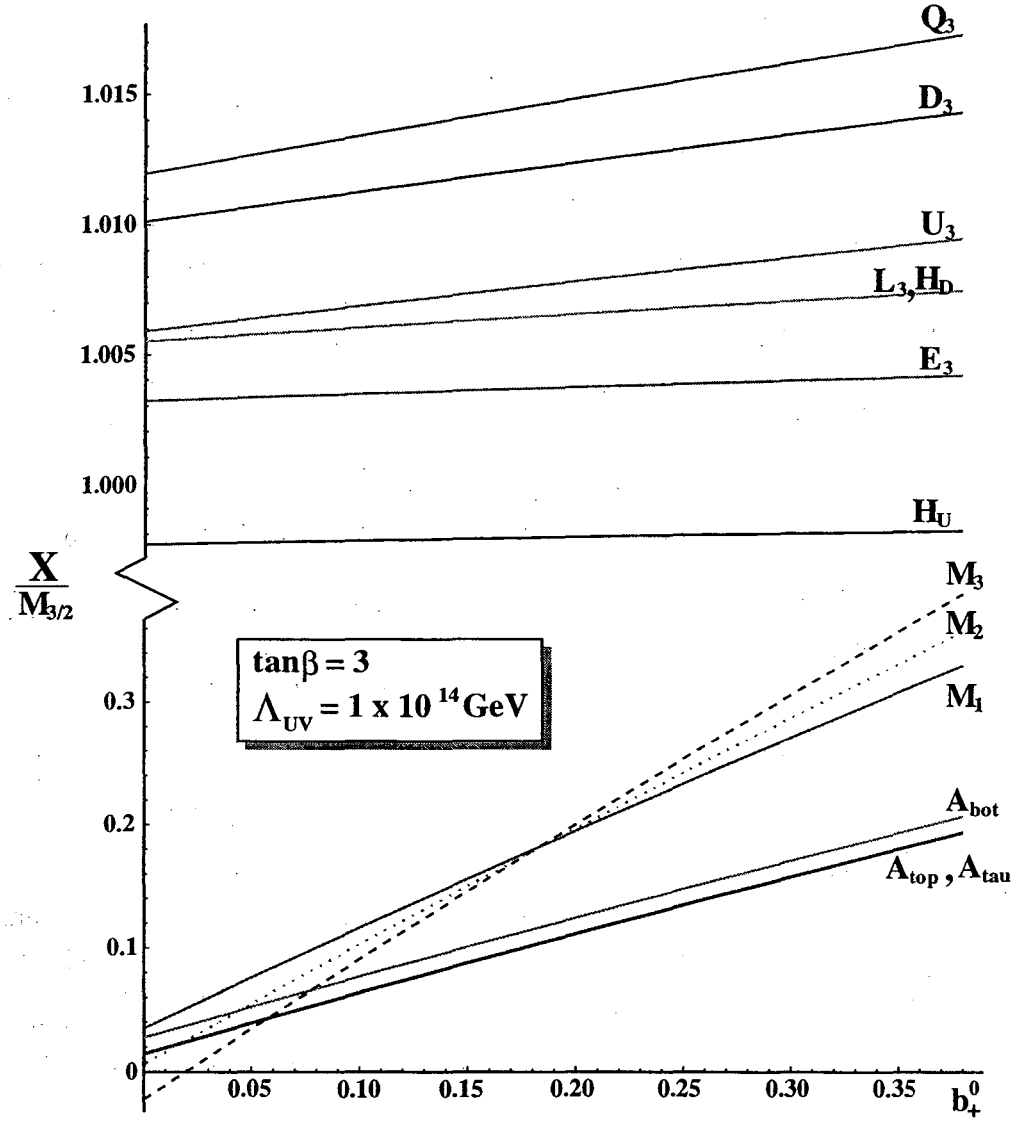

Figure 5.6: Spectrum of Soft Supersymmetry Breaking Terms in the Model of Section 5.1. All values are given relative to the gravitino mass $M_{3/2}$ at a scale $\Lambda_{\rm UV} = 1 \times 10^{14}$ GeV as a function of the condensing group β-function coefficient b_+.

Adopting the Kähler potential assumed in (5.6) and the counterterm of (1.32) with $\delta_{\rm GS} = -90$ for simplicity, the scalar masses are given in the one-condensate approximation by

$$M_A^2 = \frac{1}{16}\left\langle \rho_+^2 \frac{(p_A - b_+)^2}{(1+p_A\ell)^2}\right\rangle, \tag{5.36}$$

and the trilinear "A-terms" in the scalar potential are given by

$$A = \frac{3}{4}\langle \bar{u}_+\rangle \left\langle \frac{(p_A - b_+)}{(1+p_A\ell)} + \frac{b_+}{(1+b_+\ell)}\right\rangle. \tag{5.37}$$

As noted in [29], the fact that (5.36) and (5.37) are independent of the modular weights q_I^A of the individual observable sector fields is the result of the vanishing of the auxiliary fields F^I in the vacuum. This is a manifestation of the dilaton-dominated scenario of supersymmetry breaking [35, 36, 109] for which flavor-changing neutral currents might be naturally suppressed. For this to indeed occur, however, it is also necessary to make the assumption that the couplings p_A are the same for the first and second generations of matter.

To analyze the low energy particle spectrum it is necessary to choose a value of p_A for each generation of matter fields. If the Green-Schwarz term (1.32) is independent of the Φ^A so that $p_A = 0$, then from (5.36) $m_A = M_{3/2}$. We will call such a generation "light." On the other hand, it is possible that the Green-Schwarz term may well depend only on the combination $T^I + \overline{T}^I - \sum_A |\Phi_I^A|^2$, where Φ_I^A represents untwisted matter fields. Then for these multiplets $p_A = b$ and the scalar masses for these fields are in general an order of magnitude greater than the gravitino mass. We will call these generations "heavy."

Before giving the results of a numerical analysis using the renormalization group equations with the boundary conditions determined by equations (5.35), (5.36) and (5.37), it is worthwhile looking at what patterns of symmetry breaking are expected for various choices of the parameter p_A in the context of the MSSM. As mentioned in Section 3.1 for any generation with non-negligible Yukawa couplings a good indicator that the stable minimum of the scalar potential will yield correct electroweak symmetry breaking is the relation (3.10). For any heavy matter generation with a non-negligible coupling to a heavy Higgs field ($p_A = b$) equation (5.37) yields $A \approx 3M_A$ and so (3.9) is already nearly saturated at the condensation scale.

Another key factor in preventing dangerous color and charge-breaking minima is the ratio of scalar masses to gaugino masses and the degree of splitting between any light and heavy matter generations. In this model, both of the hierarchies, $M_A^{\text{light}}/M_{\lambda_a}$ and $M_A^{\text{heavy}}/M_A^{\text{light}}$, will turn out to be $\mathcal{O}(10)$. This pattern of soft supersymmetry breaking masses has been shown[2, 8] to lie on the boundary of the region in MSSM parameter space for which light squark masses tend to be driven negative by two loop effects arising from the heavier squarks. All of the above considerations suggest that compactification scenarios in which the observable sector matter fields couple universally to the Green-Schwarz counterterm with $p_A = b$ may have trouble reproducing the correct pattern of low energy symmetry breaking.

5.3.2 RGE Viability Analysis Within the MSSM

To determine what region of parameter space in the $\{b_+, (b_+^\alpha)_{\text{eff}}\}$ plane is consistent with current experimental data it is necessary to run the soft supersymmetry breaking parameters from the condensation scale to the electroweak scale using the renormalization group equations with the procedure described in 3.4. The RGE analysis was performed on four different scenarios:

- **Scenario A**: All three generations light.
- **Scenario B**: Third generation light, first and second generations heavy.
- **Scenario C**: All three generations heavy.
- **Scenario D**: All matter heavy except for the two Higgs doublets which remain light ($p_A = 0$).

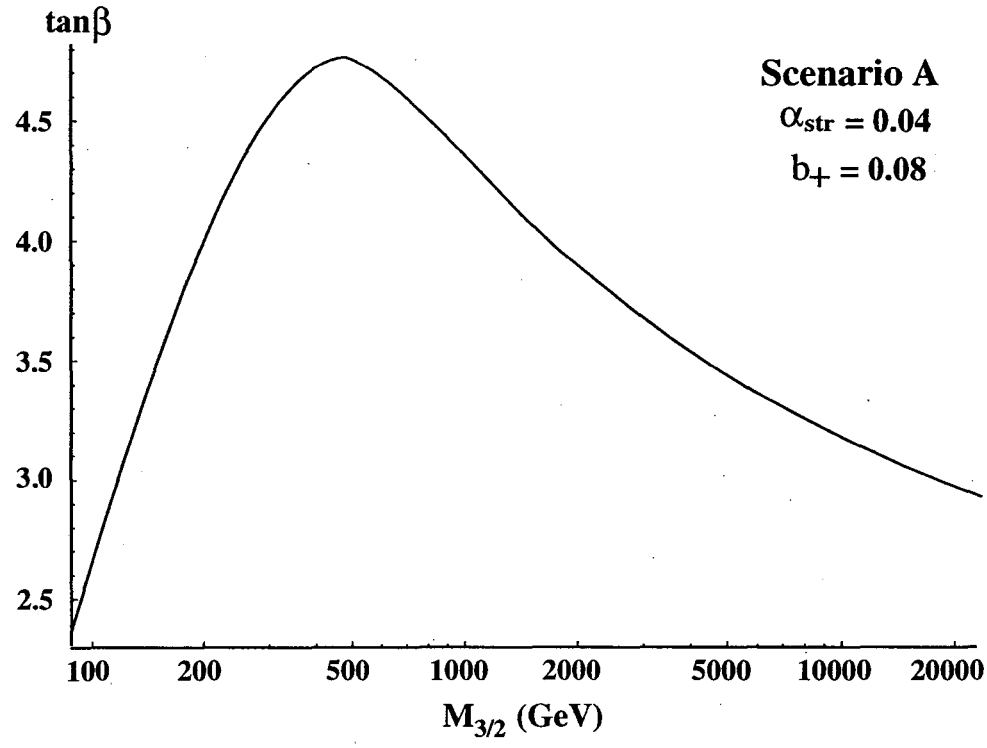

Figure 5.7: Region with Correct Symmetry Breaking for Scenario A. The maximum value of $\tan\beta$ consistent with electroweak symmetry breaking and positive squark masses is displayed as a function of the gravitino mass. The plot is shown with $b_+ = 0.08$ but the values are extremely insensitive to the choice of this parameter.

The scenarios with a heavy third generation have become popular in the literature recently [48, 62, 129] as a means of suppressing flavor-changing neutral current processes and CP-violating observables. The Higgs fields will be taken to couple to the Green-Schwarz counterterm identically to the third generation of matter, as we keep only the third generation Yukawa couplings in the MSSM superpotential. In scenario D we relax this assumption.

In the boundary values of (5.35), (5.36) and (5.37) the values of $(c_\alpha)_{\text{eff}}$ and $(b_a^\alpha)_{\text{eff}}$ appear only indirectly through the determination of the value of the condensate $\langle\rho_+^2\rangle$. It is thus convenient to cast all soft supersymmetry breaking parameters in terms of the values of b_+ and $M_{3/2}$. While the gravitino mass itself is not strictly independent of b_+, it is clear from Figure 5.3 that we are guaranteed of finding a reasonable set of values for $\left\{(c_\alpha)_{\text{eff}}, (b_+^\alpha)_{\text{eff}}\right\}$ consistent with the choice of b_+ and $M_{3/2}$ provided we scan only over values $b_+ \lesssim 0.1$ for weak string coupling. This transformation of variables allows the slice of parameter space represented by the contours of Figure 5.4 to be recast as a two-dimensional plane for a given value of $\tan\beta$ and $\text{sgn}(\mu)$. The condensation scale (the scale at which the renormalization group running begins) is also a function of the gravitino mass in this framework, found by inverting equation (5.27).

Having chosen a set of input parameters $\left\{b_+, M_{3/2}, \tan\beta, \text{sgn}(\mu)\right\}$ for a particular scenario, the model parameters are run from the condensation scale Λ_{COND} given by (5.29) to the electroweak scale $\Lambda_{\text{EW}} = M_Z$, decoupling the scalar particles at a scale approximated by $\Lambda_{\text{scalar}} = M_A$. While treating all superpartners with a common scale sacrifices precision for expediency, the results presented below are meant to be a first survey of the phenomenology of this class of

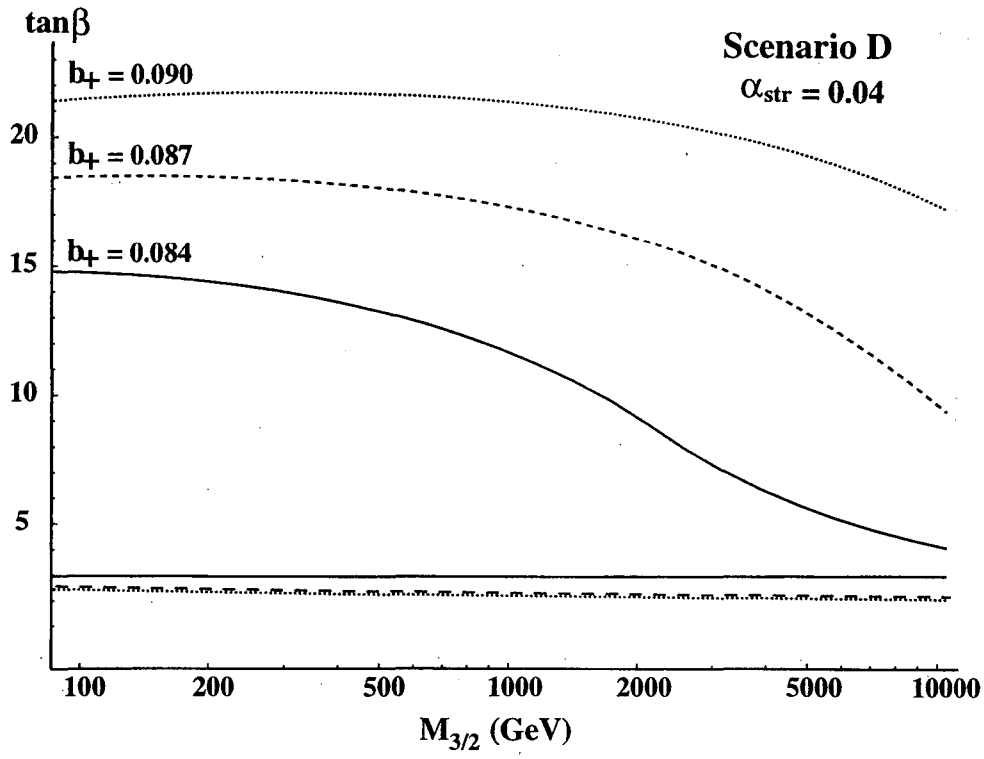

Figure 5.8: Region with Correct Symmetry Breaking for Scenario D. Three pairs of curves are shown for $b_+ = 0.084, 0.087, 0.090$. For values of $\tan\beta$ between the curves the heavy scalar contribution at two loops to the running of $m^2_{U_3}$ drives its value negative.

models.

A set of input parameters will then be considered viable if at the electroweak scale the one-loop corrected mu-term $\bar{\mu}^2$ is positive, the Higgs potential is bounded from below, all matter fields have positive scalar mass-squareds and the spectrum of physical masses for the superpartners and Higgs fields satisfy the selection criteria given in Table 4.1.[4]

The first condition to be imposed on the scenarios considered here is correct electroweak symmetry breaking, defined by (3.23), with no additional scalar masses negative. This criterion alone rules out scenario C, with all three generations coupling universally to the GS counterterm and having large scalar masses. For the opposite case of no coupling to the GS counterterm (scenario A) the allowed region is displayed in Figure 5.7. In this scenario electroweak symmetry breaking requires $1.65 \lesssim \tan\beta \lesssim 4.5$, the lower bound being the value for which the top quark Yukawa coupling develops a Landau pole below the condensation scale. This restricted region of the $\tan\beta$ parameter space is a result of the large hierarchy between gaugino masses and scalar masses in these models and has been observed in more general studies of the MSSM parameter space [106].

[4]Though the inclusive branching ratio for $b \to s\gamma$ decays was not used as a criterion, an *a posteriori* check of the region of the parameter space where this class of models wants to live – namely relatively low $\tan\beta$ and gaugino masses with high scalar masses – indicates no reason to fear a conflict with the bounds from CLEO except possibly in the case $\mathrm{sgn}(\mu) = -1$ for Scenario D [11, 52].

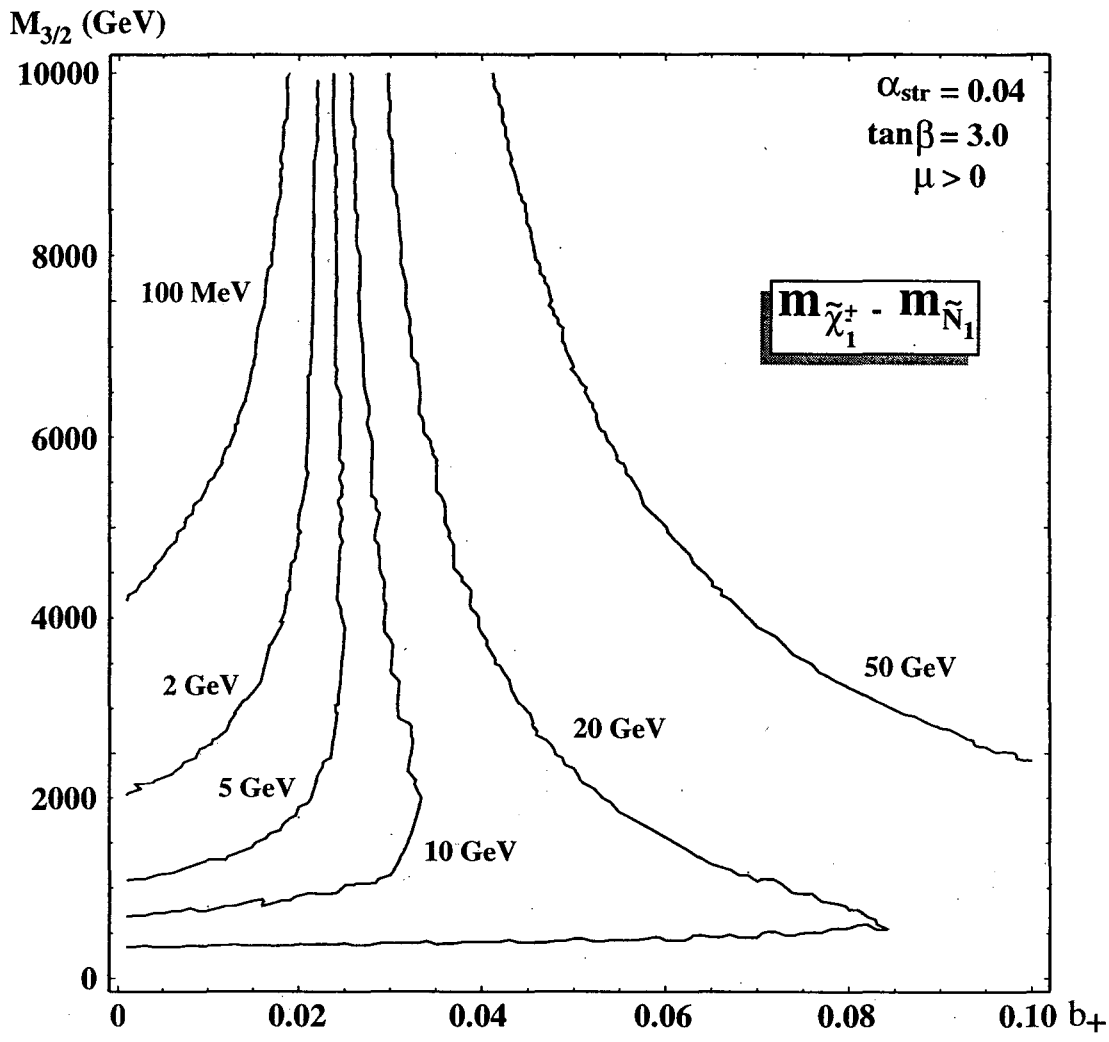

Figure 5.9: Chargino/Neutralino Mass Degeneracy in Scenario A. The mass difference between the $\chi_1^\pm$ and the $\tilde{N}_1$ is given in GeV.

Scenario B with its split generations can exist only for $0.08 \lesssim b_+ \lesssim 0.09$, where the hierarchy between the generations is small enough to prevent the two loop effects of the heavy generations from driving the right-handed top squark to negative squared-mass values. Furthermore, proper electroweak symmetry breaking in this model requires the value of $\tan\beta$ to be in the uncomfortably narrow range $1.65 \lesssim \tan\beta \lesssim 1.75$, making this pattern of Green-Schwarz couplings phenomenologically unattractive.

As for scenario D, the large third generation masses give an additional downward pressure on the Higgs squared masses in the running of the RGEs, allowing for a much wider allowed range of $\tan\beta$. In fact, electroweak symmetry is radiatively broken in the entire range of parameter space. However, as the value of b_+ is raised past the critical range $b_+ \simeq 0.08$, the scalar mass boundary values at the condensation scale start to become light enough that the right-handed stop is again driven to negative squared-mass values. This is shown in Figure 5.8 where the region between the upper and lower curves is excluded. While this region expands rapidly as the β-function coefficient is increased, the values of the β-function coefficient consistent with

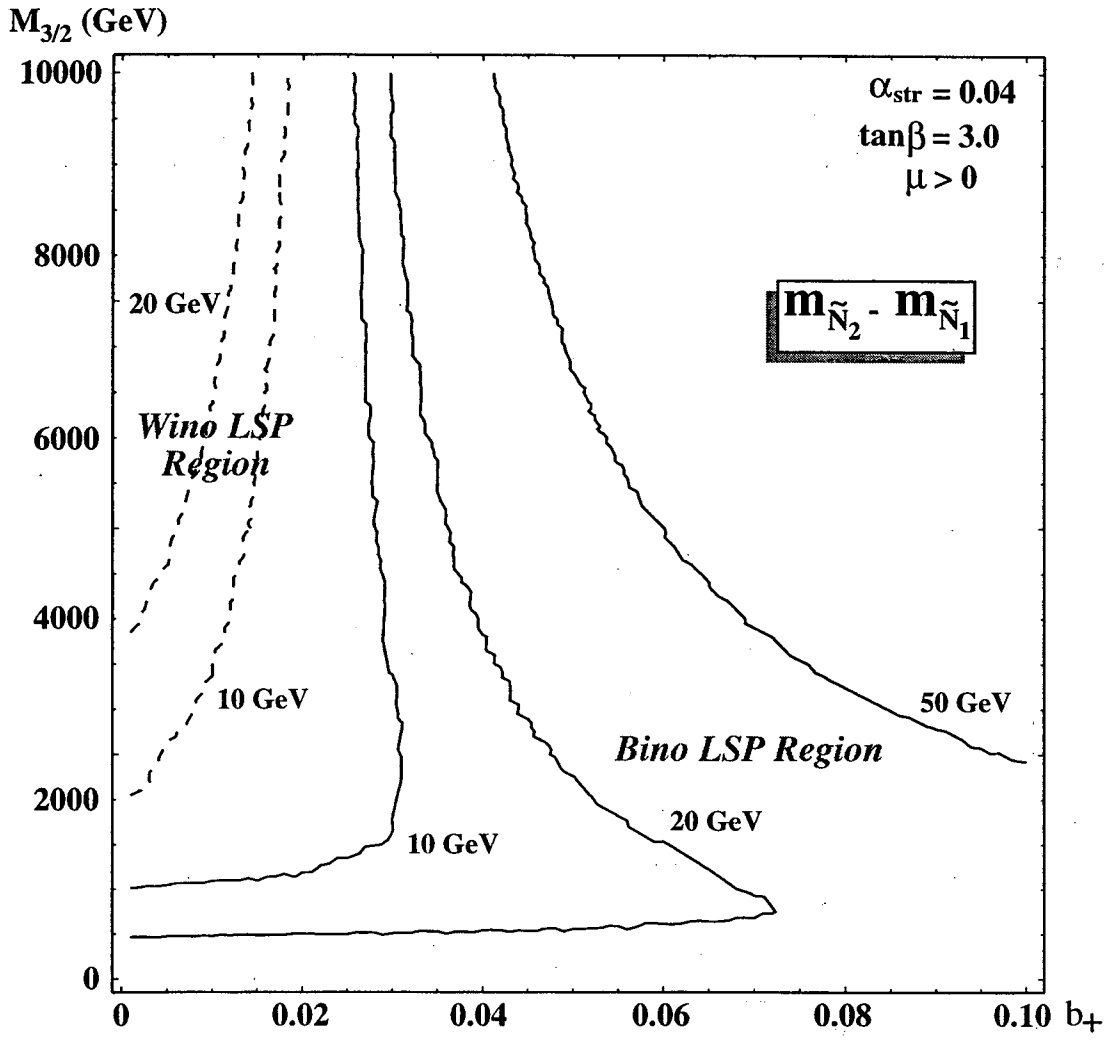

Figure 5.10: Wino-like and Bino-Like LSPs in Scenario A. The difference in mass between the two lightest neutralinos $\tilde{N}_2$ and $\tilde{N}_1$ is given. Note that a level crossing occurs and there exists a region in which the $\tilde{W}_3$ becomes the LSP, as is to be expected when the anomaly contribution to gaugino masses dominates.

$\alpha_{\rm STR} \gtrsim 0.04$ are nearly saturated when this effect arises.

The direct experimental constraints are most binding for the gaugino sector as they are by far the lightest superpartners in this class of models. Typical bounds reported from collider experiments are derived in the context of universal gaugino masses with a relatively large mass difference between the lightest chargino and the lightest neutralino. For most choices of parameters in the models studied here this is a valid assumption, but when the condensing group β-function coefficient b_+ becomes relatively small (i.e. similar in size to the MSSM hypercharge value of $b_{U(1)} = 0.028$) the pieces of the gaugino mass arising from the superconformal anomaly, the second term in (5.35), can become equal in magnitude to the first tree level term. Here there is a level crossing in the neutral gaugino sector. The lightest supersymmetric particle (LSP) becomes predominately wino-like and the mass difference between the lightest chargino and lightest neutralino becomes negligible. This effect is displayed in Figure 5.10. The phenomenology of such a gaugino sector has been studied recently in [74, 90, 101]. Note that when

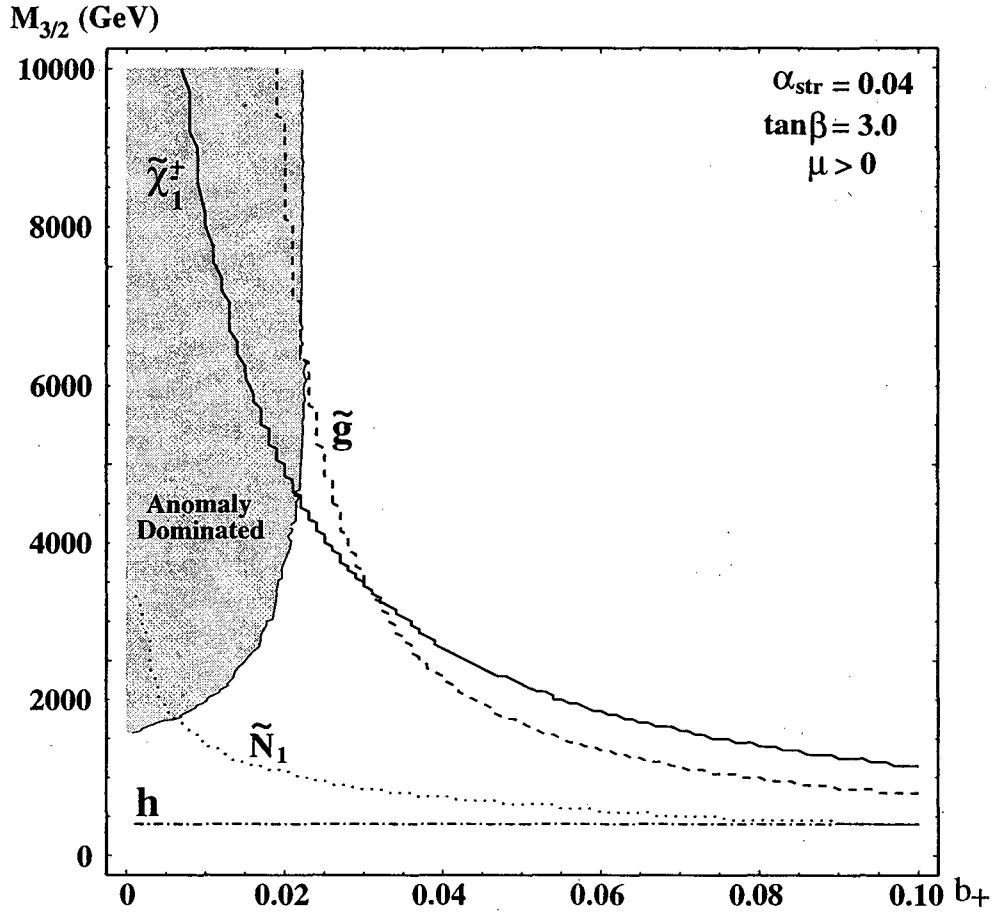

Figure 5.11: Constraints from Table 4.1 for Scenario A. Exclusion curves for lightest chargino (solid), gluino (dashed), lightest neutralino (dotted) and lightest Higgs mass (dashed-dotted) for weak coupling at the string scale. The region below the curves fails to meet the corresponding constraint from Table 4.1. The upper left corner represents the region where the difference in mass between the $\chi_1^{\pm}$ and the $\tilde{N}_1$ falls below 2 GeV.

any scalar fields couple to the GS counterterm (as in scenario D) there is a large additional, universal contribution to the gaugino masses at the condensation scale in (5.35). This eliminates any region with a non-standard gaugino sector in these cases.

Figure 5.11 gives the binding constraints from Table 4.1 for scenario A with $\tan\beta = 3$ and positive μ (the most restrictive case). The most critical constraints are for the lightest chargino and gluino.[5] The effect of varying $\tan\beta$ on these bounds is negligible over the range $1.65 \lesssim \tan\beta \lesssim 4.5$, as its effect is solely in the variation in the Yukawa couplings appearing at two loops in the gaugino mass evolution. The region for which the anomaly-induced contributions to the gaugino masses are significant is represented by the shaded region in the upper left of the figure. In general, the light gaugino masses at the condensation scale require a large gravitino mass (and hence, a large set of universal soft scalar masses since $M_A = M_0 = M_{3/2}$ in this scenario) in order to evade the observational bounds coming from LEP and the Tevatron. While current theoretical prejudice would disfavor such large soft scalar masses, this pattern of soft

[5]The gluino mass determination takes into account the difference between the running mass (M_3) and the physical gluino mass [119]. This difference is neglected for the other mass parameters.

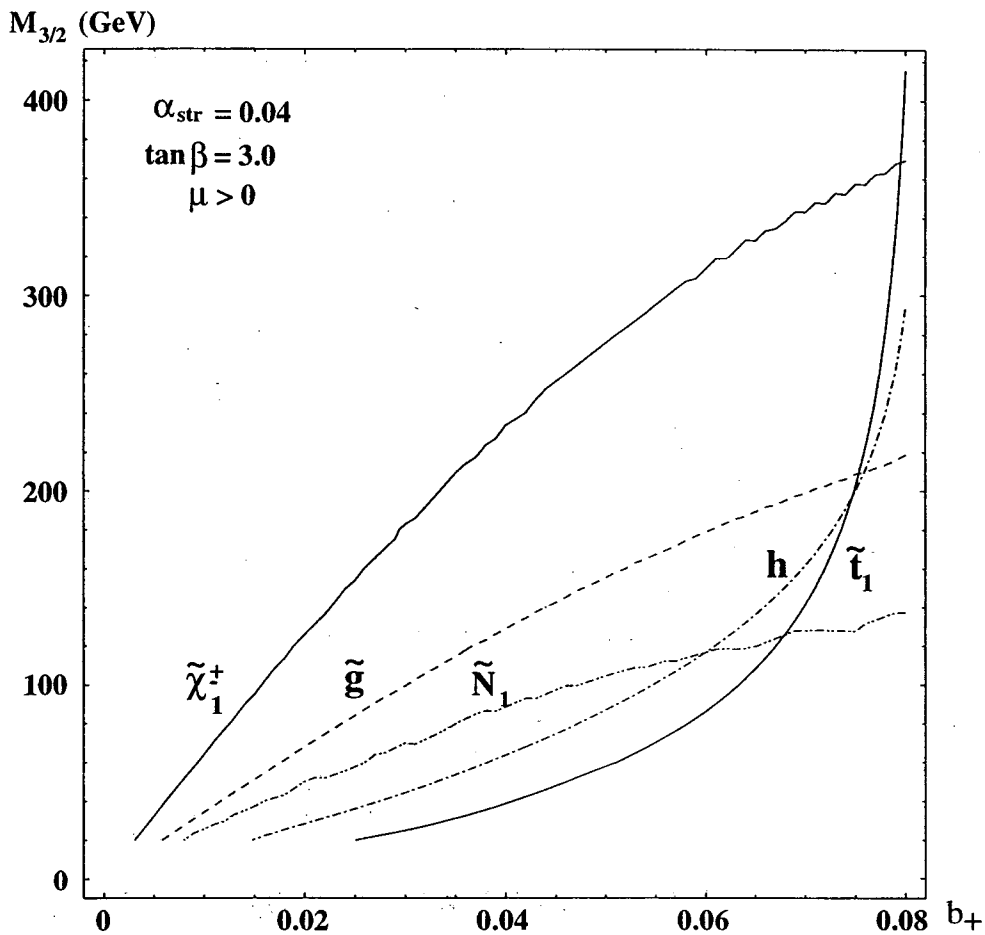

Figure 5.12: Constraints from Table 4.1 for Scenario D. Exclusion curves for lightest chargino (thick solid), gluino (dashed), lightest neutralino (dotted), lightest Higgs (dashed-dotted) and lightest stop (thin solid) mass. Curves are for weak coupling at the string scale. The region below the curves fails to meet the corresponding constraint from Table 4.1.

parameters may not necessarily be a sign of excessive fine-tuning [71, 72]. Nevertheless, we refrain from making any statements about the "naturalness" of this class of models as we have not specified any mechanism for generating the μ-term.

Figure 5.12 gives the binding constraints from Table 4.1 for scenario D with $\tan\beta = 3$ and positive μ. Note the change of scale in both axes for these plots relative to those of scenario A. As in Figure 5.11, varying $\tan\beta$ over the range $1.65 \lesssim \tan\beta \lesssim 40$ has a negligible effect on the gaugino constraint contours and only a very small effect on the contours of constant stop mass. Here the gaugino masses start at much larger values so a lower supersymmetry breaking scale is sufficient to evade the bounds from LEP and the Tevatron. Though the gravitino mass can now be much smaller, recall that the scalars in this scenario have masses at the condensation scale roughly an order of magnitude larger than the gravitino. Thus the typical size of scalar masses at the electroweak scale continues to be about 1 TeV for the first two generations and a few hundred GeV for the third generation scalars. As opposed to the case where all the matter fields of the observable sector decouple from the GS counterterm, here smaller values of the condensing group β-function coefficient *enhance* the gaugino masses via the last term in (5.35). We end this section by giving mass contours for the lightest Higgs, chargino, neutralino and top

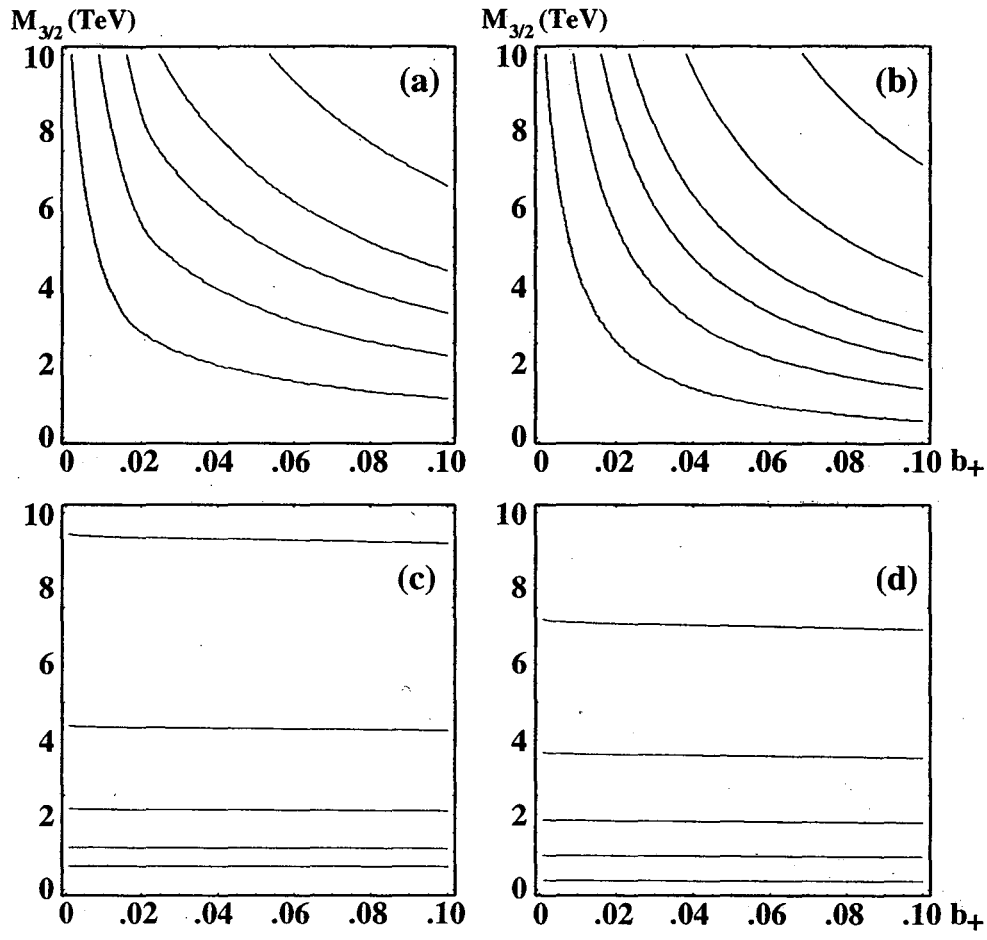

Figure 5.13: Mass Contours for Scenario A. *Panel A:* Contours for the lightest neutralino mass of 40, 80, 120, 160 and 240 GeV. *Panel B:* Contours of lightest chargino mass of 40, 80, 120, 160, 240 and 400 GeV. *Panel C:* Contours of lightest Higgs mass of 90, 100, 110, 120 and 130 GeV. *Panel D:* Contours of lightest stop mass of 200, 500, 1000, 2000 and 4000 GeV. All contours increase from the bottom to the top of each panel.

squark for $\tan\beta = 3$ and positive μ for scenarios A and D in Figures 5.13 and 5.14, respectively.

5.3.3 Gauge Coupling Unification

In Section 5.2.3 the possibility of larger values of the unified coupling constant $g^2_{\rm STR}$ at the string scale was considered in a very general way. It is well known [56] that the apparent unification of coupling constants at a scale $\Lambda_{\rm MSSM} \approx 2 \times 10^{16}$ GeV, assuming only the MSSM field content, is at odds with the string prediction that unification must occur at a scale given by

$$\Lambda^2_{\rm STR} = \lambda g^2_{\rm STR} M^2_{\rm PL} \tag{5.38}$$

where λ represents the (scheme-dependent) one loop correction from heavy string modes. In [28] this factor was computed for the $\overline{\rm MS}$ scheme and it is given by

$$\lambda = \frac{1}{2}\,(f+1)\,e^{g-1}, \tag{5.39}$$

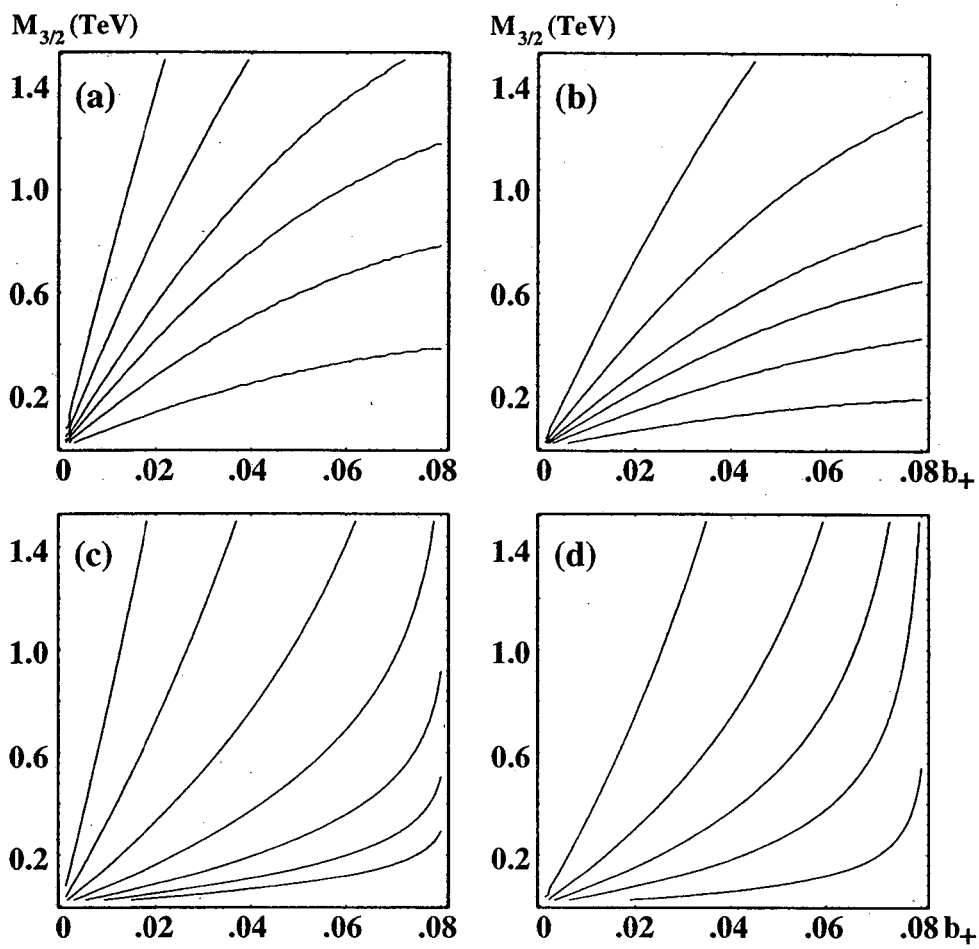

Figure 5.14: Mass Contours for Scenario D. *Panel A:* Contours for the lightest neutralino mass of 40, 80, 120, 160, 240 and 400 GeV. *Panel B:* Contours of lightest chargino mass of 40, 80, 120, 160, 240 and 400 GeV. *Panel C:* Contours of lightest Higgs mass of 80, 90, 100, 110, 120, 130 and 140 GeV. *Panel D:* Contours of lightest stop mass of 200, 500, 1000, 2000 and 4000 GeV. All contours increase from the bottom to the top of each panel.

where f and g are the vacuum values of the nonperturbative corrections in (5.4) and (5.22). For the vacua considered in this work this parameter is typically $\lambda \sim 0.19$.

Even after taking into account one loop string corrections there is still an order of magnitude discrepancy between the scale of unification predicted by string theory and the apparent scale of unification as extrapolated from low energy measurements under the MSSM framework. One possible solution to the problem is the inclusion of additional matter fields in incomplete multiplets of SU(5) at some intermediate scale which will alter the running of the coupling constants, causing them to converge at some value higher than Λ_{MSSM} [88, 118]. These solutions tend to involve slightly larger values of the coupling constant at the string scale than that of the MSSM ($\alpha_{\text{MSSM}}^{-1} \approx 24.7$).

In the model in question here, the intermediate scale (Λ_{COND}) at which this additional matter might appear is not independent of the scale of the superpartner spectrum ($\Lambda_{\text{SUSY}} \sim M_{3/2}$), but the two are in fact related by equation (5.28). Thus if we assume this additional matter has a typical mass of the condensation scale, each point in the $\{b_+, M_{3/2}\}$ plane can be tested for

potential compatibility with string unification given a certain set of additional matter fields. We will not specify the origin of these fields (though such incomplete multiplets are not uncommon in string theory compactifications [91]), but merely posit their existence with masses on the order of the condensation scale.

Our procedure for carrying out this investigation is similar to that used in the literature by a number of authors [3, 12, 102]. The standard model coupling constants α_3, α_2 and α_1 are determined from $\alpha_{\rm EM}(M_Z) = 1/127.9$, $\alpha_3(M_Z) = 0.119$ and $\sin^2\theta_{\rm EW}(M_Z) = .23124$ and these $\overline{\rm MS}$ values are converted to the $\overline{\rm DR}$ scheme. As we will not be concerned with performing a precision survey, these coupling constants are run at one loop from their values at the electroweak scale using only the standard model field content up to the scale $\Lambda = M_{3/2}$. At this scale the entire supersymmetric spectrum is added to the equations until the scale $\Lambda = \Lambda_{\rm COND}$ is reached. Here incomplete multiplets of SU(5) are added and the couplings are run to the scale at which the SU(2) and U(1) fine structure constants coincide. This scale will be defined as the string scale.

We now require $\alpha_3 = \alpha_2 = \alpha_1$ at this scale and invert equation (5.38) to find the implied Planck scale. Consistency requires that this value be the reduced Planck mass of 2.4×10^{18} GeV *and* that the QCD gauge coupling, when the renormalization group equations are solved in the reverse direction, give a value for α_3 at $\Lambda = M_Z$ within two standard deviations of the measured value.[6]

The results of the analysis for a typical choice of extra matter fields are shown in Figure 5.15, where a pair of vector like $(Q, \overline{Q})$ and two pairs of vector-like $(D, \overline{D})$'s are introduced at the condensation scale with quantum numbers identical to their MSSM counterparts. The two sigma window about the current best-fit value of α_3 can indeed accomodate a consistent Planck mass while allowing for perturbative unification of gauge couplings. From this base configuration additional **5**s and **10**s of SU(5) can be added at will to increase the value of the unified coupling at the string scale, but the contours of constant implied Planck mass shown in Figure 5.15 will not move significantly. While these combinations of matter fields have been known to allow for gauge coupling unification for some time [88, 118], the relationships (5.28) and (5.38) between the various scales involved makes this a nontrivial accomplishment for this class of models.

5.4 Dark Matter in Condensation Models

As a supergravity model with a unification scale, many of the typical results of mSUGRA continue to hold in the models of gaugino condensation considered in Section 5.1, in particular the few number of parameters necessary to determine the low energy spectrum. However the contribution to the gaugino masses resulting from the superconformal anomaly (2.32) gives a correction to the standard gaugino mass unification that was demonstrated in Figure 5.5. Thus in this model one is able to determine the ratio (M_2/M_1) as a function of the parameters of the hidden sector.

[6] It is worth remarking that even the celebrated supersymmetric SU(5) unification of couplings fails to predict the strong coupling at the electroweak scale at the level of two sigma and calls for a rather large value of $\alpha_3(M_Z)$ [3, 12, 102]. This is usually taken as an indication of the size of model-dependent threshold corrections. We therfore demand no more from the models considered here.

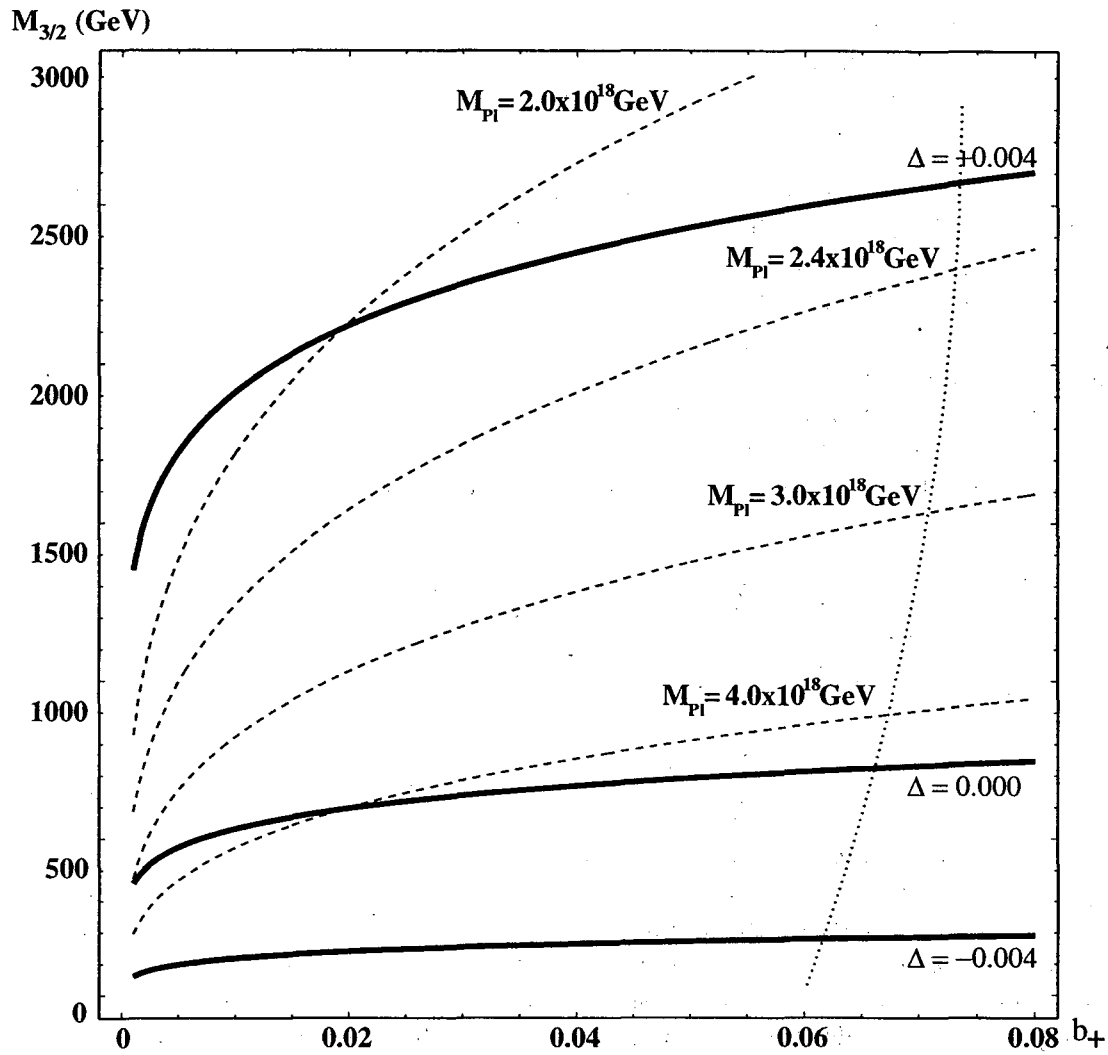

Figure 5.15: Gauge Coupling Unification. Results of adding one pair of $(Q, \overline{Q})$ and two pairs of $(D, \overline{D})$ at the condensation scale. Contours of constant implied Planck mass are overlaid on the region for which $\Delta = \alpha_3^{\text{RGE}} - \alpha_3^{\text{OBS}}$ is within the two-sigma experimental limit of $\delta\alpha = \pm 0.004$. The dotted line represents the maximum value of b_+ consistent with $M_{3/2} \leq 10$ TeV and the RGE determined string coupling. The values of α_{STR} here range from 0.044 at the $\Delta = +0.004$ contour to 0.050 at the $\Delta = -0.004$ contour.

From (5.35) is is clear that the key variable (M_2/M_1) depends on the value of b_+ when $p_A = 0$:

$$\frac{M_2(\Lambda_{\text{COND}})}{M_1(\Lambda_{\text{COND}})} = \frac{g_2^2(\Lambda_{\text{COND}})\,(1 + b_2'\ell) - (b_2/b_+)\,(1 + b_+\ell)}{g_1^2(\Lambda_{\text{COND}})\,(1 + b_1'\ell) - (b_1/b_+)\,(1 + b_+\ell)} \tag{5.40}$$

Figure 5.16 shows contours of constant LSP (χ_0) relic density for the model of Section 5.1 in the $\{b_+, M_0\}$ plane, where M_0 is the usual universal scalar mass whose value is given by $M_0 = M_{3/2}$ in the model we will consider here. While the axes of Figure 5.16 are very similar to those of Figures 4.3, 4.5 and 4.6 there are some notable differences in this model. The gluino mass parameter M_3 relates to M_2 and M_1 through an identical relationship to Equation (5.40) and therefore changes with b_+. In the previous figures M_3 was held constant at the high scale within a single plot, but in Figure 5.16 the ratio M_3/M_1 at the condensation scale varies from

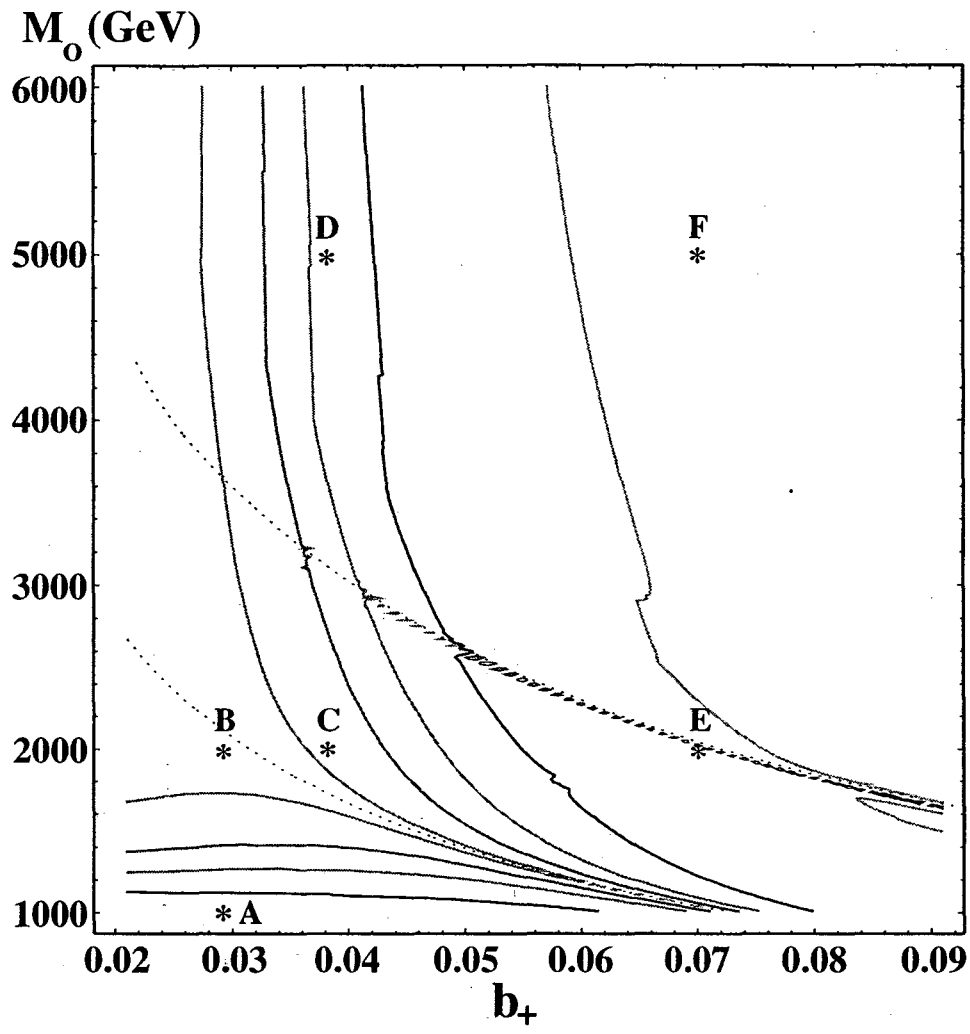

Figure 5.16: Cosmologically Preferred Region in Gaugino Condensation Models. Contours of constant relic density are given as a function of M_0 and b_+ by the solid lines while the Higgs resonance and $W^\pm$ resonance are indicated by the upper and lower dotted lines, respectively. Moving outward from the lower dotted line are contours of $\Omega_\chi h^2 = 0.01$, 0.1, 0.3, 1.0 and 10. The labeled points are examined in detail in Figure 5.18.

0.2 at $b_+ = 0.02$ to 0.8 at $b_+ = 0.09$. Nevertheless, there is still a region of viable dark matter largely independent of the universal scalar mass, as in the general nonuniversal cases studied in Section 4.2, for the same reasons: a smaller value of (M_2/M_1) for lower b_+ results in higher wino content as well as more degeneracy between the lightest neutralino and chargino, resulting in conannihilation.

In Figure 5.16 it is evident that this is not a result of the masses being tuned to sit on a pole. The Higgs pole, given by the locus of points for which $2m_{\chi_1^0} = m_h$, is indicated by the uppermost dotted line. More important is the W-pole, denoted by the second lower dotted line in the left plot, where a neutralino and chargino go to an on-shell W-boson, severely warping the lower part of the plot. However, both of these resonant regions are excluded experimentally by the criteria of Table 4.1 as indicated in Figure 5.17 by the shaded region. The key constraints include the gluino mass (given by the dashed line) and the chargino mass (given by two parallel

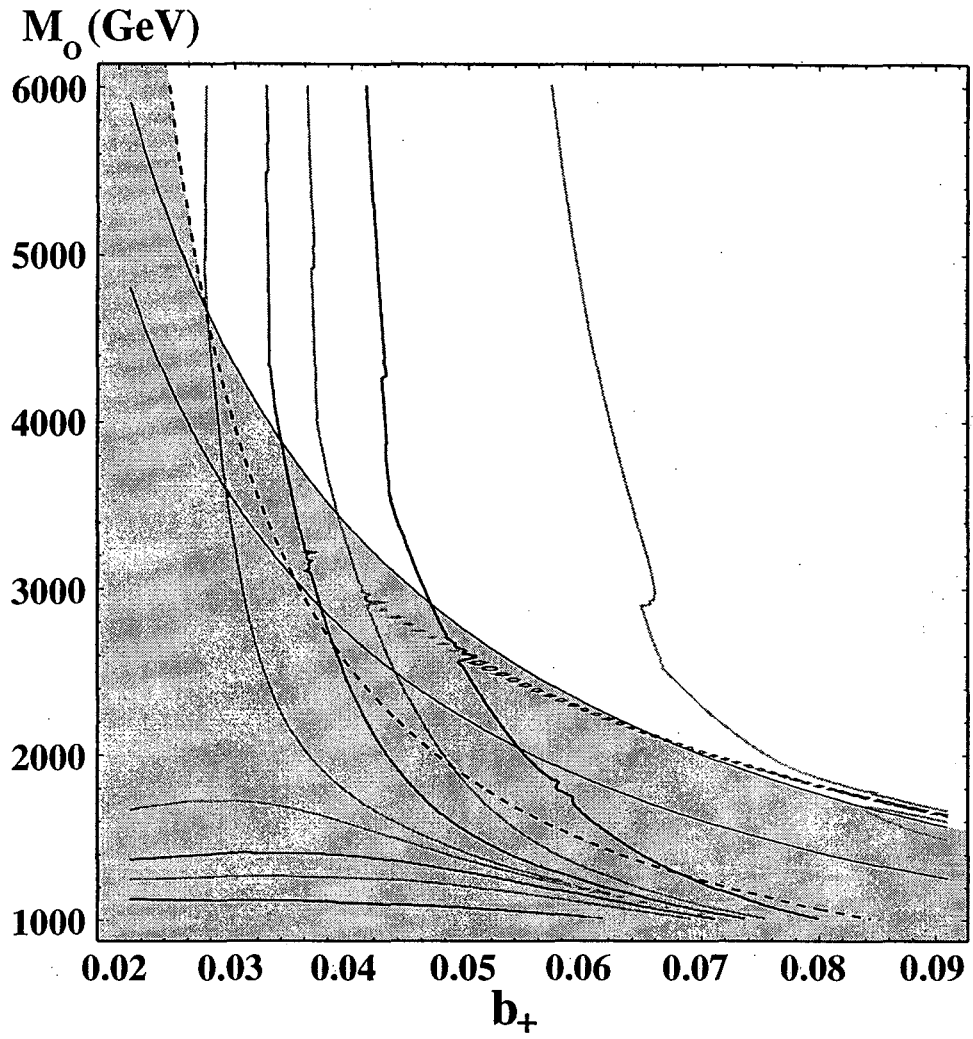

Figure 5.17: Cosmologically Preferred Region and Experimental Constraints. Contours of $\Omega_\chi h^2 = 0.01$, 0.1, 0.3, 1.0 and 10 are again shown along with the experimental constraints from Table 4.1. The shaded region is excluded: the dashed curve represents a 190 GeV gluino mass while the two parallel solid curves represent a 75 GeV and a 90 GeV chargino mass from bottom to top.

solid curves representing a chargino mass of 75 and 90 GeV from bottom to top).

As with the previous cases the additonal physics contained in this plot is easily seen through a few representative points given in more detail in Figure 5.18. Starting from the top right in Figure 5.16, point F sits at far too high a value of M_0 for the normal cMSSM annihilation channels to be effective. Its high value of b_+ also gives a high value of $(M_2/M_1)_{\rm low}$ (between 1.3 and 1.4), so the wino content of the LSP is low. The dominant channels are neutralino-chargino coannihilation but this is not sufficient to deplete the relic density to acceptable levels. Point E lies exactly on the pole for two neutralinos going to an on-shell Higgs which then naturally decays to two fermions, making this the dominant final state. A lowered scalar mass scale also allows coannihilation to two fermions to increase. Nevertheless, the net effect is still too small to bring the relic density down far enough.

Point D is in the region where one would not expect much annihilation to fermions, but for this

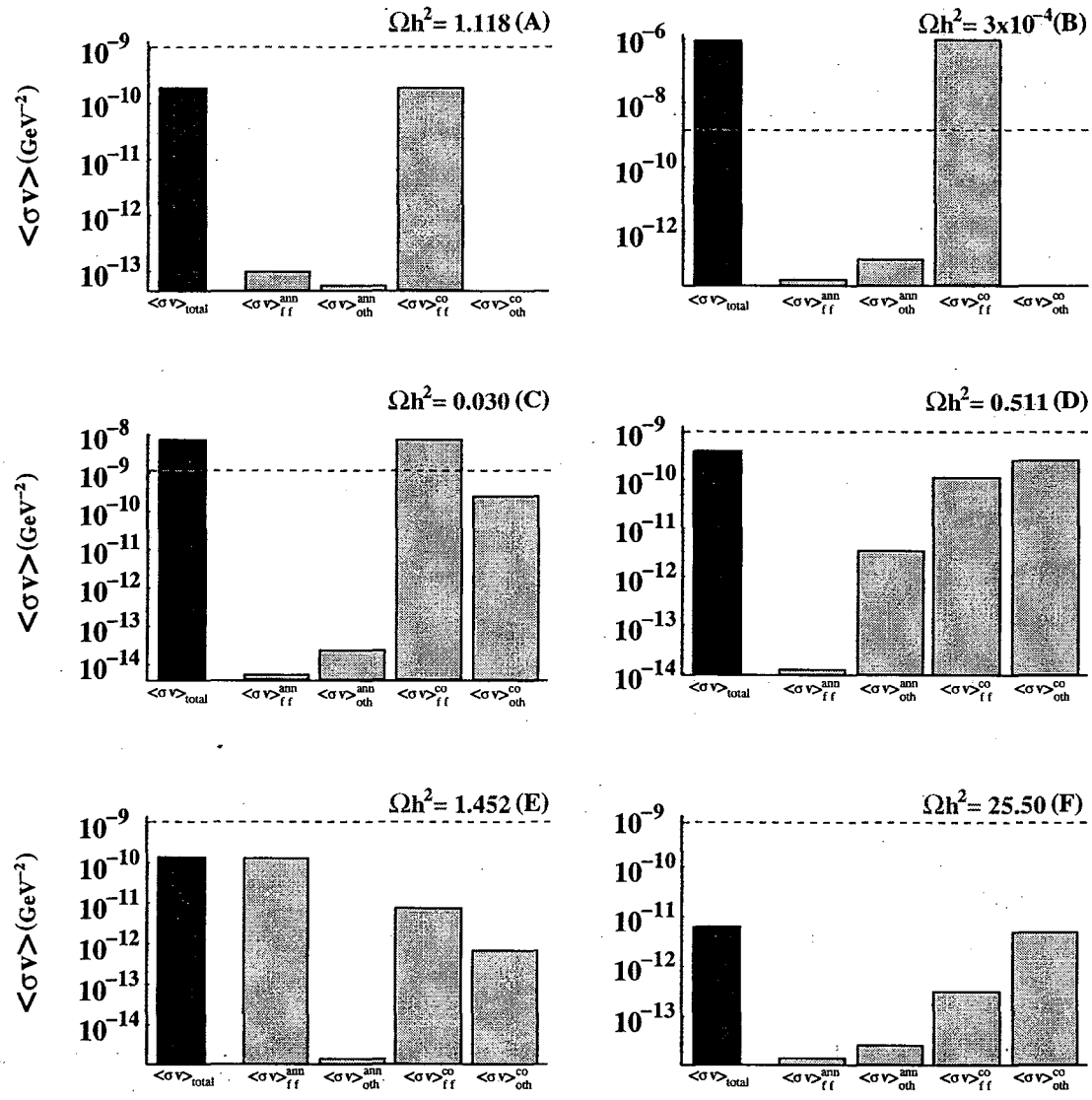

Figure 5.18: Annihilation Cross Sections for Selected Points From Figure 5.16. These graphs are identical in nature to those of Figure 4.4.

b_+ value the neutralino and chargino are becoming more degenerate, increasing coannihilation and bringing the relic density down towards the cosmologically preferred region. Additionally, points D and F are the only two points which kinematically allow $\chi^\pm\chi^0 \to W^\pm Z$. Once this channel is open it is the main determining factor in the relic density.

Points B and C both lie near the region where the masses of the lightest chargino and the LSP add up to exactly the mass of the charged W-boson. This enhances the efficiency of most channels of chargino-neutralino coannihilation, resulting in a relic density that is now a little too low to account for astrophysical observations. For point A, by contrast, the particles are off-shell so these processes are too inefficient and the relic density is too high. Note that for points A, B and C the value of the lightest chargino mass is below the experimental limit so these points are excluded.

Figure 5.19 shows how the parameters of this model determine wino content and the ratio

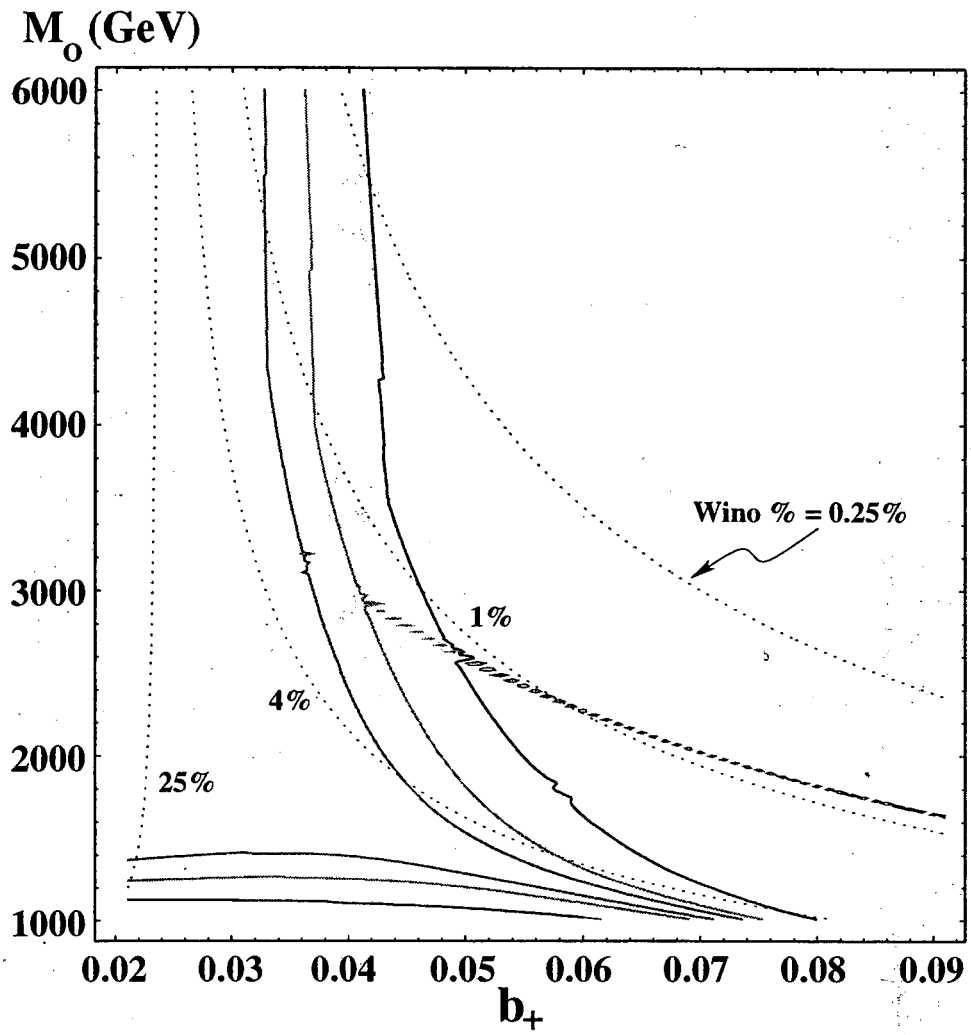

Figure 5.19: Relic Densities vs. Wino Content in Gaugino Condensation Models. Contours of constant relic density are given as in Figure 5.16 by the solid lines for $\Omega_\chi h^2 = 0.1$, 0.3, and 1.0 only. Dotted lines are contours of constant wino content of 25%, 4%, 1%, 0.25% from left to right.

$(M_2/M_1)_{\text{low}}$. As in the case of Figures 4.5 and 4.6 from Section 4.2, cosmological observations favor a mild wino content of 0.1% to 5% and single out the region $1.15 \lesssim (M_2/M_1)_{\text{low}} \lesssim 1.25$. The correspondence between the value of b_+ and $(M_2/M_1)_{\text{high}}$ is clear from the comparison of Figure 5.20 with Figures 4.5 and 4.6, in particular panels (A) for lower values of b_+ and (B) for higher values.

To see the discriminatory power that cosmological considerations can have on model building, consider Figure 5.21. We sampled 25,000 combinations of $\{b_+, (b_a^\alpha)_{\text{eff}}, (c_\alpha)_{\text{eff}}\}$ which give rise to gravitino masses between 100 GeV and 10 TeV and which yield a particle spectrum consistent with the bounds in Table 4.1 [34]. In Figure 5.21 we display those combinations which implied a relic density in the range $0.1 \leq \Omega_\chi h^2 \leq 0.3$ (fine points), as well as the slightly higher range $0.3 < \Omega_\chi h^2 \leq 1.0$ (coarse points).

Figure 5.21 clearly favors a very specific region of hidden sector parameter space with a preferred value of b_+ in the neighborhood of $b_+ = 0.036$ and a corresponding range in $(b_a^\alpha)_{\text{eff}}$

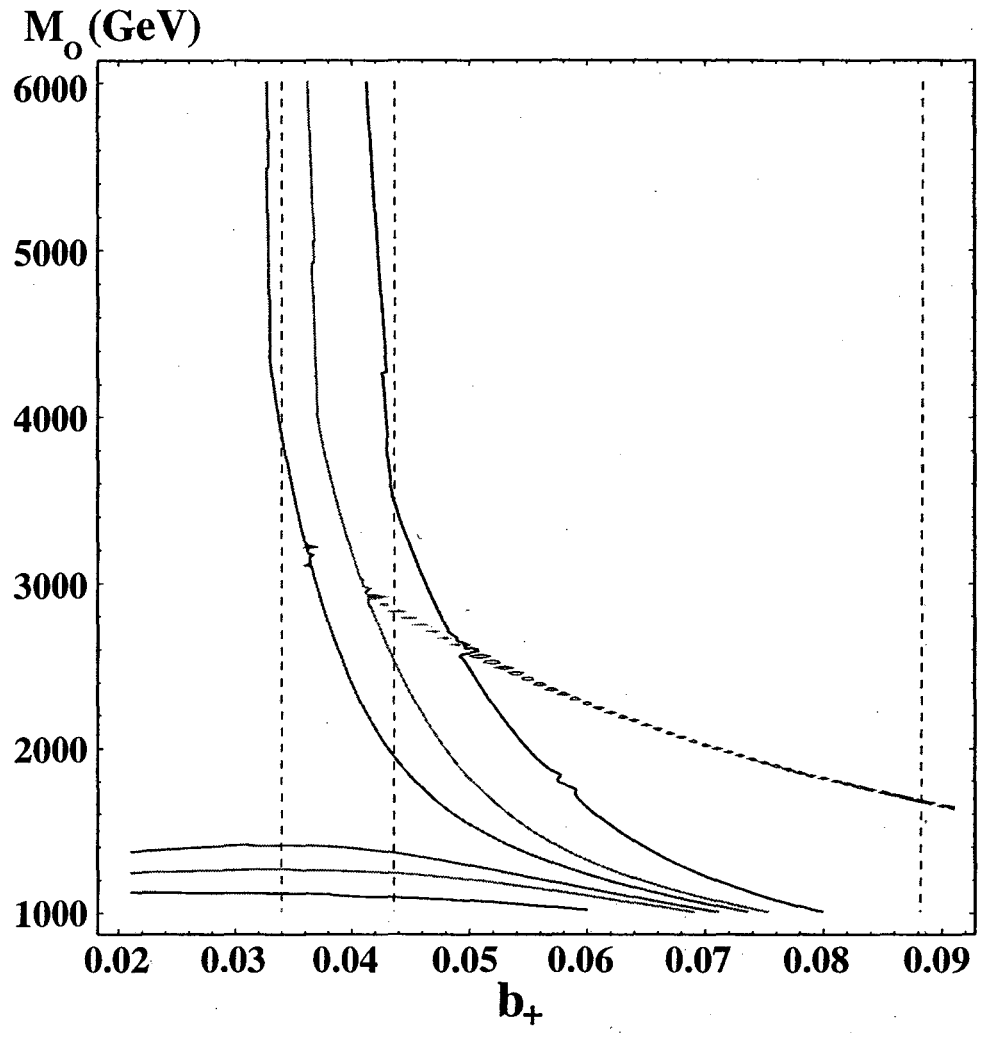

Figure 5.20: Relic Densities vs. Gaugino Mass Ratios in Gaugino Condensation Models. Contours of constant relic density are given as in Figure 5.16 by the solid lines for $\Omega_\chi h^2 = 0.1$, 0.3, and 1.0. Dashed lines are contours of constant ratio $(M_2/M_1)_{\rm low}$ of 1.15, 1.25, and 1.5 from left to right.

of $0.2 \lesssim (b_a^\alpha)_{\rm eff} \lesssim 0.6$, which points towards a large condensing group such as $SO(12)$, $SO(14)$, $SO(16)$, E_6 or E_7. A typical matter configuration for the hidden sector would be represented in Figure 5.21 by a point on one of the gauge group lines. The number of possible configurations consistent with a given choice of $\{\alpha_{\rm str}, (c_\alpha)_{\rm eff}\}$ and supersymmetry breaking scale $M_{3/2}$ is quite restricted. For example, if we ask for a hidden sector configuration charged under the E_6 gauge group for which $C_{E_6} = 12$ and $C_{E_6}^{\rm fund} = 3$, and require that our matter condensates be gauge invariant so that fundamentals must come in groups of three, then from (5.8) and (5.9) the only combination that falls in the preferred region of Figure 5.21 is $N_{\rm fund} = 9$. This combination is notable in that it was shown in [84] to possess many desirable phenomenological features. A similar analysis for the other allowed gauge groups leaves only a handful of possible hidden sector configurations, summarized in Table 5.1, where we have included some examples with various hidden sector effective Yukawa couplings $(c_\alpha)_{\rm eff}$ and the implied values of $M_{3/2}$ and $\Omega_\chi h^2$. As is evident from the table and from Figure 5.21, using the dark matter constraint on LSP relic densities is a very powerful tool in restricting the high energy physics of the underlying theory.

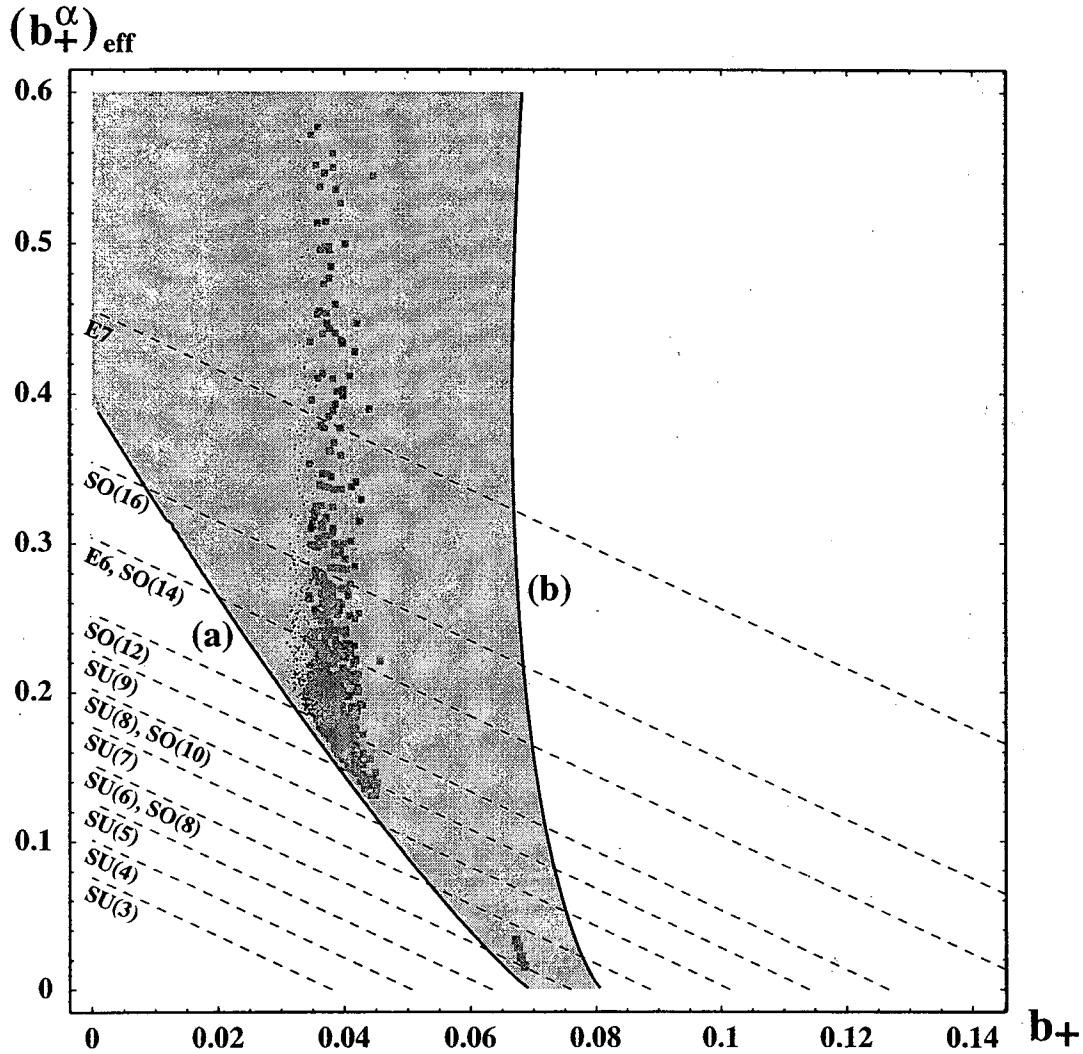

Figure 5.21: Preferred Dark Matter Region in Hidden Sector Configuration Space. This plot illustrates the dark matter parameter space in terms of the gauge group and matter content parameters of the hidden sector. The fine points on the left have the preferred value $0.1 \leq \Omega_\chi h^2 \leq 0.3$ and the coarse points have $0.3 < \Omega_\chi h^2 \leq 1.0$. The swath bounded by lines (a) and (b) is the region in which the $0.1 \leq (c_\alpha)_{\rm eff} \leq 10$ and the gravitino mass is between 100 GeV and 10 TeV. The dotted lines are the possible combination of gauge parameters for different hidden sector gauge groups.

In summary, the prospects for cMSSM dark matter at low $\tan\beta$ are rapidly diminshing, barring a curious conspiracy between M_0 and $M_{3/2}$. This is due to the inefficient annihilation of a dominantly bino-like LSP. Departure from the standard cMSSM GUT relation allows values of (M_2/M_1) that accomodate small admixtures of wino content for the LSP. Lowering this ratio at the electroweak scale increases the LSP annihilation efficiency by virtue of its higher wino content and the tightening degeneracy between the lightest chargino and the LSP, resulting in increased coannihilation. Ranges of $(M_2/M_1)_{\rm low}$ exist with $0.1 \leq \Omega h^2 \leq 0.3$ and where the value of M_0 is restricted to be anything *above* 1 TeV – quite in contrast to the light scalars required at low $\tan\beta$ in the standard cMSSM case.

The requirement of cosmologically interesting relic densities, or at least the demand that

Gauge group	C_a	C_a^{fund}	b_a	$(b_a^\alpha)_{\text{eff}}$	N_{fund}	$(c_\alpha)_{\text{eff}}$	$M_{3/2}$ (GeV)	$\Omega_\chi h^2$
E_6	12	3	0.038	0.23	9	3.8	5967	0.633
$SO(16)$	14	1	0.034	0.29	34	2.7	7011	0.194
$SO(14)$	12	1	0.034	0.24	28	4.4	3383	0.069
$SO(12)$	10	1	0.034	0.19	22	6.3	1438	0.076

Table 5.1: Gauge group Casimirs and allowed condensate numbers. Possible hidden sector gauge group configurations that might give rise to thermal relic neutralino densities compatible with observations.

$\Omega_\chi h^2 \leq 1$, can be a powerful constraint on models with nonuniversal gaugino masses which is often quite complementary to the constraints arising from direct search limits for superpartners. For example, in the model of gaugino condensation considered here, the number of possible hidden sector gauge groups and matter configurations could be restricted to a very small number. Similar analyses on models with small deviations from universality should prove equally fruitful. While relic densities of supersymmetric particles that were once in thermal equilibrium need not be the explanation for the missing nonbaryonic mass in the universe,[7] it is nevertheless one of the most compelling aspects of low energy supersymmetric phenomenology and promises to remain so even in scenarios with heavy squarks and sleptons.

[7]In [124], for example, nonthermal mechanisms are used to provide adequate relic densities in the case of the highly wino-like LSP characteristic of the standard anomaly mediated supersymmetry breaking scenario.

Conclusions

In conclusion, we have shown in Section 2 that even in the absence of soft supersymmetry breaking at tree level, the loop-induced soft supersymmetry breaking operators are not uniquely determined by anomalies. In particular, the hidden sector Kähler potential and superpotential must be separately specified. This is closely related to the well-known fact[8] that Kähler invariance of supergravity is broken at the quantum level, as is manifest in the expressions (2.39); F^n is Kähler covariant while K_n is not. Once the full low energy Lagrangian is specified, including any hidden sector, the one loop gaugino masses are completely determined by the requirements of finiteness and supersymmetry of the Kähler anomaly. However the soft terms in the scalar potential depend on the details of Planck scale physics, since the corresponding PV couplings are not sufficiently constrained. In particular, scalars can acquire masses at one loop in the absence of tree level soft supersymmetry breaking. This is the case in the no-scale model when the PV couplings are chosen so that the renormalized Kähler potential does not break Kähler invariance. Kähler invariance is necessarily broken by gauge coupling renormalization (unless specific constraints are imposed on the low energy theory) because there is no similar freedom to adjust the relevant PV couplings. In the context of string-derived supergravity, field theory anomalies for Kähler transformations associated with the exact perturbative symmetries of string theory must be canceled, for example by the introduction of a Green-Schwarz counterterm in the case of gauge coupling renormalization. This breaks the no-scale structure of the untwisted matter sector, and there are generally soft supersymmetry terms at tree level, with supersymmetry broken in the dilaton (S) sector. One loop effects can nevertheless be important, especially for gaugino masses.

Let us stress that even though we have been studying specific classes of superstring models, the types of spectra that we obtained and discussed in Section 3 appear to be quite generic. For example, scenarios from models with extra dimensions tend to give spectra which can be related to one or another type considered here, whether it is the model of Randall and Sundrum [131], or models of gaugino mediation [108, 134]. In particular, soft terms that are proportional to β-function coefficients and anomalous dimensions can be realized in a variety of ways in string-derived supergravity. The case that is generally referred to as "anomaly mediation" is just one limiting value in a continuum of such models. The importance of these anomaly-induced terms depends on the absence or suppression of tree level contributions to the soft supersymmetry breaking parameters and on the assumptions made regarding the underlying theory when regulating the effective supergravity theory.

Once supersymmetry is discovered, the central issue will be to unravel the mechanism of supersymmetry breaking. The search strategy will be of the most value if it is based on large

[8] For a recent discussion of this and related issues, see [14].

classes of different models, not just on a single "minimal" model. The models studied above tend to show that a possible strategy could be based on three steps:

(1) identifying gaugino masses (the least model dependent aspect of these theories) and the nature of the LSP;

(2) identifying where (approximately) the bulk of the scalar masses lie and whether there is an order of magnitude between gaugino and scalar masses;

(3) then using the details of the scalar masses, in particular the mixing in the stop sector and the degree of nonuniversality, to disentangle the possible scenarios.

Observation of nonuniversal supersymmetric parameters obeying the relations described in Sections 3.1 – 3.3 will likely shed light on the scale of supersymmetry breaking, the nature of the fields responsible for this breaking and the origin of the μ-term, if not the properties of the underlying superstring theory itself.

The preceding pages should be cause for guarded optimism with regard to string phenomenology. As we saw in Section 5, the initial challenge of dilaton stabilization has been met without resorting to strong coupling in the effective field theory nor requiring delicate cancellations. Reasonable values of the supersymmetry breaking scale can be achieved over a fairly large region of the parameter space, but a given combination of coupling strength at the string scale and hidden sector matter content will single out a tantalizingly small slice of this space. These successful combinations do not destroy the potential solutions to the coupling constant unification problem by the introduction of additional matter at the condensation scale. Tighter restriction on the hidden sector will require more precise knowledge of the size of Yukawa couplings in the corresponding superpotential.

Requiring a vacuum configuration which gives rise to successful electroweak symmetry breaking seems to demand that either the Green-Schwarz counterterm be independent of the matter fields or that all matter fields couple in a universal way but that the Higgs fields are distinct. The pattern of soft supersymmetry breaking parameters in the former case pushes the theory towards large gravitino masses and very low values of $\tan\beta$. The low gaugino masses relative to scalar masses favors larger β-function coefficients for the condensing group of the hidden sector, while smaller values may result in phenomenology in the gaugino sector similar to that of the "anomaly dominated" scenarios. These same values tend to lie in the region of the parameter space for which relic neutralinos could account for the majority of the "dark" matter in the universe.

A more realistic model may alter these results to some degree and uncertainty remains in the general size and nature of the Yukawa couplings of the hidden sector of these theories. Nevertheless this survey suggests that eventual measurement of the size and pattern of supersymmetry breaking in our observable world may well point towards a very limited choice of hidden sector configurations (and hence string theory compactifications) compatible with low energy phenomena.

Appendix A

Chiral vs. Linear Multiplet Formulation for the Dilaton

In this appendix we show the correspondence between various terms in the component Lagrangian of the linear formalism and of the expressions given in Section 2. In the presence of a nonperturbatively induced potential for the dilaton, the tree level scalar Lagrangian takes the form (dropping gauge charged matter)

$$\mathcal{L}_{\text{scalar}} = -\sum_{\alpha} \frac{\partial_m t^\alpha \partial^m t^\alpha}{(t^\alpha + \bar{t}^\alpha)^2} - \frac{k'(\ell)}{4\ell}\partial_m \ell \partial^m \ell - \frac{\ell}{k'(\ell)}\partial_m a \partial^m a - V, \tag{A.1}$$

where the axion a is related to the two-form b_{mn} of the linear multiplet by a duality transformation:

$$\frac{1}{2}\epsilon^{mnpq}\partial_n b_{pq} = -\frac{2\ell}{k'(\ell)}\partial^m a. \tag{A.2}$$

The potential V can be written in the form

$$\begin{aligned} V &= \sum_{\alpha} \frac{1}{(t^\alpha + \bar{t}^\alpha)^2} F^\alpha \overline{F}^\alpha + \frac{\ell}{k'(\ell)} F^2 - \frac{1}{3} M \overline{M}, \\ F &= \frac{k'(\ell)}{4\ell} f(\ell, t^\alpha, z^i), \end{aligned} \tag{A.3}$$

where $f(\ell, t^\alpha, z^i)$ is a complex but nonholomorphic function of the scalar fields.

To cast this result in a form resembling the standard chiral formulation we introduce the variable $x(\ell) = 2g^{-2}(\Lambda_{\text{STR}})$, which is twice the inverse squared gauge coupling (1.18). It is related to the dilaton Kähler potential k by the differential equation [31]

$$k'(\ell) = -\ell x'(\ell), \quad \partial \ell = -\frac{\ell}{k'(\ell)}\partial x, \tag{A.4}$$

giving

$$\begin{aligned} &\frac{\partial k(x)}{\partial x} = k'(\ell)\frac{\partial \ell}{\partial x} = -\ell, \quad \frac{\partial^2 k(x)}{\partial x^2} = -\frac{\partial \ell}{\partial x} = \frac{\ell}{k'(\ell)}, \\ &\frac{k'(\ell)}{4\ell}\partial_m \ell \partial^m \ell = -\frac{\ell}{4k'(\ell)}\partial_m x \partial^m x = \frac{1}{4}\frac{\partial^2 k(x)}{\partial x^2}\partial_m x \partial^m x. \end{aligned} \tag{A.5}$$

Then setting

$$x = s + \bar{s}, \quad a = \mathrm{Im} s, \tag{A.6}$$

(A.1) and (A.3) take the standard form (now including gauge-charged chiral matter)

$$\begin{aligned} \mathcal{L}_{\text{scalar}} &= -\sum_N K_{N\overline{N}} \left(\partial_m z^N \partial^m \bar{z}^{\overline{N}} + F^N \overline{F}^{\overline{N}} \right) + \frac{1}{3} M \overline{M}, \\ K &= k\,(s+\bar{s}) + K(t^\alpha) + \sum_i \kappa_i |z^i|^2, \end{aligned} \tag{A.7}$$

provided we identify $F = F^S$ and $K_{S\bar{S}} = \ell/k'(\ell)$. When the fermion part of the Lagrangian is included, one obtains for the gaugino masses

$$M_a^{(0)} = \frac{g_a^2}{2} F, \tag{A.8}$$

in agreement with (2.49) for $f_a = s$ and $F = F^S$.

The replacements (A.6) amount to a duality transformation to the chiral formulation for the dilaton. When the GS term is included, after a two-form/scalar duality transformation, Eqs. (A.1)–(A.7) are modified by the replacements

$$\begin{aligned} \partial_m a &\to \partial_m a + \frac{b}{2} \sum_\alpha \frac{\partial_m \mathrm{Im} t^\alpha}{\mathrm{Re} t^\alpha}, \quad (t^\alpha + \bar{t}^\alpha)^{-2} \to (1 + b\ell)\,(t^\alpha + \bar{t}^\alpha)^{-2}, \\ b &= -\delta_{\text{GS}}/24\pi^2. \end{aligned} \tag{A.9}$$

We may make a full superfield duality transformation by the additional replacements

$$x = s + \bar{s} = \tilde{s} + \bar{\tilde{s}} + b \sum_\alpha \ln(t^\alpha + \bar{t}^\alpha), \quad k(s+\bar{s}) \to k\left[\tilde{s} + \bar{\tilde{s}} - bK(t^\alpha)\right], \tag{A.10}$$

where $\tilde{s}$ is the complex scalar component ($\mathrm{Im}\tilde{s} = a$) of the dilaton chiral superfield. This introduces mixing of the moduli with the dilaton in the Kähler metric [35, 36]. Working in the linear multiplet formalism for the dilaton, there is no mixing of the dilaton with chiral fields;[1] in this case (A.1) and (A.3) are modified only by (A.9). With this modification (A.3) is completely general; it includes the effects of the GS term on the potential for ℓ and t in the presence of a source of supersymmetry breaking such as gaugino condensation. In fact the GS term coupling to the confined hidden gauge sector, as in the model of Section 5, must be included to make the effective supersymmetry breaking "tree" Lagrangian perturbatively modular invariant.

In the linear multiplet formulation for the dilaton, the tree level scalar potential takes the form

$$\begin{aligned} V_{\text{tree}} &= \sum_N \widehat{K}_{N\overline{N}} F^N \overline{F}^{\overline{N}} - \frac{1}{3} M \overline{M}, \\ M &= -3e^{K/2} w, \quad F^N = -w^{-1} e^{-K/2} \widehat{K}^{N\overline{N}} \partial_{\overline{N}} \left(e^K w \bar{w} \right), \end{aligned} \tag{A.11}$$

where the effective metric $\widehat{K}_{N\overline{N}}$ is defined by

$$K_{M\overline{N}} \to \widehat{K}_{M\overline{N}} = K_{M\overline{N}} + \frac{g_s}{2} \partial_M \partial_{\overline{N}} V_{\text{GS}}, \tag{A.12}$$

[1] See for example the discussion of Eq. (4.20) in [87].

and $\widehat{K}_{S\overline{S}} = K_{S\overline{S}} = \ell/k'(\ell)$. If $p_i = 0$, the effect of (A.12) is to multiply the *vev* of F^α by the numerical factor $1 \leq 1 - g^2_{\rm STR}\delta_{\rm GS}/48\pi^2 \lesssim 1.1$ if $g^2_{\rm STR} = 1/2$. Additional corrections are unimportant if $\delta_{\rm GS}(t^\alpha + \bar{t}^\alpha)^{-1}|F^\alpha W_S/W|/48\pi^2 \ll |M/3|$: for example when supersymmetry breaking is dilaton dominated or if the superpotential is independent of the dilaton.

The expression in (A.11) reduces to the standard form if w is holomorphic. If a duality transformation to the chiral formulation for the dilaton is always possible [38] in the effective theory below the supersymmetry breaking scale, we must have

$$w = w(\tilde{s}, t^\alpha, z^i), \quad s = \frac{x}{2} + ia, \quad \tilde{s} = s + \frac{1}{2}V_{\rm GS}. \tag{A.13}$$

For example, in the gaugino condensation model of Section 5 we have

$$w = W(t^\alpha, z^i) + v(\tilde{s}, t^\alpha), \quad v = -e^{-K/2}\frac{b_+}{4}u, \quad u = ce^{K/2}e^{-\tilde{s}/b_+}\prod_\alpha \eta(t^\alpha)^{2(b-b_+)/b_+}, \tag{A.14}$$

where c is a constant. In this case we have

$$\begin{aligned} \partial_{\overline{N}} w &= \frac{1}{2}w_S\partial_{\overline{N}}V_{\rm GS}, \quad w_{\overline{s}} = 0, \quad F^S = -e^{K/2}\widehat{K}^{S\overline{S}}\left[\bar{w}_{\overline{S}} + K_{\overline{S}}\bar{w}\right] \\ F^N &= -e^{K/2}\widehat{K}^{N\overline{N}}\left[\bar{w}_{\overline{N}} + K_{\overline{N}}\bar{w} + \frac{1}{2}(\partial_{\overline{N}}V_{\rm GS})\partial_s \ln w\right]. \end{aligned} \tag{A.15}$$

Inserting these expressions in the potential (A.11) we obtain the following expressions for the soft supersymmetry breaking terms at tree level:

$$\begin{aligned} A^{\rm tree}_{ijk} &= A^{(0)}_{ijk} - \frac{b}{2(t^\alpha + \bar{t}^\alpha)}\left(F^\alpha\partial_s \ln\bar{w} + \text{ h.c. }\right), \\ \left[B^{\rm tree}_{ij}\right]_{\rm superpotential} &= \left[B^{(0)}_{ij}\right]_{\rm superpotential} - \frac{b}{2(t^\alpha + \bar{t}^\alpha)}\left(F^\alpha\partial_s \ln\bar{w} + \text{ h.c. }\right), \\ \left[B^{\rm tree}_{ij}\right]_{\text{Kähler potential}} &= \left[B^{(0)}_{ij}\right]_{\text{Kähler potential}} - \frac{b}{2(t^\alpha + \bar{t}^\alpha)}F^\alpha\partial_s \ln\bar{w}, \end{aligned} \tag{A.16}$$

where the expressions with index 0 are the tree level expressions given in the text with $W(Z^N) \to w(Z^N, V_{\rm GS})$ and

$$F^\alpha = -e^{K/2}\widehat{K}^{t^\alpha\bar{t}^\alpha}\left[\bar{w}_{\bar{t}^\alpha} + K_{\bar{t}^\alpha}\bar{w} - \frac{b}{2(t^\alpha + \bar{t}^\alpha)}\partial_s \ln w\right]. \tag{A.17}$$

The scalar masses depend on the curvature of the effective scalar metric $\widehat{K}_{N\overline{N}}$. If $p_i \neq 0$ they are complicated expressions in the general case but if $p_i = 0$, they reduce to the result given in Section 2, with the substitutions $W \to w$ and (A.17).

If $p_i = 0$ the expressions receive no corrections if supersymmetry breaking is dilaton mediated, $F^\alpha = 0$. If there is no dilaton "superpotential", $w_s = 0$, the only correction is the rescaling $F^\alpha \to (1 + b\ell)F^\alpha$. If a dilaton "superpotential" v is generated by a single dominant gaugino condensate (and the associated matter condensates), the dilaton dependence of v in (A.14) follows quite generally from anomaly matching, giving

$$\partial_s \ln w = v/b_+ w. \tag{A.18}$$

Since $b_+ \leq b$, the corrections in (A.16) can be significant if $|v/w|, \cos\theta$ and $1/t^\alpha$ are all order one. The moduli dependence of v in (A.14) follows from perturbative modular invariance.[2] To the extent that modular invariant condensation dominates supersymmetry breaking, one gets essentially the expressions in the text with negligible contributions from F^α. On the other hand if $\langle W \rangle$ is dominant, the corrections found in (A.14) again become negligible. They are significant only if there are two comparable sources of supersymmetry breaking. Even in this case they are unimportant in the large T limit if $\partial_s \ln w$ is not too large. Note that the correction to the A-term does not vanish at the self-dual points for the moduli, so in this case we would not get an "anomaly mediated" scenario at these points when $F^S = 0$. In the chiral formulation [35, 36], there is mixing between dilaton and moduli F-terms. In that language, the corrections to the results of Section 2, aside from the rescaling of F^α, arise from terms proportional to $F^S \overline{F}^\alpha K_{S\overline{T}^\alpha} +$ h.c. in the potential.

[2]Modular invariance could be broken in v if corrections to $k(\ell)$ from string nonperturbative effects are moduli dependent [137]. We have ignored this possibility throughout.

Appendix B

Complete One Loop Expressions in Orbifold Models

In this appendix we collect the complete expressions (tree plus one loop correction) for the soft supersymmetry breaking terms in orbifold models defined by (1.14), (1.19) and (1.24) with supersymmetry breaking *vevs* parameterized by (3.1) and (3.2).

The gaugino mass is determined from (2.59) and (2.53):

$$\begin{aligned} M_a^{tot} &= \frac{g_a^2(\mu)}{2\sqrt{3}}\overline{M}\left\{\frac{2}{3}\cos\theta\sum_\alpha(t^\alpha+\bar{t}^\alpha)G_2^\alpha\Theta_\alpha\left[\frac{\delta_{\rm GS}}{16\pi^2}+b_a^0-\frac{1}{8\pi^2}\sum_i C_a^i(1+3n_i^\alpha)\right]e^{-i\gamma_T}\right. \\ &\left.+\frac{2b_a^0}{\sqrt{3}}+\frac{\sin\theta}{k_{s\bar{s}}^{1/2}}\left[1+\frac{g_s^2}{16\pi^2}\left(C_a-\sum_i C_a^i\right)\right]e^{-i\gamma_S}\right\}. \end{aligned} \tag{B.1}$$

The trilinear A-terms are obtained from (2.57). The expression is simplified by utilizing (2.8) to obtain the identities

$$F^S\partial_s\gamma_i^a=-\gamma_i^a M_a^{(0)};\quad \partial_s\gamma_i^{lm}=k_s\gamma_i^{lm}, \tag{B.2}$$

where the last relation is true if $\kappa_i\neq\kappa_i(s)$. This yields A-terms of the form:

$$\begin{aligned} A_{ijk}^{tot} &= \frac{\overline{M}}{\sqrt{3}}\left\{-\frac{\gamma_i}{\sqrt{3}}+\cos\theta\left[\sum_\alpha(t^\alpha+\bar{t}^\alpha)G_2^\alpha\Theta_\alpha\left(\frac{1}{3}(n_i^\alpha+n_j^\alpha+n_k^\alpha+1)\right.\right.\right. \\ &\left.-\sum_{lm}\gamma_i^{lm}\left(p_{lm}^\alpha-(n_i^\alpha+n_l^\alpha+n_m^\alpha+1)\ln(\tilde{\mu}_{lm}^2)\right)-\sum_a\gamma_i^a p_{ia}^\alpha\right) \\ &\left.-\sum_\beta\ln\left[(t^\beta+\bar{t}^\beta)|\eta(t^\beta)|^4\right]\sum_{lm}\gamma_i^{lm}p_{lm}^\beta\sum_\alpha(t^\alpha+\bar{t}^\alpha)G_2^\alpha\Theta_\alpha(n_i^\alpha+n_l^\alpha+n_m^\alpha+1)\right] \\ &+\frac{\sin\theta}{k_{s\bar{s}}^{1/2}}\left[-\frac{k_s}{3}+\sum_a\gamma_i^a\left(\partial_s\ln(\tilde{\mu}_{ia}^2)+\frac{g_a^2}{2}\ln(\tilde{\mu}_{ia}^2)\right)+\sum_{lm}\gamma_i^{lm}\partial_s\ln(\tilde{\mu}_{lm}^2)\right. \\ &\left.\left.-\sum_\alpha\ln\left[(t^\alpha+\bar{t}^\alpha)|\eta(t^\alpha)|^4\right]\left(\sum_a g_a^2\gamma_i^a p_{ia}^\alpha-k_s\sum_{lm}\gamma_i^{lm}p_{lm}^\alpha\right)\right]e^{-i\gamma_S}\right\}+\text{ cyclic (ijk)}. \end{aligned} \tag{B.3}$$

The bilinear B-terms have a similar form

$$
\begin{aligned}
B_{ij}^{tot} \;=\; & \frac{\overline{M}}{3}\left(\frac{1}{2}-\gamma_i\right)+\frac{\overline{M}}{\sqrt{3}}\Bigg\{\cos\theta\Bigg[\frac{1}{2}\sum_\alpha \Theta_\alpha\left((n_i^\alpha+n_j^\alpha+1)-\partial_{t^\alpha}\ln\mu_{ij}\right) \\
& -\sum_\alpha (t^\alpha+\bar{t}^\alpha)G_2^\alpha\Theta_\alpha\left(\sum_a \gamma_i^a p_{ia}^\alpha+\sum_{lm}\gamma_i^{lm}p_{lm}^\alpha\right) \\
& -\sum_\beta \ln\left[(t^\beta+\bar{t}^\beta)|\eta(t^\beta)|^4\right]\sum_{lm}\gamma_i^{lm}p_{lm}^\beta\sum_\alpha (t^\alpha+\bar{t}^\alpha)G_2^\alpha\Theta_\alpha(n_i^\alpha+n_l^\alpha+n_m^\alpha+1) \\
& +\sum_{lm}\gamma_i^{lm}\sum_\alpha (t^\alpha+\bar{t}^\alpha)G_2^\alpha\Theta_\alpha(n_i^\alpha+n_l^\alpha+n_m^\alpha+1)\ln(\tilde{\mu}_{lm}^2)\Bigg]e^{-i\gamma_\alpha} \\
& +\frac{\sin\theta}{k_{s\bar{s}}^{1/2}}\Bigg[\sum_a \gamma_i^a\left(\frac{g_a^s}{2}\ln(\tilde{\mu}_{ia}^2)+\partial_s\ln(\tilde{\mu}_{ia}^2)\right)+\sum_{lm}\gamma_i^{lm}\partial_s\ln(\tilde{\mu}_{lm}^2) \\
& -\sum_\alpha \ln\left[(t^\alpha+\bar{t}^\alpha)|\eta(t^\alpha)|^4\right]\left(\sum_a \gamma_i^a g_a^2 p_{ia}^\alpha-\sum_{lm}\gamma_i^{lm}k_s p_{lm}^\alpha\right)-(k_s+\partial_s\ln\mu_{ij})\Bigg]e^{-i\gamma_s}\Bigg\} \\
& +(i\leftrightarrow j)
\end{aligned}
\tag{B.4}
$$

The scalar masses arise from (2.75) and (2.76). Some degree of consolidation can be obtained by employing the relation (B.2) as well as

$$
|F^S|^2\partial_s\partial_{\bar{s}}\ln g_a^2=|M_a^{(0)}|^2, \tag{B.5}
$$

to allow the following identifications:

$$
\begin{aligned}
\overline{F}^{\overline{S}}\partial_{\bar{s}}\sum_{lm}\gamma_i^{lm}A_{ilm}^{(0)}\ln(\tilde{\mu}_{lm}^2) &= \sum_{lm}\gamma_i^{lm}\left\{A_{ilm}^{(0)}\overline{F}^{\overline{S}}\partial_{\bar{s}}\ln(\tilde{\mu}_{lm}^2)+k_{\bar{s}}\overline{F}^{\overline{S}}A_{ilm}^{(0)}\ln(\tilde{\mu}_{lm}^2)-k_{s\bar{s}}|F^S|^2\ln(\tilde{\mu}_{lm}^2)\right\} \\
\overline{F}^{\overline{S}}\partial_{\bar{s}}\sum_a \gamma_i^a M_a^{(0)}\ln(\tilde{\mu}_{ia}^2) &= \sum_a \gamma_i^a\left\{\overline{F}^{\overline{S}}M_a^{(0)}\partial_{\bar{s}}\ln(\tilde{\mu}_{ia}^2)-2(M_a^{(0)})^2\ln(\tilde{\mu}_{ia}^2)\right\}
\end{aligned}
\tag{B.6}
$$

With these, the complete expression for the tree level plus one loop scalar masses is given by

$$
\begin{aligned}
(M_i^{tot})^2 \;=\; & |M|^2 \Bigg\{ \frac{1}{9}(1+\gamma_i) + \frac{1}{9}\sum_\alpha \ln\left[(t^\alpha+\bar{t}^\alpha)|\eta(t^\alpha)|^4\right] \left(\sum_a \gamma_i^a p_{ia}^\alpha - 2\sum_{jk}\gamma_i^{jk} p_{jk}^\alpha\right) \\
& -\frac{1}{9}\sum_a \gamma_i^a \ln(\tilde{\mu}_{ia}^2) + \frac{2}{9}\sum_{jk}\gamma_i^{jk}\ln(\tilde{\mu}_{jk}^2) + \\
& \frac{\sin\theta}{k_{s\bar{s}}^{1/2}}\left[\frac{1}{3\sqrt{3}}\left(\sum_a \gamma_i^a g_a^2 \cos\gamma_S - \frac{1}{2}\sum_{jk}\gamma_i^{jk}\left(k_s e^{-i\gamma_S} + k_{\bar{s}} e^{i\gamma_S}\right)\right)\right] \\
& +\frac{\cos\theta}{3\sqrt{3}}\left[\sum_\alpha (t^\alpha+\bar{t}^\alpha) G_2^\alpha \Theta_\alpha \sum_{jk}\gamma_i^{jk}(n_i^\alpha + n_j^\alpha + n_k^\alpha + 1)\right]\cos\gamma_\alpha \\
& +\cos^2\theta\left[\frac{1}{3}\sum_\alpha n_i^\alpha \Theta_\alpha^2 - \frac{1}{3}\sum_\alpha \Theta_\alpha^2\left(\sum_a \gamma_i^a p_{ia}^\alpha + \sum_{jk}\gamma_i^{jk} p_{jk}^\alpha\right)\right. \\
& -\frac{1}{3}\sum_a \gamma_i^a \sum_\alpha n_i^\alpha \Theta_\alpha^2 \ln(\tilde{\mu}_{ia}^2) + \frac{1}{3}\sum_{jk}\gamma_i^{jk}\sum_\alpha (n_j^\alpha + n_k^\alpha)\Theta_\alpha^2 \ln(\tilde{\mu}_{jk}^2) \\
& -\sum_\alpha \ln\left[(t^\alpha+\bar{t}^\alpha)|\eta(t^\alpha)|^4\right]\left(-\frac{1}{3}\sum_a \gamma_i^a p_{ia}^\alpha \sum_\beta n_i^\beta \Theta_\beta^2 + \frac{1}{3}\sum_{jk}\gamma_i^{jk} p_{jk}^\alpha \sum_\beta (n_j^\beta + n_k^\beta)\Theta_\beta^2\right. \\
& \left.+\frac{1}{3}\sum_{jk}\gamma_i^{jk} p_{jk}^\alpha \sum_\beta\sum_\gamma (t^\beta+\bar{t}^\beta)(t^\gamma+\bar{t}^\gamma) G_2^\beta G_2^\gamma \Theta_\beta\Theta_\gamma (n_i^\beta + n_j^\beta + n_k^\beta + 1)(n_i^\gamma + n_j^\gamma + n_k^\gamma + 1)\right) \\
& \left.+\frac{1}{3}\sum_{jk}\gamma_i^{jk} p_{jk}^\alpha \sum_\alpha\sum_\beta (t^\alpha+\bar{t}^\alpha)(t^\beta+\bar{t}^\beta) G_2^\alpha G_2^\beta \Theta_\alpha\Theta_\beta (n_i^\beta + n_j^\beta + n_k^\beta + 1)\cos(\gamma_\beta - \gamma_\alpha)\right] \\
& +\frac{\sin\theta\cos\theta}{k_{s\bar{s}}^{1/2}}\left[-\frac{1}{6}\sum_\alpha (t^\alpha+\bar{t}^\alpha) G_2^\alpha \Theta_\alpha \sum_{jk}\gamma_i^{jk} p_{jk}^\alpha \left(k_s e^{-i(\gamma_S-\gamma_\alpha)} + k_{\bar{s}} e^{i(\gamma_S-\gamma_\alpha)}\right)\right. \\
& +\frac{1}{3}\sum_\alpha (t^\alpha+\bar{t}^\alpha) G_2^\alpha \Theta_\alpha \sum_a g_a^2 \gamma_i^a p_{ia}^\alpha \cos(\gamma_S - \gamma_\alpha) \\
& +\frac{1}{6}\sum_{jk}\gamma_i^{jk}\sum_\alpha (t^\alpha+\bar{t}^\alpha) G_2^\alpha \Theta_\alpha (n_i^\alpha + n_j^\alpha + n_k^\alpha + 1)\left(\partial_{\bar{s}}\ln(\tilde{\mu}_{jk}^2) + k_{\bar{s}}\ln(\tilde{\mu}_{jk}^2)\right) e^{i(\gamma_S-\gamma_\alpha)} \\
& \left.+\frac{1}{6}\sum_{jk}\gamma_i^{jk}\sum_\alpha (t^\alpha+\bar{t}^\alpha) G_2^\alpha \Theta_\alpha (n_i^\alpha + n_j^\alpha + n_k^\alpha + 1)\left(\partial_s\ln(\tilde{\mu}_{jk}^2) + k_s\ln(\tilde{\mu}_{jk}^2)\right) e^{-i(\gamma_S-\gamma_\alpha)}\right] \\
& +\frac{\sin^2\theta}{k_{s\bar{s}}}\left[-\frac{1}{4}\sum_a g_a^4 \gamma_i^a \ln(\tilde{\mu}_{ia}^2) - \frac{1}{3}\sum_a \gamma_i^a \partial_s\partial_{\bar{s}}\ln(\tilde{\mu}_{ia}^2) + \frac{1}{3}\sum_a \gamma_i^a g_a^2\left(\partial_s\ln(\tilde{\mu}_{ia}^2) + \partial_{\bar{s}}\ln(\tilde{\mu}_{ia}^2)\right)\right. \\
& -\sum_{jk}\gamma_i^{jk}\left(\frac{1}{3}(k_s k_{\bar{s}} + 2k_{s\bar{s}})\ln(\tilde{\mu}_{jk}^2) + \frac{1}{3}\partial_s\partial_{\bar{s}}\ln(\tilde{\mu}_{jk}^2) + \frac{1}{2}(k_s\partial_{\bar{s}}\ln(\tilde{\mu}_{jk}^2) + k_{\bar{s}}\partial_s\ln(\tilde{\mu}_{jk}^2))\right) \\
& \left.\left.-\sum_\alpha \ln\left[(t^\alpha+\bar{t}^\alpha)|\eta(t^\alpha)|^4\right]\left(\frac{1}{4}\sum_a g_a^4 \gamma_i^a p_{ia}^\alpha + \frac{1}{3}\sum_{jk}\gamma_i^{jk} p_{jk}^\alpha k_s k_{\bar{s}}\right)\right]\Bigg\}. \qquad \text{(B.7)}
\end{aligned}
$$

Bibliography

[1] P. Adamietz, P. Binétruy, G. Girardi and R. Grimm, *Nucl. Phys.* **B401** (1993) 257.

[2] K. Agashe and M. Graesser, *Phys. Rev.* **D59** (1999) 015007.

[3] U. Amaldi, W. de Boer and H. Fürstenau, *Phys. Lett.* **B260** (1991) 447.

[4] D. Amati, K. Konishi, Y. Meurice, G.C. Rossi and G. Veneziano, *Phys. Rept.* **162** (1988) 169.

[5] I. Antoniadis, E. Gava, K.S. Narain and T.R. Taylor, *Nucl. Phys.* **B432** (1994) 187.

[6] I. Antoniadis, K.S. Narain and T.R. Taylor, *Phys. Lett.* **B267** (1991) 37.

[7] N. Arkani-Hamed, G.F. Giudice, M.A. Luty and R. Rattazzi, *Phys. Rev.* **D58** (1998) 115005.

[8] N. Arkani-Hamed and H. Murayama, *Phys. Rev.* **D56** (1997) 6733.

[9] R. Arnowitt and P. Nath, *Phys. Rev.* **D46** (1992) 3981.

[10] H. Baer and M. Brhlik, *Phys. Rev.* **D53** (1996) 597.

[11] H. Baer and M. Brhlik, *Phys. Rev.* **D55** (1997) 3201.

[12] J. Bagger, K. Matchev and D. Pierce, *Phys. Lett.* **B348** (1995) 443.

[13] J. Bagger, T. Moroi and E. Poppitz, *JHEP* **0004** (2000) 009.

[14] J. Bagger, T. Moroi and E. Poppitz, *Nucl. Phys.* **B594** (2001) 354.

[15] N. Bahcall, J.P. Ostriker, S. Perlmutter and P.J. Steinhardt, *Science* **284** (1999) 1481.

[16] T. Banks and M. Dine, *Phys. Rev.* **D50** (1994) 7454.

[17] T. Banks, D. Kaplan and A. Nelson, *Phys. Rev.* **D49** (1994) 779.

[18] R. Barbieri, S. Ferrara, L. Maiani, F. Palumbo and C.A. Savoy, *Phys. Lett.* **B115** (1982) 212.

[19] V. Barger et al., *Report of the SUGRA Working Group for Run II of the Tevatron*, hep-ph/0003154.

[20] V. Barger and C. Kao, *Phys. Rev.* **D57** (1998) 3131.

[21] T. Barreiro, B. de Carlos and E.J. Copeland, *Phys. Rev.* **D57** (1998) 7354.

[22] P. Binétruy, S. Dawson, M.K. Gaillard and I. Hinchliffe, *Phys. Rev.* **D37** (1988) 2633.

[23] P. Binétruy and M.K. Gaillard, *Phys. Lett.* **B232** (1989) 82.

[24] P. Binétruy and M.K. Gaillard, *Nucl. Phys.* **B358** (1991) 121.

[25] P. Binétruy, M.K. Gaillard and B.D. Nelson, *One Loop Soft Supersymmetry Breaking Terms in Superstring Effective Theories*, hep-ph/0011081, to appear in *Nucl. Phys.* **B**.

[26] P. Binétruy, M.K. Gaillard and T.R. Taylor, *Nucl. Phys.* **B455** (1995) 97.

[27] P. Binétruy, M.K. Gaillard and Y.-Y. Wu, *Nucl. Phys.* **B481** (1996) 109.

[28] P. Binétruy, M.K. Gaillard and Y.-Y. Wu, *Nucl. Phys.* **B493** (1997) 27.

[29] P. Binétruy, M.K. Gaillard and Y.-Y. Wu, *Phys. Lett.* **B412** (1997) 288.

[30] P. Binétruy, G. Girardi and R. Grimm, *Phys. Lett.* **B265** (1991) 111.

[31] P. Binétruy, G. Girardi and R. Grimm, *Phys. Rept.* **343** (2001) 255.

[32] P. Binétruy, G. Girardi, R. Grimm and M. Müller, *Phys. Lett.* **B189** (1987) 83.

[33] P. Binétruy, G. Girardi, R. Grimm and M. Müller, *Phys. Lett.* **B195** (1987) 389-396.

[34] A. Birkedal-Hansen and B.D. Nelson, *The Role of Wino Content in Neutralino Dark Matter*, hep-ph/0102075, to appear in *Phys. Rev.* **D**.

[35] A. Brignole, C.E. Ibáñez and C. Muñoz, *Nucl. Phys.* **B422** (1994) 125.
ERRATUM *Nucl. Phys.* **B436** (1995) 747.

[36] A. Brignole, C.E. Ibáñez, C. Muñoz and C. Scheich, *Z. Phys.* **C74** (1997) 157.

[37] R. Brustein and P. Steinhardt, *Phys. Lett.* **B302** (1993) 196.

[38] C.P. Burgess, J.-P. Derendinger, F. Quevedo and M. Quirós, *Phys. Lett.* **B348** (1995) 428.

[39] G.L. Cardoso and B.A. Ovrut , *Nucl. Phys.* **B369** (1993) 351.

[40] G.L. Cardoso and B.A. Ovrut , *Nucl. Phys.* **B418** (1994) 535.

[41] J.A. Casas, *Phys. Lett.* **B384** (1996) 103.

[42] D.J. Castaño, E.J. Piard and P. Ramond, *Phys. Rev.* **D49** (1994) 4882.

[43] S. Cecotti, S. Ferrara and M. Villasante, *Int. J. Mod. Phys.* **A2** (1987) 1839.

[44] C.-H. Chen, M. Drees and J.F. Gunion, *Phys. Rev.* **D55** (1997) 330.
ERRATUM *Phys. Rev.* **D60** (1999) 039901.

[45] T.P. Cheng and L.F. Li, *Gauge Theories of Elementary Particle Physics*, (Clarendon Press, 1988).

[46] K. Choi and J.E. Kim, *Phys. Lett.* **B154** (1985) 39.

[47] K. Choi and J.E. Kim, *Phys. Lett.* **B165** (1985) 71.

[48] A.G. Cohen, D.B. Kaplan and A.E. Nelson, *Phys. Lett.* **B388** (1996) 588.

[49] A. Corsetti and P. Nath, *Gaugino Mass Nonuniversality and Dark Matter in SUGRA, Strings and D-Brane Models*, hep-ph/0003186.

[50] P. de Bernardis et al., *Nature* **404** (2000) 955.

[51] W. de Boer, H.J. Grimm, A.V. Gladyshev and D.I. Kazakov, *Phys. Lett.* **B438** (1998) 281.

[52] B. de Carlos and J.A. Casas, *Phys. Lett.* **B349** (1995) 300.

[53] DELPHI Collaboration, *Phys. Lett.* **B489** (2000) 38.

[54] J.-P. Derendinger, S. Ferrara, C. Kounnas and F. Zwirner, *Nucl. Phys.* **B372** (1992) 145.

[55] J.-P. Derendinger, F. Quevedo and M. Quirós, *Nucl. Phys.* **B428** (1994) 282.

[56] K.R. Dienes, *Phys. Rept.* **287** (1997) 447.

[57] M. Dine and D. MacIntire, *Phys. Rev.* **D46** (1992) 2594.

[58] M. Dine and N. Seiberg, *Phys. Lett.* **B162** (1985) 299.

[59] L.J. Dixon, V.S. Kaplunovsky and J. Louis, *Nucl. Phys.* **B355** (1991) 649.

[60] S. Dodelson, *Int. J. Mod. Phys.* **A15** (2000) 2629.

[61] M. Drees and M.M. Nojiri, *Phys. Rev.* **D47** (1993) 376.

[62] G. Dvali and A. Pomarol, *Phys. Rev. Lett.* **77** (1996) 3728.

[63] J. Edsjo and P. Gondolo, *Phys. Rev.* **D56** (1997) 1879.

[64] J. Ellis, T. Falk, G. Ganis and K.A. Olive, *Phys. Rev.* **D62** (2000) 075010.

[65] J. Ellis, T. Falk and K.A. Olive, *Phys. Lett.* **B444** (1998) 367.

[66] J. Ellis, T. Falk, K.A. Olive and M. Schmitt, *Phys. Lett.* **B388** (1996) 97.

[67] J. Ellis, T. Falk, K.A. Olive and M. Schmitt, *Phys. Lett.* **B413** (1997) 355.

[68] J. Ellis, T. Falk, K.A. Olive and M. Srednicki, *Astropart. Phys.* **13** (2000) 181.

[69] J. Ellis, J.S. Hagelin, D.V. Nanopoulos, K.A. Olive and M. Srednicki, *Nucl. Phys.* **B238** (1984) 453.

[70] J. Ellis and L. Roszkowski, *Phys. Lett.* **B283** (1992) 252.

[71] J.L. Feng, K.T. Matchev and T. Moroi, *Phys. Rev. Lett.* **84** (2000) 2322.

[72] J.L. Feng, K.T. Matchev and T. Moroi, *Phys. Rev.* **D61** (2000) 075005.

[73] J.L. Feng, K.T. Matchev and F. Wilczek, *Phys. Lett.* **B482** (2000) 388.

[74] J.L. Feng, T. Moroi, L. Randall, M. Strassler and S. Su, *Phys. Rev. Lett.* **83** (1999) 1731.

[75] A. Font, L. Ibáñez, F. Quevedo and A. Sierra, *Nucl. Phys.* **B331** (1990) 421.

[76] W.L. Freedman, *Phys. Rept.* **333-334** (2000) 1.

[77] M.K. Gaillard, *Phys. Lett.* **B342** (1995) 125.

[78] M.K. Gaillard, *Phys. Rev.* **D58** (1998) 105027.

[79] M.K. Gaillard, *Phys. Rev.* **D61** (2000) 084028.

[80] M.K. Gaillard and V. Jain, *Phys. Rev.* **D49** (1994) 1951.

[81] M.K. Gaillard, V. Jain and K. Saririan, *Phys. Lett.* **B387** (1996) 520.

[82] M.K. Gaillard, V. Jain and K. Saririan, *Phys. Rev.* **D55** (1997) 833.

[83] M.K. Gaillard, D.H. Lyth and H. Murayama, *Phys. Rev.* **D58** (1998) 123505.

[84] M.K. Gaillard and B.D. Nelson, *Nucl. Phys.* **B571** (2000) 3.

[85] M.K. Gaillard and B.D. Nelson, *Nucl. Phys.* **B588** (2000) 197.

[86] M.K. Gaillard, B.D. Nelson and Y.-Y. Wu, *Phys. Lett.* **B459** (1999) 549.

[87] M.K. Gaillard and T.R. Taylor, *Nucl. Phys.* **B381** (1992) 577.

[88] M.K. Gaillard and R. Xiu, *Phys. Lett.* **B296** (1992) 71.

[89] S.J. Gates, M. Grisaru, M. Roček and W. Siegel, *Superspace*, (Benjamin/Cummings, 1983).

[90] T. Gherghetta, G. Giudice and J.D. Wells, *Nucl. Phys.* **B559** (1999) 27.

[91] J. Giedt, *Nucl. Phys.* **B595** (2001) 3.

[92] L. Girardello and M.T. Grisaru, *Nucl. Phys.* **B194** (1982) 65.

[93] G.F. Giudice, M. Luty, H. Murayama and R. Rattazzi, *JHEP* **9812** (1998) 027.

[94] G.F. Giudice and A. Masiero, *Phys. Lett.* **B206** (1988) 480.

[95] G.F. Giudice and R. Rattazzi, *Nucl. Phys.* **B511** (1998) 25.

[96] H. Goldberg, *Phys. Rev. Lett.* **50** (1983) 1419.

[97] P. Gondolo and G. Gelmini, *Nucl. Phys.* **B360** (1991) 145.

[98] K. Griest, M. Kamionkowski and M.S. Turner, *Phys. Rev.* **D41** (1990) 3565.

[99] K. Griest and L. Roszkowski, *Phys. Rev.* **D46** (1992) 3309.

[100] K. Griest and D. Seckel, *Phys. Rev.* **D43** (1991) 3191.

[101] J.F. Gunion and S. Mrenna, *Phys. Rev.* **D62** (2000) 015002.

[102] R. Hempfling, *Phys. Lett.* **B351** (1995) 206.

[103] L.E. Ibáñez, H.-P. Nilles and F. Quevedo, *Phys. Lett.* **B187** (1987) 25.

[104] A.H. Jaffe et al., *Phys. Rev. Lett.* **86** (2000) 3475.

[105] G. Jungman, M. Kamionkowski and K. Griest, *Phys. Rept.* **267** (1996) 195.

[106] G.L. Kane, C. Kolda, L. Roszkowski, J.D. Wells, *Phys. Rev.* **D49** (1994) 6173.

[107] G.L. Kane, C. Kolda, L. Roszkowski and J.D. Wells, *Phys. Rev.* **D50** (1994) 3498.

[108] D. Kaplan, G. Kribs and M. Schmaltz, *Phys. Rev.* **D62** (2000) 035010.

[109] V.S. Kaplunovsky and J. Louis, *Phys. Lett.* **B306** (1993) 269.

[110] V.S. Kaplunovsky and J. Louis, *Nucl. Phys.* **B444** (1995) 191.

[111] Y. Katsuki et al., *KEK Preprint DPKU-8904.*

[112] C. Kolda and J.-M. Russell, *Phys. Rev.* **D55** (1997) 4252.

[113] L3 Collaboration: M. Acciarri et al., *Phys. Lett.* **B482** (2000) 31.

[114] A.B. Lahanas and D.V. Nanopoulos, *Phys. Rept.* **145** (1987) 1.

[115] A.B. Lahanas, D.V. Nanopoulos and V.C. Spanos, *Phys. Lett.* **B464** (1999) 213.

[116] A. Love and P. Stadler, *Nucl. Phys.* **B515** (1998) 34.

[117] D. Lüst and T.R. Taylor, *Phys. Lett.* **B253** (1991) 335.

[118] S.P. Martin and P. Ramond, *Phys. Rev.* **D51** (1995) 6515.

[119] S.P. Martin and M.T. Vaughn, *Phys. Lett.* **B318** (1993) 331.

[120] S.P. Martin and M.T. Vaughn, *Phys. Rev.* **D50** (1994) 2282.

[121] P. Mayr and S. Stieberger, *Nucl. Phys.* **B412** (1994) 502.

[122] S. Mizuta, D. Ng and M. Yamaguchi, *Phys. Lett.* **B300** (1993) 96.

[123] S. Mizuta and M. Yamaguchi, *Phys. Lett.* **B298** (1993) 120.

[124] T. Moroi and L. Randall, *Nucl. Phys.* **B570** (2000) 455.

[125] Particle Data Group, *Eur. Phys. J.* **C15** (2000) 1.

[126] S. Perlmutter et al., *Astrophys. J.* **517** (1999) 565.

[127] J. Polchinski, *Phys. Rev.* **D50** (1994) 6041.

[128] A. Pomarol and R. Rattazzi, *JHEP* **9905** (1999) 013.

[129] A. Pomarol and D. Tommasini, *Nucl. Phys.* **B466** (1996) 3.

[130] J.R. Primack, *Cosmological Parameters 2000*, astro-ph/0007187.

[131] L. Randall and R. Sundrum, *Nucl. Phys.* **B557** (1999) 79.

[132] L. Roszkowski, *Phys. Lett.* **B262** (1991) 59.

[133] L. Roszkowski, *Phys. Lett.* **B278** (1991) 147.

[134] M. Schmaltz and W. Skiba, *Phys. Rev.* **D62** (2000) 095005.

[135] S.H. Shenker, in *Random Surfaces and Quantum Gravity*, Proceedings of the NATO Advanced Study Institute, Cargese, France, 1990, Ed. O. Alvarez, E. Marinari and P. Windey, NATO ASI Series, (Plenum, New York, 1990).

[136] M.A. Shifman and A.I. Vainshtein, *Nucl. Phys.* **B277** (1986) 456.

[137] E. Silverstein, *Phys. Lett.* **B396** (1997) 91.

[138] T.R. Taylor, *Phys. Lett.* **B164** (1985) 43.

[139] T.R. Taylor, G. Veneziano and S. Yankielowicz, *Nucl. Phys.* **B218** (1983) 493.

[140] G. Veneziano and S. Yankielowicz, *Phys. Lett.* **B113** (1982) 231.

[141] S. Weinberg, *Phys. Rev. Lett.* **50** (1983) 387.

[142] J. Wess and J. Bagger, *Supersymmetry and Supergravity*, (Princeton University Press, 1983).

[143] E. Witten, *Nucl. Phys.* **B443** (1995) 85.

[144] Y.-Y. Wu, *Dilaton Stabilization and Supersymmetry Breaking by Dynamical Gaugino Condensation in the Linear Multiplet Formalism of String Effective Theory*, hep-th/9610089.

Ernest Orlando Lawrence Berkeley National Laboratory
One Cyclotron Road | Berkeley, California 94720

Prepared for the U.S. Department of Energy under Contract No. DE-AC03-76SF00098